# optimize sedimentation tank and lab flocculation unit by cfd

duo zhang

Norwegian University of Life Sciences
Department of mathematical science and technology
Master Thesis 60 credits 2014

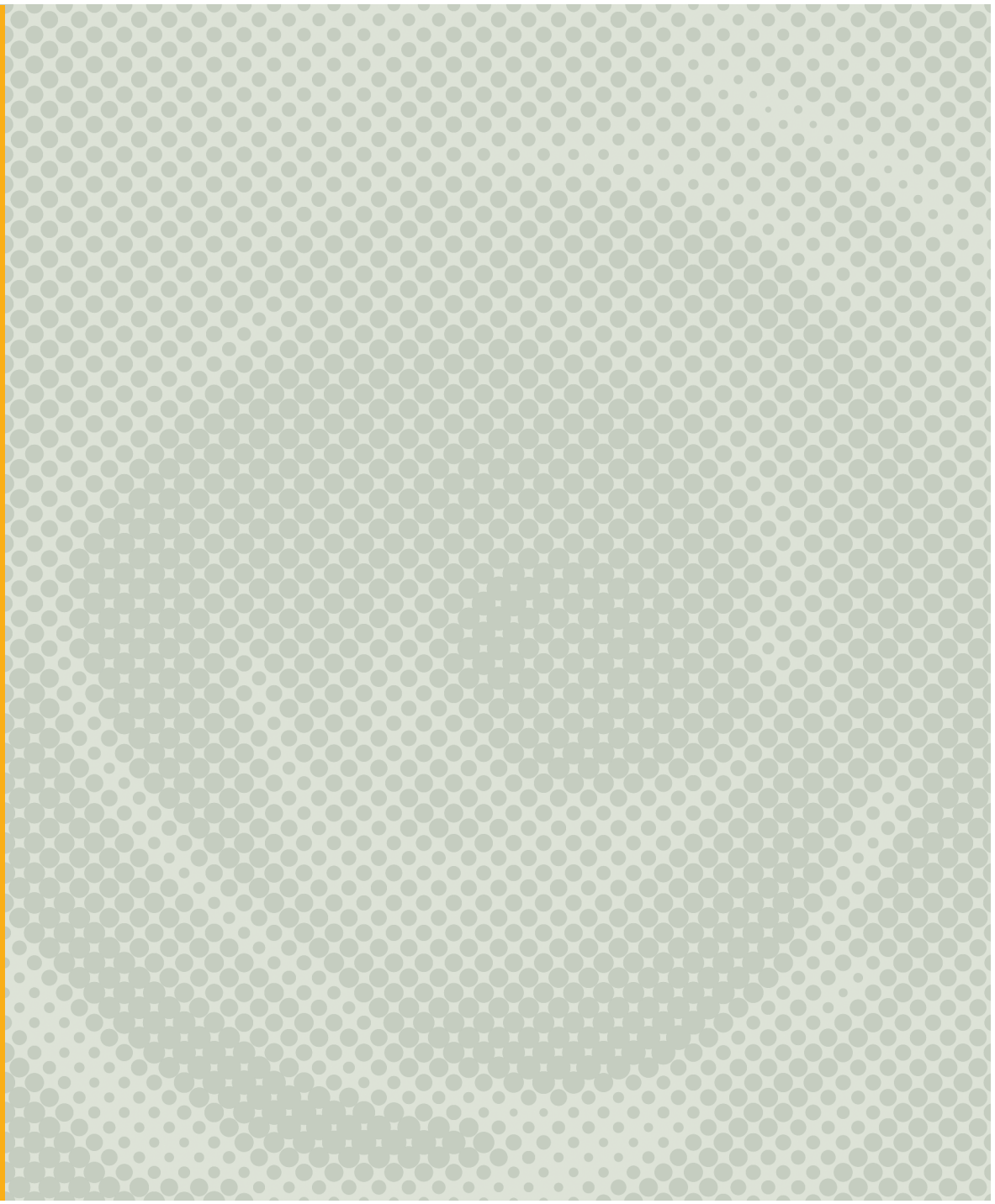

# Optimize sedimentation tank and lab flocculation unit by CFD

**Master Thesis**

by

**Duo Zhang**

Norwegian University of Life Sciences

Ås, Norway

February, 2014

## Acknowledgements

The simulation work of this master's thesis was carried out at the computer lab of Department of Mathematical Science and Technology (IMT), Norwegian University of Life Sciences (NMBU), Norway.

It was my dream that embed modern computer technology into wastewater treatment research, thanks to my supervisor, Dr. Harsha Ratnaweera, I got this opportunity to realize my dream. I would like to express my sincere gratitude to Dr. Harsha Ratnaweera, for his support and patience throughout my simulation work and thesis writing. Special thanks to Dr. Lelum Manamperuma for conducting the tracer test at the Drøbak wastewater treatment plant.

I express my sincere thanks and love to my mother Chun Xu (徐春) and my wife Jingjing Li (李晶晶). Without their support and understanding, I could not have the opportunity to study abroad.

I will be grateful to all who had helped me and supported me in these three years.

Ås, Norway
February, 2014
Duo Zhang

*Abbreviations:*
CAD: Computer Aided Design
CAE: Computer Aided Engineering
CAF: Computer Aided Manufacture
CEPT: Chemically Enhanced Primary Treatment
CFD: Computational Fluid Dynamics
DAF: Dissolved Air Flotation
DNS: Direct Numerical Simulation
DPM: Discrete Phase Model
FBT: Flat Blade Turbine
FDM: Finite Differential Method
FEA: Finite Element Analysis
FEM: Finite Element Method
FTC: Flow Through Curve
FVM: Finite Volume Method
HVAC: Heating, ventilating and Air Conditioning
LES: Large Eddy Simulation
MRF: Multi Reference Frame
PDE: Partial Differential Equations
PBM: Population Balance Model
PBT: Pitched Blade Turbine
RANS: Reynolds Averaged Navier-Stokes
RNG: Re-Normalisation Group
RSM: Reynolds Stress Model
RTD: Residence Time Distributed
SBR: Sequencing Batch Reactor
SIMPLE: Semi-Implicit Method for Pressure Linked Equations
SST: Shear Stress Transport
UDF: User Defined Function
VOF: Volume of Fluid
WWTP: Wastewater Treatment Plant

*Figures and table:*

**Abstract**

This work aim at introduce basic knowledge of CFD and it's application in optimization of sedimentation tank and lab flocculation units. A series of specialized strategies are developed for the simulation of the sedimentation tanks and lab flocculation units. Chapter 1 is general introduction of particle removal in water and wastewater treatment, includes particle separation, as well as particle removal during chemical treatment and biological treatment.

In chapter 2, background and application of CFD is introduced, development of CFD, application of CFD in different water and wastewater treatment processes are illustrated, the advantage of introduce CFD into water and wastewater treatment processes optimize and design then apparent.

Governing equations and basic numerical solution procedure of CFD are introduced in chapter 3, a compact direct numerical solution of Navier-stokes equation is demonstrated in this chapter, the demonstration could help readers gain quickly understanding about some basic concepts of CFD. Some concepts used in commercial CFD software, such as pressure-velocity coupling, residual, convergence criteria and under relaxation factor, also briefly explained, these concepts will be used in following chapters.

The major content of chapter 4 is turbulence model, because most flows in reality are turbulence flow, to ensure accuracy of CFD simulation, turbulence model is necessary, an appropriate turbulence model in addition to governing equations is prerequisite of acceptable CFD simulation, main stream turbulence model, includes zero equation model, one equation model, two equations k-$\varepsilon$ model, two equations k-$\omega$ model, seven equations Reynolds stress model as well as large eddy simulation, is introduced in this chapter.

Chapter 5 introduce the species transport and reaction model, Residence Time Distributed (RTD) is a very important parameter in reactor design, in commercial CFD software, RTD can be obtained by solve the species transport and reaction model with assistance of continuity equation, Navier-stokes equation and turbulence models.

Chapter 6 mainly focus on different multi-phase models available in current commercial CFD software, because most flows in reality consist of more than one phase, in order to increase accuracy of CFD simulation, also modeling multi-phase phenomena, different multi-phase models are coupled into commercial CFD software, multi-phase models should be selected carefully according to characteristic of phases in flow, another factor need taken into consideration when choosing a multi-phase model is computer power, since multi-phase models require higher CPU usage compare to single phase simulation. The major task of chapter 6 is introduce different multi-phase models and explain why Mixture model is selected as multi-phase model used in this study.

Chapter 7 demonstrate and analyze single phase and RTD simulation result for seven different sedimentation tank models, contour of velocity gradient, velocity vector, kinetic energy and RTD curve for different designs is demonstrated. According to simulation result, several failures such as strong surface current and re-circulating current is detected in the original design, the hydraulic performance is improved in modified designs.

Chapter 8 demonstrate and analyze the multi-phase simulation result, the multi-phase simulation in this chapter use transient solver, so that simulation result at different simulate times are recorded, “density current” is detected in the multi-phase simulation result, through analyze distribution of sediments, the function of sludge hopper and stability of sludge layer is studied.

Chapter 9 demonstrate and analyze simulation result for one Flat Blade Turbine (FBT) and two Pitched Blade Turbines (PBT) with different inclined angles, a special mesh generation technique, namely “Multi Reference Frame (MRF)”, also illustrate in this chapter, the mixing effect of different mixing devices is demonstrated through display contour of velocity gradient and velocity vector.

**Keywords:** sedimentation; flocculation; CFD

# list of content

# Chapter 1 Background and objective

## 1.1 Particle separation in water and wastewater treatment

Water is one of the most valuable resources in this world, although 70 percent of the earth's surface covered by water, nevertheless, of which only around 2-3 percent is fresh water. With the growth of the world population and development of the world economy, the amount of wastewater and demand of drinking water are growing rapidly, thereby the demand of water and wastewater treatment are increasing significantly.

Particle removal plays an important role in all kinds of water and wastewater treatment process, the primary goal of particle removal is remove water turbidity, produce water without visible particles. Particle separation technology mainly includes filtration, Dissolved Air Flotation (DAF), membrane filtration and sedimentation. Particles also can be removed by biological processes, according to requirement of oxygen, biological treatment can be divided into aerobic and anaerobic processes, biological treatment also can be classified into suspended growth and attached growth processes according to growth method of microorganism. Besides, although not technically a particle separation process, coagulation and flocculation still regarded as a kind of particle separation technology since it enlarge particle size and therefore enhance particle removal efficiency.

In most water and wastewater treatment plants, particle separation is the first treatment step, namely primary treatment. The particle separation processes could locate upstream of chemical or biological treatment, such as screening, primary sedimentation or grit chamber, also can be implemented downstream of the secondary treatment units, play the role of tertiary treatment, such as membrane filtration. Generally speaking, when used as primary treatment, the major task of particle separation is reduce treatment load for secondary treatment, when used as tertiary treatment, particle separation aim at removing particles generated in upstream units.

### 1.1.1 Major particle separation technology

*Sedimentation tank*

Sedimentation is one of the most common particle separation methods, although simple in principle, sedimentation tank still effective and essential in modern water and wastewater treatment. In water treatment, sedimentation tank usually aim at removing impurities, turbidity and color that produced by coagulation and flocculation. In wastewater treatment, sedimentation is the most popular primary treatment method, sand, grit and other big particles is removed by primary sedimentation process. Sedimentation tank not only have good performance in sewage treatment, but also play an important role in industrial wastewater treatment, Thompson et al (2001) summarized that sedimentation is the preferred treatment method for wastewater generated by the pulp and paper mill factory, on average, sedimentation could contribute to more than 80 percent removal of the suspended

particles. Rajvaidya and Markandey (1998) reported that 70-80 percent of suspended particles can be removed by sedimentation process.

According to the function of the sedimentation tank in water and wastewater treatment process, sedimentation tank can be classified into primary sedimentation tank and secondary sedimentation tank. Primary sedimentation tank mainly used as pretreatment, it locates upstream of chemical or biological treatment. In primary sedimentation tank, larger particles such as sand, natural particles, natural biological particles and large debris are removed, it could efficiently reduce treatment load for downstream treatment units.

Secondary sedimentation tank usually locates downstream of chemical or biological treatments, in the secondary sedimentation tank, finer particles generate in upstream chemical or biological processes are removed. In water treatment, the secondary sedimentation tank could settle flocs generated during flocculation or coagulation. In wastewater treatment, secondary sedimentation tank usually combined with activated sludge process, it settle waste sludge from the activated sludge tank, the waste sludge collected by the secondary sedimentation tank then can be reused (Metcalf 2002).

Sedimentation tank can be classified into the horizontal sedimentation tank, vertical flow sedimentation tank and circular sedimentation tank according to the sharp and flow direction of fluids in the sedimentation tank.

•Horizontal sedimentation tank

The horizontal sedimentation tank is a kind of rectangular shaped tank, wastewater inflow from one side of the tank, flow horizontally through the tank, and finally flow out of the tank at the outlet side.

•Vertical flow sedimentation tank

The vertical sedimentation tank is a kind of circular tank. Wastewater flow into the tank from an inlet locate in the center, directed by the feed pipe, flow downward and reflected by a reflector at the end of feed pipe, after reflected by the reflector, wastewater is distributed and flow towards the rim of sedimentation tank.

•Circular sedimentation tank

Circular sedimentation tank quite similar to the vertical sedimentation tank, the difference is in the circular sedimentation tank, wastewater flow upward in the central inlet, reflected by a baffle at the top of the feed pipe, then distributed and flow towards the rim of sedimentation tank.

Sedimentation is an important step no matter in primary treatment or secondary treatment, without sedimentation tank, sludge generated in chemical or biological treatment processes can’t be removed efficiently.

*Dissolved air flotation (DAF)*

Dissolved air flotation (DAF) mainly used as primary treatment, besides remove solids, DAF can also remove suspended pollutants such as oil, when used as

secondary treatment, DAF mainly responsible for removing particles generated in flocculation process. In some cases, DAF can be enhanced by adding coagulants into DAF plant (Edzwald 2010).

The DAF tank consists of three zones, namely the inlet zone, the contact zone and the separation zone respectively. After incoming wastewater pass through the inlet zone, air bubbles are added into the untreated wastewater in the contact zone, air bubbles interact with particles in incoming wastewater, generate the suspension of floc–bubble aggregates, then free bubbles and unattached floc particles carried by wastewater flows to the separation zone. In the separation zone, free bubbles and floc–bubble-aggregates float to the surface of the tank.

DAF is a kind of compact, high load rate and efficient treatment process, DAF could achieve very good performance in both domestic wastewater and industrial wastewater treatment. For example, Gubelt et al (2000) reported 65–95% removal of suspended solids in DAF, Wenta and Hartmen (2002) mentioned that dissolved DAF is able to remove 95% of the suspended solids.

### 1.1.2 Particle removal during biological treatment

*Activated sludge*

Biological treatments are normally used as secondary treatment. The major principle of biological treatments is removes the suspended solids and the dissolved organic matter by using microorganisms. Microorganisms involved in biological treatment process are responsible for the degradation of the organic matter. Microorganisms in wastewater treatment systems use the organic content as energy source, according to requirement of oxygen during degradation processes, biological treatment processes can be classified into aerobic and anaerobic processes. The most common aerobic processes include: activated sludge, sequence batch reactor and trickling filter.

Activated sludge is the most widely applied biological treatment process, usually used as secondary treatment. Activated sludge is one of the most representative aerobic technology, it dominantly applied for the treatment of domestic wastewater. Gavrilescu (1999) summarized that the advantages of activated sludge process are high biological particle removal efficiency, the possibility for nutrient removal (such as remove nitrogen via nitrification and de-nitrification) and the high operational flexibility.

In activated sludge, the plant must be aerated in order to get aerobic condition. The organic pollutants enter into the first tank namely aeration tank, mix with the activated sludge, after organic pollutants react with microorganisms in the activated sludge, the mixture then enter into the second tank namely settling tank where the mixture are settled. The settled activate sludge is recycled to the aeration tank to maintain sufficient microorganisms to degrade the organic matter. In activated sludge system, the treatment efficiency is influenced significantly by the sludge separation process,

which is affected by the sedimentation efficiency of activated sludge in the secondary sedimentation tank (Kim et al 2006).

*Sequencing batch reactor (SBR)*

Sequencing batch reactor (SBR) is a kind of transformation of activated sludge process, the SBR process includes the following six steps, namely anoxic fill, aerated fill, react, settle, decant and idle (Wilderer et al 2001).

In a SBR plant, firstly the wastewater is injected into reactor after pass through the influent distribution manifold, due to distribution of the influent distribution manifold, the incoming wastewater is distributed evenly inside the whole reactor, thereby in SBR microorganisms and the pollutants have better connection and interaction than activated sludge process (Norcross 1992). The mixture consists of influent wastewater and sludge then is drawn through the influent distribution manifold, merged with flow in the motive liquid pump, and discharged to the jet aerator. When microorganisms react with pollutants in wastewater, the reactor is continually aerated until biodegradation of BOD and nitrification of nitrogen is completed. After reaction, the aeration is stop, solids generated through previous stage begin to settle, a sludge blanket then appeared at the bottom of reactor, a clear, treated effluent layer appear on the top of reactor. At last, the treated effluent layer withdrawal from the top of the reactor, the settled sludge layer at the bottom of reactor withdrawal from the reactor. A portion of sludge recycled for next reaction cycle. Backwashing of the jet aerator also happened in this step (Chambers 1993).

*Trickling filter*

Both activated sludge and SBR are suspended growth processes, rather than being suspended as in activated sludge or SBR, in attached growth processes, microorganisms are attached to some support media over which they grow. The trickling filter is one of the most common attached growth processes. The trickling filter is a circular tank filled with the packing media where the microorganisms could grow. The bottom of the tank must be constructed stable enough in order to support the packing media above it. The wastewater spread on the top of the trickling tank, then pass through the packing media, by contact and react with microorganisms attached on the packing media, the organic pollutants is degraded by the microorganisms while the treated wastewater drains to the bottom (Metcalf 2002).

### 1.1.3 Particle removal during chemical treatment

*Chemical Enhanced Primary Treatment (CEPT)*

In some cases, in order to enhance phosphate and BOD removal while still maintain sedimentation effect, as well as increase treatment capacity of the sedimentation tank, Chemically Enhanced Primary Treatment (CEPT) usually introduced, CEPT means primary treatment enhanced by the addition of coagulants. With coagulants added into sedimentation tank, smaller particles will aggregate into larger particles, coagulation process and sedimentation process then happen simultaneously in sedimentation tank,

thus enhance sedimentation effect as well as P and BOD removal. CEPT is considered as an alternative or complementary technique to biological treatment (Žarković et al 2011). CEPT is particularly suitable for rapidly growing cities (Harleman 1999).

*Coagulation and flocculation*

Particle separation is a very important step in water and wastewater treatment, particle removal efficiency increase with increasing particle size (Bridgeman et al 2009). To enlarge particle size, coagulation and flocculation often combined with particle separation processes.

Unlike larger particles which can be removed via physical treatment unit, smaller particles such as dissolved organic matter and colloids are almost impossible to remove by physical treatment method, size of these small particles range from 0.01 to 1 μm. These collides and particles surface are negatively charged, so that ions with opposite charge attached at the surface of collides or particles, this ion layer known as fixed layer, surround this fixed layer, is a diffusion layer of ions, the compact layer and diffuse layer form double layers of ions surround particle. Repelling forces between these particles are considerably larger than attractive body force, under this condition, particles keep suspended by Brownian motion. In order to remove these smaller particles, chemical treatment is a preferable option, assisted by add chemicals into wastewater, dissolved material transform from smaller particles into larger particles, thus increase particle separation efficiency (Ravina 1993).

Add coagulants into wastewater changes the surface charge of particles, reduce the repulsive energy and energy barrier between two particles, with compress double layers which consist of positive and negative ions surround colloids, distance between two particles narrower, then particles attached by polymer chain, small particles further aggregate into larger particles by bridging effect (Crittenden et al 2012).

Based on particle size, flocculation can be classified into two types, micro-flocculation (also known as perikinetic flocculation) and macro-flocculation (orthokinetic flocculation), micro-flocculation refer to particles aggregated by Brownian motion, particle involved in micro-flocculation have particle size from 0.001 to 1 μm, for macro-flocculation, particle size in range 1 to 2 μm. Rapid mixing is necessary in flocculation process, through de-stabilisation (coagulation) and subsequent agglomeration (flocculation) process, fine particles and colloids aggregate into larger particles, thus improve removal efficiency of the subsequent particle separation devices. For macro-flocculation, mixing speed have significant effect on particle aggregation, in same velocity field, particles with higher velocity gradient will catch up slower moving particles, thus a larger particles generated (Bridgeman 2009).

In this research, in order to study the possibility of optimize water and wastewater treatment devices by using CFD, we will simulate the hydraulic behavior of

sedimentation tank and lab flocculation unit, and compare the CFD assisted design process with traditional design process.

## 1.2 Traditional design theory of sedimentation tank and flocculation unit

### 1.2.1 Traditional design theory of sedimentation tank

Traditionally, sedimentation tank design mostly based on simple hydro-dynamics or experience, due to lack of fully understanding about hydraulic mechanism inside sedimentation processes, traditional design method leads to potential failures easily (Metcalf 2002). Traditional sedimentation tank design based on some simple concepts such as detention time, surface loading rate and weir loading rate, Problems in sedimentation tank includes density current, dead zone, strong surface current, recirculating current, channeling and inefficient sludge removal.

One of the earliest sedimentation tank design theory proposed by Hazen (1904) in 1904, which is a major model for flow pattern and suspended solids distribution in sedimentation tank design, his theory assume that on the same cross section, horizon velocity of fluid is a constant u, settle of suspended solid in sedimentation tank decided by both fluid velocity u and settling velocity (vertical velocity) of suspended solid v, once suspended solid reach bottom of sedimentation tank, suspended solid is regarded as removed. For example, use Q denote flow rate, use W, L and D denote width, length and depth of sedimentation tank respectively, use Th denote horizontally transport time of particles and Tv denote time for vertical movement of particles, then we have following calculation:

Horizontal velocity of particle is:

$$Vh = Q/(W*D)$$

Horizontal transport time for particles is:

$$Th=L*W*D/Q$$

Vertical transport time for particles is:

$$Tv=D/Vv$$

According to above assumption:

$$Th = Tv$$

Thus:

$$Vv = D*(Q/(W*D))/L$$

$$Vv = Q/(W*L)$$

As implied from above formulas, we could concluded that according to Hazen’s assumption, removal efficiency of solids depends on surface area of sedimentation tank and detention time, while depth of the sedimentation tank have limited influence, the shorter retention time in a shallow tank (sludge accumulation) will be compensated by the shorter sedimentation distance. however, this theory assume all the solids in wastewater are discrete particles, with uniform density, size and sharp, with development of sedimentation tank design theory, more accurate design regulations for sedimentation tank are proposed.

Kynch (1952) proposed a more accurate sedimentation tank design theory in 1952.

His theory assume in any horizontal layer of sedimentation tank, concentration of suspended solid is evenly distributed, in the same layer, all particles settled with similar velocity, particle sharp, size and characteristic have no influence on settle velocity. Settle velocity of particles link to concentration of suspended solids surround particles.

Particles may be discrete particle, such as sand, or flocculent, such as organic materials or biological particles. If particle concentration is very high, adjacent particles are actually in contact thus particle concentration may influence settle effect. In reality, according to aggregation ability of suspended solid and concentration, sedimentation can be divided into following four types:
Class I - Unlimited settling
Class II - Settling of flocculent particles
Class III - Hindered settling and zone settling
Class IV - Compression settling

Unlimited settling also called unhindered settling, which mainly represent removal of discrete particles, under this situation, suspended solids have low concentration, each particle settles freely without interaction from adjacent particles, particle settles accelerated by gravity, velocity of particle keep moving until drag force of the particle is equal to the gravity force of the particle, then the particle will reach its terminal velocity and settled.

Settlement of flocculent particles is recognized as collides aggregate after flocculation. In sedimentation tank, some particles settle faster as result of increase particle size, longer detention time gives more time for particle growth so that ultimate settling velocity also increase. With the same retention time, a longer, shallower sedimentation tank with slower horizontal flow rate would more benefits in promoting collisions, because the opportunity for collision would become even greater. Because the advantage of shallower depths, baffles or tubes is introduced, which push the particles settled to the bottom of the sedimentation tank.

With the concentration of particles increased, particles further close together and interaction of particles enhanced, settle of particles will depend on each other, particles depends on adjacent particles rather than velocity fields of the fluid. This effect results to a reduced particle-settling velocity, this phenomena is known as hindered settling. When hindered settling occurs in the extreme condition, particle concentration is so high, the particles tends to form a ‘blanket’. This phenomena then known as zone settling.

Compression settling is very important in gravity thickening processes, compression settling means with high particle concentrations, particles settles to the bottom of the sedimentation tanks, adjacent particles interact with each other. This is known as compression settling. When compression settling occurs, settled particles are

compressed under the weight of particles on the top.

### 1.2.2 Traditional design theory of flocculation unit

A lot of factors could influent flocculation process, such as pH, temperature and mixing. Mixing could encourage particle agglomeration, in practical, flocculation mixing efficiency could increase via mechanical method or hydraulic method, in hydraulic flocculation process, fluid pass through baffled, “plug flow” condition reactor, hydraulic head loss caused by baffle will increase flocculation. In mechanical flocculation process, mixing of agitator will increase particle-particle interaction and flocculation, mechanical mixing should arranged enough to promote particle interaction and avoid existing floc breakage (Bridgeman et al 2010). In wastewater treatment processes, mechanical mixing aim at promote mixing of chemicals, aeration or blending, mechanical mixing mainly use turbine or propeller mixers, available mixers includes flat blade turbine (FBT), pitched blade turbine (PBT), Rushton turbine and propeller (Paul et al , 2004).

Mixing effect is difficult to study, a roughly measurement of mixing effect is energy input into per unit volume of vessel, more energy input means more turbulence, Camp and Stein (1943) proposed the following equations to characteristic mixing effect of mechanical mixing devices:

$$G = \sqrt{\frac{P}{\mu V}}$$

Where P is the power dissipated, V is tank volume, $\mu$ is dynamic viscosity, and G is average velocity gradient. Use concept of velocity gradient G is popular in wastewater field, however, it only applicable for macro-flocculation and only supply an approximate parameter for mixing optimization.

## 1.3 Objectives of this study

According to above introduction, in this study, we will use CFD optimize water and wastewater treatment processes, the objectives of this study are summarized to:

- Explore the possibility and advantage of using CFD as an alternative design tool for water and wastewater treatment devices.
- Develop a three dimensional CFD single phase model that describes flow pattern in sedimentation tanks.
- Develop the strategy for Residence Time Distribution (RTD) simulation by using the species transport and reaction model.
- Based on the single phase simulation result and RTD simulation result, as well as tracer test result, evaluate hydraulic performance of the sedimentation tank in Drøbak wastewater treatment plant (WWTP), then propose modified design towards failures of the original design, and evaluate the hydraulic performance of modified designs.
- In order to systematically study hydraulic performance of different sedimentation tanks, in addition to study the hydraulic efficiency of different horizontal sedimentation tanks, the performance of circular sedimentation tanks should also be studied.

•Develop a three-dimensional multiphase flow model that describes density current, sludge accumulation and particle separation in sedimentation tanks, use the simulation result further evaluate the performance of different sedimentation tank designs.
•Simulate the flow fields in lab jar test units with different agitators.

# Chapter 2 Background of CFD

## 2.1 History of CFD

One of the earliest contributions of CFD could track back to 1910, Richardson (1910) introduced approximate arithmetical solution by finite differences of physical problems, also application of this solution to stresses in a masonry dam in his paper, his computational work use hand calculations with human computers. Although the calculation extremely slow (only 2000 operations per week), it still provide ideal for numerical research, he thereby is regarded as pioneer of CFD.

After World War 2, with development of semi-conductor technology, computer architecture and electronic engineering, computer power was increased dramatically, computer was employed to solve fluid problems governed by Navier-Stokes equations, Francis H. Harlow and his group (Khalil 2012) developed a series of numerical methods for unsteady, two dimensional problems. Some of milestone of CFD was developed during this period (from early 1950s to late 1960s), such as Marker and Cell methods developed by Harlow and Welch (1965) in 1965, Fluid-in-cell method proposed by Gentry, Martin and Daly (1966) in 1966 and velocity stream function method provided by Fromm (1963) in 1963.

Three-dimensional models began to appear in late 1960s, with launch of space program, as well as stimulated by cold war, more fluid dynamics solution is required, CFD appeared in development and manufacture of aerospace and military equipment, such as submarines, helicopters, aircraft and missile. In 1967, Hess and Smith (1967) published the first paper about three-dimensional problem, they proposed the Panel Method, which is performance discretization according to geometry of panels based on requirement of aircraft manufacture. Lifting panel code also described by engineers from major aircraft company, such as Boeing, Douglas and NASA.

In 1970s, report about Finite difference methods for Navier-Stokes equations and Finite element methods for stress analysis appeared, however, finite difference methods based on structured mesh, suitable for problems with rectangular and cubic sharp only, finite element methods require more computer power. To compensate limitation of finite difference method and finite element method, Finite volume methods was proposed by the CFD group at Imperial College in 1970s, they launched a program which aim at solve simple shear flows and jet flows, from 1970s to 1980s, some algorithm and models which employed by nowadays commercial CFD software was developed, such as the SIMPLE (Semi-Implicit Method for Pressure Linked Equations) algorithm, which supply a straight forward solution of the Navier Stokes Momentum Equations. Additionally, the most popular turbulence model, Standard k-ε turbulence model, also proposed during this time, the Standard k-ε turbulence model is developed by Launder and Spalding in 1974, this model could describe turbulent flow with high Reynolds numbers. These achievement made fluid dynamic problems suitable for programming and solved by computer, thus create features that differ

CFD with traditional fluid dynamics problems. More two equations turbulent models was developed in late 1970s, application of turbulence flow transfer from simple shear flow to flow with strong swirling, circulation and turbulent chemical reaction in complex geometries. k-ε turbulence model was validated in a series of applications with and without swirl. Additionally, besides solve fluid dynamics problems, k-ε turbulence model also testify in turbulent reacting furnace configuration with and without swirl.

CFD was encouraged to apply in a variety of industrial applications in 1980s, in 1985, CFD already commonly used in aero industries, at that time, although assisted by more advanced models, CFD still use simple structured grid and difficult to handle unstructured boundary and wall conditions. Other drawbacks of CFD at that time include slow convergence and numerical diffusion caused by limited computer power, as well as difficult to handle simulation with three dimensional complex geometries (Anderson 1995).

In early 1980s, commercial CFD codes became available in market, more and more CFD users began to choose commercial CFD software rather than develop their own CFD codes. Commercial CFD software based on a series of very complex non-linear mathematical expressions, these expressions defined the basic governing equations of fluid dynamics, such as continuity equation, Navier-Stokes equation and energy equation, as well as additional models available in commercial CFD software, such as multi-phase models, turbulence models, species transport model etc, assisted by algorithms embedded in commercial CFD software, these equations are solved. Commercial CFD software enable users define geometry of flow field need to simulate, identity physical and chemical condition of fluids, also specific initial and boundary condition, with above condition as input, a converged solution as output with information of the flow field is provided. Output of commercial CFD software can be viewed graphically, such as contour plot, velocity vector, path-line, or numerically, such as output data and x-y plot.

In 1990s, CFD spread from traditional aero industries to non-aero industries, more and more applications of CFD appeared in a variety of industries, CFD is now regarded as an essential part of the Computer aided engineering (CAE), have similar function as Finite element analysis (FEA), CAE technology together with Computer aided design (CAD) and Computer aided manufacture (CAF), could completely change traditional industries.

CFD supply a “virtual wind tunnel” on engineer’s desktop, engineers could simulate fluid flow, equipment performance and reactor hydraulics before really construction work start, all they need is only a computer, CFD can supply fully information of the whole computational zone, with all conditions well controlled and almost without any constrains, with appropriate conceptualization of model geometry, mesh generation and select proper solution method, as well as proper verification and calibration, CFD

could supply acceptable accuracy. Nowadays, CFD has become an indispensable part of industries, aerodynamics and hydrodynamics simulation for airfare, car, train, missile, ship and submarine has been popular, in last two decades, CFD also contribution in non-traditional field, such as in-door environment simulation and pollutants transport. In water and wastewater industry, CFD also employed by some institution while still infancy and need further research.

**2.2 CFD in wastewater research**

To avoid potential failures and obtain fully understanding about hydraulic mechanism in particle separation processes such as flocculation or sedimentation, CFD could supply new solutions. Originated from aerospace engineering in late 1960s, CFD had been employed by engineers from variable fields, included chemical engineering, hydraulic engineering and civil engineering (Anderson 1995).

With the development of computer science, nowadays personal computer is getting greater and greater computational power, CFD is not only limited in academic environment or specialized consultant company, it's more and more popular in water and wastewater treatment research, technically, CFD is applicable for every water and wastewater treatment processes. This section aim at give a briefly introduction of CFD in varies water and wastewater treatment research, includes sedimentation, flocculation, flotation, biological treatment, disinfection and sludge treatment.

*CFD and sedimentation tank*

As one pioneer in numerical simulation of sedimentation tank, Larsen (1977) applied CFD simulation to several sedimentation tanks, although with simplification and conceptualization, he still shown several major hydraulic phenomena of sedimentation tank, such as "density waterfall" due to heavier fluid sink into bottom of sedimentation tank soon after entering, bottom current and surface return current, Nowadays, thanks to effort of computer engineers, mathematicians and fluid dynamics scientists, several more advanced models has been developed and available in commercial CFD software, based on these models and today's high performance computer, we could run advanced simulation which far beyond than 1970's.

Goula et al (2008) researched influence of baffle on sedimentation tank in potable water treatment by using CFD, a circulation zone is detected in the original tank without baffle. After equipped baffle, the recirculation zone around inlet in original tank decreased, the baffle enhanced setting of particles. Due to effect of baffle, particles around inlet move downwards and reach the bottom of the tank.

Density current, or turbidity current, means when two fluids with different density due to temperature, concentration or salinity confront each other, fluid with higher density sinks and flow along the bottom of fluid with smaller density, Goula et al (2008) studied the influence of temperature variation on density current in sedimentation tank. He found temperature difference between incoming fluid and fluid in tank could leads

to density current. Under density current phenomenon, a rising buoyant plume appears in the tank, and changes the direction of the main circular current.

Shahrokhi et al (2012) studied effect of baffles on sedimentation tanks, result show that baffle at optimum location could reduce the circulation zone, kinetic energy and maximum velocity magnitude, uniform velocity vector inside the settling zone from CFD simulation result could indicate better sedimentation effect.

*CFD and flocculation*

To investigate the most suitable parameters for flocculation process, it requires a large numbers of experiments. Nowadays, flocculation research were focused mainly at improving chemical conditions for treatment, ignore study the influence of hydraulic mechanism on flocculation, it's because hydraulic mechanism is difficult to study under lab conditions. So, the CFD is the most suitable method for explore the performance of flocculation tank during changing the parameters, almost without any cost and restrictions (Thomas 1999).

There were a lot of studies about effect of different types of coagulants, PH and coagulant dose by jar test approach, CFD start to employed for lab scale reactor research in recent years, Bridgeman et al (2010) used CFD simulate mixing in lab scale cylinder and square vessels for jar test, he use velocity gradient distribution and turbulence dissipation rates demonstrate mixing efficiency in different jar test units. More evenly distributed velocity gradient indicates better mixing efficiency, velocity gradient distribution also help users find dead zone, through plot path-line or velocity vector, flow direction can be detected thus problems such as circulation or bypass can be shown. Turbulence dissipation rate also used for mixing efficiency evaluation, when the two jar test vessels were mixed at the same speed, the turbulence dissipation rates of circular section vessel is lower than turbulence dissipation rates of square section vessel, means fluids in the circular vessel is better distributed, besides configuration of jar test units, the geometry of paddle also important and could influent performance of flocculation process.

*CFD and DAF*

Change of flow rate, size of tank and baffle height will influent performance of DAF, to show how velocity variable as function of operating factors, CFD is a useful tool. Two-phase simulation consists of water and air bubbles are more suitable for DAF simulation, three-phase model include water, air and particles also available although difficult to implement. Despite ignore a lot of details in reality, such as air bubble size, particle interaction and coagulation effect, CFD still a useful tool and will contribute a lot for DAF optimization in feasible future (Edzwald 2010).

*CFD in biological treatment*

Ding et al (2006) described particle aggregation simulation by using CFD-Population balance model (PBM), with assistance of CFD, hydro-dynamics as well as biological

kinetics could be predicted, simulation result supply reference for activated sludge treatment unit operating.

Besides activated sludge plant, CFD can be employed in both suspended growth processes and attached growth processes. Fayolle et al (2007) studied aeration in activated sludge process, two kinds of aeration tank geometry, oblong and annular, and two types of mixer, axial mixer and large blade slow speed mixer, is taken into consideration, different combination of tank geometry and mixer is studied in this paper, in addition to hydraulics, oxygen transfer also simulated in his work.

*CFD in sludge treatment and odour control*

In wastewater treatment processes, sludge generated from primary sedimentation tank, dissolved air filtration, excess sludge from aeration tank and secondary sedimentation tank, sludge contains almost all the organic matters removed from the treated wastewater. Organic matter in sludge may eventually decompose, be offensive and become contaminant if not treated properly. Normally, sludge treatment techniques include compost, disposal, fertilizer, anaerobic digest and incineration. Anaerobic digest of sludge have several advantages, firstly, anaerobic digest need less volume compare to aerobic treatment, secondly, methane can be produced through anaerobic digest, methane could transfer into energy, thus reduce the total energy demand of the treatment plant.

Terashima et al (2009) developed a three dimensional model in order to study effect of quantify mixing in a full-scale anaerobic digester. For full scale digester, CFD can be applied to determine required time for fully distributed mixing. According to rheological characteristics of sludge, turbulence model and non-newtonian fluid model is activated in anaerobic digest simulation. Meroney and Colorado (2009) simulate mixing effect of draft impeller tube mixers for anaerobic digest tanks under complex mixing situation, different mixer position, influent and effluent of sludge and different mixing speed is taken into consideration, after simulation, some “rule of thumb” design criteria for anaerobic digester, such as digester volume turnover time, mixture diffusion time, and hydraulic retention time can be determined by CFD directly, it save a lot of time and experimental investment.

Odour generated during sludge treatment processes, odour control also could be optimized by CFD, CFD simulation and optimization of heating, ventilating, and air-conditioning (HVAC) system is reported (Kim et al 2001), based on similar principle, odour from sludge treatment or wastewater treatment plant also can be simulated.

*CFD in disinfection*

Rauen (2012) summarized application of CFD in chlorine contact tank, from aspect of hydrodynamics, simulation of chlorine contact tank could be conducted under steady condition or unsteady condition, steady state simulation aim at assess the hydraulic

behavior of a chlorine tank under certain flow rate. Unsteady simulation could study long term effect of chlorine tank, such as daily supply-demand cycle of a service reservoir. Another consideration of chlorine contact tank is soluble transport and chlorine kinetics, soluble transport ability of chlorine contact tank correlated to chlorine-fluid contact, soluble transport governed by advection-diffusion equation, through solve governing equation of soluble transport, Flow Through Curve (FTC) or Residence Time Distribution (RTD) could obtain, then flow pattern and soluble transport could be evaluated.

# Chapter 3 Basic mathematical concepts of CFD

## 3.1 Governing equations

CFD based on basic governing equations of fluid dynamics (Anderson 1995), which is: continuity equation, momentum equation (Navier-Stokes equation) and energy equation. The physical statement of the continuity equation is the mass of a fluid is conserved. The momentum equation (Navier-Stokes equation) denote the change rate of momentum as same as the total forces act on fluid particles, in classical physics, this statement also known as the Newton's second law. The energy equation represent the change rate of energy same with the total heat addition plus the work done on a fluid particle, the energy equation is another statements of the first law of thermodynamics (Malalasekra 2007).

### 3.1.1 Continuity equation

The whole flow domain can be divided into numerous infinitesimal volumes V, which we name these infinitesimal volume control volume. Use $\partial V$ denote the boundary surface of control volume V. According to the physical statement of the continuity equation, mass is conserved in control volume V, so that the mathematical statement of continuity equation is:

Mass flow into a control volume = Mass flow out of a control volume

Obviously, if the density of mass is constant, the total mass in the control volume is controlled by two terms, which is: 1) Source term S, means the total amount of mass in the control volume V. and 2) Flux term F, means flux of mass pass through the boundary surface of control volume $\partial V$. So that the continuity equation can be written as:

$$dS/dt = F$$

The S and F can be denoted in terms of density functions, the density function expressed by two components: space r and time t:

$$S = \int_V \rho \, dV, \ \rho=\rho(r,t)$$

$$F = -\oint_{\partial V} j \cdot n \, d\sigma, \ j=j(r,t)$$

Where ρ is the density, j is the current density, n is the outward unit normal at the boundary surface $\partial V$, dV is the volume of an infinitesimal part of the control volume V, dσ is the area of an infinitesimal part of the boundary surface $\partial V$, j·n denote mass pass through the boundary surface $\partial V$ and flow into or out of the control volume V,

By combine the equation of S and F, we can rewrite the continuity equation on the form:

$$\frac{d}{dt}\left(\int_V \rho \, dV\right) = -\oint_{\partial V} j \cdot n \, d\sigma$$

The equation above is conservation law on integral form. If we assume $\frac{\partial \rho}{\partial t}$ is a

continuous function, the left hand side of conservation law on integral form can be rewritten on the form:

$$\frac{\mathrm{d}}{\mathrm{dt}}(\int_V \rho \, \mathrm{dV}) = \int_V \frac{\partial \rho}{\partial t} \, \mathrm{dV}$$

According to Gauss's theory (Katz, V. J. 1979), we could convert the right hand side of conservation law on integral form from surface intergration $\oint_{\partial V} j \cdot n \, \mathrm{d}\sigma$ into volumetric intergration $\oint_V \nabla \bullet j \mathrm{dV}$. So that the whole conservation law on integral form can be rewritten on the form:

$$\int_V \frac{\partial \rho}{\partial t} + \nabla \bullet j \, \mathrm{dV} = 0$$

Or on the form:

$$\frac{\partial \rho}{\partial t} + \nabla \bullet j = 0$$

### 3.1.2 Momentum equation

The momentum equation derived from the Newton's second law, The forces act on a control volume equals to the rate of change of momentum, in each control volume, if u, v and w is velocity on the x, y and z direction, the rate of increase of momentum on x, y and z direction can be written as $\rho \frac{\mathrm{du}}{\mathrm{dt}}$ ,$\rho \frac{\mathrm{dv}}{\mathrm{dt}}$ and $\rho \frac{\mathrm{dw}}{\mathrm{dt}}$ respectively. There are two types of forces on a control volume, which is body force and surface force, body force means forces acts throughout the control volume, such as gravity force and electromagnetic force, surface force means forces which are exerted to the surface of control volume, such as pressure force and viscous force.

In the following part, we use P denote pressure force, $\tau$ denote viscous forces and S denote body force, to specify direction and location of viscous forces, we use subscript i and j. For example, $\tau_{ij}$ denote that the viscous force acts in the j direction on a surface perpendicular to the i-direction.

In a control volume has length in x, y and z directions are $\partial x$, $\partial y$ and $\partial z$ respectively, the momentum equation on x, y and z direction can be written as:

$$\rho \frac{\mathrm{du}}{\mathrm{dt}} = \frac{\partial(-\mathrm{p} + \tau_{xx})}{\partial x} + \frac{\partial \tau_{yx}}{\partial y} + \frac{\partial \tau_{zx}}{\partial z} + S_x$$

$$\rho \frac{\mathrm{dv}}{\mathrm{dt}} = \frac{\partial(-\mathrm{p} + \tau_{yy})}{\partial y} + \frac{\partial \tau_{xy}}{\partial x} + \frac{\partial \tau_{zy}}{\partial z} + S_y$$

$$\rho \frac{\mathrm{dw}}{\mathrm{dt}} = \frac{\partial(-\mathrm{p} + \tau_{zz})}{\partial z} + \frac{\partial \tau_{xz}}{\partial x} + \frac{\partial \tau_{yz}}{\partial y} + S_z$$

The detailed procedure about how to find above equations can be found in Malalasekra, W.'s book "An introduction to computational fluid dynamics: The finite

volume method" (Malalasekra 2007).

*Navier-stokes equation*

The viscous stress components in the momentum equations are unknown, a suitable model for the viscous stress components should be introduced, one of the most common methods is express the viscous stress components as function of local deformation rate. In three-dimensional flows, the local deformation rate includes the linear deformation rate and the volumetric deformation rate. Assume the fluid is isotropic and Nnewtonian fluid, using s denote the deformation, deformations includes three linear elongating deformations, six linear shearing deformations and volumetric deformations, to specify direction and location of deformations, subscript i and j are introduced.

Then the deformation could be written as (Schlichting and Gersten 2000):

Three linear elongating deformations:

$$s_{xx}=\frac{\partial \mathrm{u}}{\partial \mathrm{x}}$$

$$s_{yy}=\frac{\partial \mathrm{v}}{\partial \mathrm{y}}$$

$$s_{zz}=\frac{\partial \mathrm{w}}{\partial \mathrm{z}}$$

Six linear shearing deformations:

$$s_{xy}=s_{yx}=\frac{1}{2}\left(\frac{\partial \mathrm{u}}{\partial \mathrm{y}}+\frac{\partial \mathrm{v}}{\partial \mathrm{x}}\right)$$

$$s_{xz}=s_{zx}=\frac{1}{2}\left(\frac{\partial \mathrm{u}}{\partial \mathrm{z}}+\frac{\partial \mathrm{w}}{\partial \mathrm{x}}\right)$$

$$s_{yz}=s_{zy}=\frac{1}{2}\left(\frac{\partial \mathrm{v}}{\partial \mathrm{z}}+\frac{\partial \mathrm{w}}{\partial \mathrm{y}}\right)$$

And volumetric deformation:

$$\frac{\partial \mathrm{u}}{\partial \mathrm{x}}+\frac{\partial \mathrm{v}}{\partial \mathrm{y}}+\frac{\partial \mathrm{w}}{\partial \mathrm{z}}=\nabla\bullet\mathrm{U}$$

In Newtonian fluid, the viscous force is proportional to the deformation rate, based on this relationship, we could denote viscous force by deformation, so that the deformation then could be re-written as:

Three linear elongating deformation:

$$\tau_{xx}=2\mu\frac{\partial \mathrm{u}}{\partial \mathrm{x}}+\lambda\bullet\nabla\bullet\mathrm{U}$$

$$\tau_{\mathrm{yy}}=2\mu\frac{\partial \mathrm{v}}{\partial \mathrm{y}}+\lambda\bullet\nabla\bullet\mathrm{U}$$

$$\tau_{\mathrm{zz}}=2\mu\frac{\partial \mathrm{w}}{\partial \mathrm{z}}+\lambda\bullet\nabla\bullet\mathrm{U}$$

Six linear shearing deformation:

$$\tau_{xy}=\tau_{yx}=\mu(\frac{\partial u}{\partial y}+\frac{\partial v}{\partial x})$$

$$\tau_{xz}=\tau_{zx}=\mu(\frac{\partial u}{\partial z}+\frac{\partial w}{\partial x})$$

$$\tau_{yz}=\tau_{zy}=\mu(\frac{\partial v}{\partial z}+\frac{\partial w}{\partial y})$$

Where μ is the first viscosity, it denotes the viscous stresses by linear deformations, and λ is the second viscosity, it relates viscous stresses to the volumetric deformation. If the only body force is gravity, then we can re-write the momentum equation as

$$\frac{d(\rho u)}{dt}+\nabla\bullet(\rho uU)=-\frac{\partial p}{\partial x}+\mu\nabla^2 u+\rho g$$

$$\frac{d(\rho v)}{dt}+\nabla\bullet(\rho vU)=-\frac{\partial p}{\partial x}+\mu\nabla^2 v+\rho g$$

$$\frac{d(\rho w)}{dt}+\nabla\bullet(\rho wU)=-\frac{\partial p}{\partial x}+\mu\nabla^2 w+\rho g$$

Due to heat transfer is not taken into consideration in the following simulation, introduction of the energy equation is neglected in this section.

### 3.2 General components of CFD software

Nowadays commercial CFD software consists of three major modules: 1) pre-processor, 2) solver and 3) post-processor.

*Pre-processor*

Pre-processing include geometry establish and mesh generation. In this step, the aim of pre-processor is establish a computer model based on the really object need to simulate, thereby proper simplification and conceptualization is necessary, not all geometry details from reality need transfer into computer model, professional computer assist design (CAD) software is suggested for complex configurations creation

*Mesh generation*

Mesh generation is the most important procedure in pre-processing, meshing means divide the whole computational zone into a number of small control volumes, these control volumes will used for numerical study according to Finite Volume Method (FVM). Mesh quality as well as configuration of control volumes, could influence solution accuracy and convergence behavior, inappropriate meshing will leads to divergence or poor accuracy of simulation result. Another aspects need to consider during mesh generation is numbers and size of the mesh, larger numbers of control volumes could improve simulation accuracy but increase computing time as well, so in order to get high quality mesh, both solution accuracy and computing time should be taken into consideration.

Mesh spatially separate the whole computational domain, through meshing, the continuous fluid problem in reality transform into a discrete numerical problem in CFD, we name this step discretization, the discrete numerical problems then solved by computer. Three major group of discretization in CFD is: equation discretization, spatial discretization and temporal discretization (Laari 2010).

The most popular equation equation discretization method includes finite differential method (FDM), finite element method (FEM) and finite volume method (FVM). Deng et al (Peyret 1996) reported use finite-difference and finite-volume methods solve Navier-Stokes equations for incompressible flows, as the easiest equation discretization method, FDM is a kind of straightforward method, it employs the Taylor expansion to solve the partial differential equations, the major advantage of FDM is simple and easy to understand, however, due to FDM only works for structured mesh, application of FDM is limited to simple geometry problems, another advantage of FDM is it's algorithm quite similar to FVM, so nowadays FDM usually used to demonstrate numerical solution procedure for educational purpose.

Unlike FDM, FEM could be applied for complex geometry problems, it normally use unstructured mesh, the unstructured mesh divided computational zone into finite numbers of elements, each elements contain several nodes, upon each nodes numerical values could be determined. Although have advantage towards complex geometry problems, the FEM require higher computer power than FDM. Traditionally, FEM usually used in structural engineering, because the mesh structure of FEM similar to geometry structure of bridge, truss structure or beam. Implementation of finite-element methods to solve Navier-Stokes equations for incompressible flows could found in Gunzburger's paper. (Peyret 1996)

FVM is currently the most common equation discretization method employed by commercial CFD software, the FVM method have the advantages of both FDM and FEM. FVM discrete computational zone into finite numbers of control volumes, intergration of governing equations are performance and solved across each control volume, FVM applicable for both structured and unstructured mesh, Grasso et al demonstrate use finite-volume methods solve Euler and Navier-Stokes equations for compressible flows (Peyret 1996).

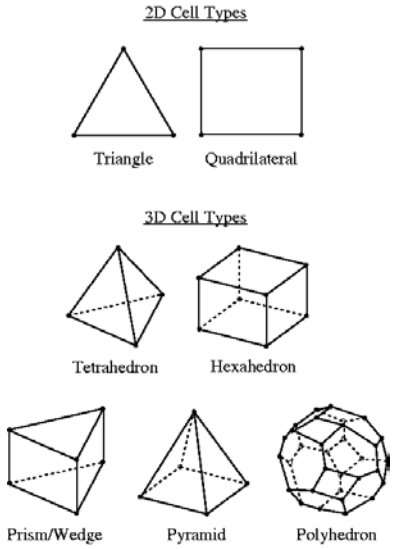


**Figure 3.1** Structured and unstructured mesh (Fluent, I. N. C. 2006)

Spatial discretization aims at divide the whole computational domain into small control volumes, this process also known as meshing. There are two types of mesh in general, structured mesh and unstructured mesh (Fluent,I.N.C. 2006), the structured mesh build on coordinate system, it usually used in simple geometry problems, the quadrilateral mesh and hexahedron mesh in Figure 3.1 is typical structured mesh, however, the structured mesh have very bad performance in complex geometry problems, because complex geometry problems is very common in reality, unstructured mesh is necessary, the pyramid mesh and polyhedron mesh in Figure 3.1 is typical unstructured mesh, in unstructured mesh, control volumes is arranged according to the sharp of the computational domain, so that the unstructured mesh have good performance for complex geometry problems, but it require higher computing cost compare to structured mesh.

Temporal discretization, also known as time discretization, means split the time in fluid problems into separately time steps. Compare to steady solver, transient solver have an additional variable time t, use unsteady solver or transient solver, the simulation could performance with discrete time steps.

After establish geometry model and mesh generation, the next step is defines boundary conditions, boundary conditions now available in common commercial software includes: velocity inlet, outflow, pressure inlet, pressure outlet, symmetric boundary, wall and interface etc. Inappropriate boundary conditions will leads to poor convergence behavior or even di-convergence, or cause inaccurate simulation result. According to mathematical theory of Partial differential equations (PDE), boundary condition could be classified into three groups: Dirichlet boundary condition (the first-type boundary condition), means the values that a solution needs to take on the boundary of computational domain, Neumann boundary condition (the second-type boundary condition), means the derivative of solution is take on the boundary of computational domain, and Cauchy boundary condition (mixed type boundary

condition), means mixture of Dirichlet boundary condition and Neumann boundary condition.

*Solver*

Solver is the most sophisticated part of CFD software, in the solver, user could define governing equations, turbulence models, multi-phase models, species transport and reaction model or more advanced models. Boundary conditions, such as inlet velocity, also need to be defined in this part, after confirm equations need to solve and initial conditions, the next step is define solution methods, such as algorithm for velocity-pressure coupling, as well as solution methods for pressure, convection and diffusion terms, user also could set up the under relaxation factor in order to control convergence behavior. Solver inherit mesh from the pre-processing step.

*Post-processing*

To successfully solve engineering problems with assistance of CFD, post-processing play equal important role as model accuracy (Wu 2012), high quality image which contain necessary information from simulation result is major objective of post-processing. Post-processing usually achieved by display contours of velocity gradient, volume fraction (if use multi-phase simulation) and temperature, direction and speed of flow pattern can be presented by displaying velocity vectors, streamline could indicate flow line or particle tracking behavior. Besides image, simulation result also can be presented by x-y plot, histogram as well as table.

### 3.3 General numerical procedure of FVM

In this section, we demonstrate a compact solution procedure for Navier-stokes equation proposed by Tryggvason in a series of his work (Tryggvason 2001, Prosperetti and Tryggvason 2007, Tryggvason and Scardovelli 2011). We assume it's a two dimension problem, solved by structured rectangular grids in Cartesian coordinate system (Calhoun et al 2008).

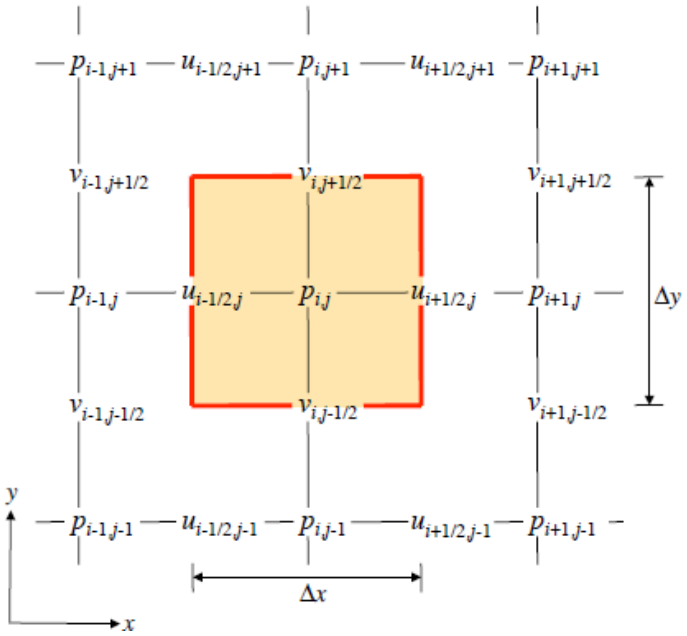


**Figure 3.2** The coordinate system used for numerical calculation (Tryggvason 2012)

The Navier-Stokes equation used for demonstration is written on the form:

$$\rho\frac{\partial \mathrm{u}}{\partial \mathrm{t}} + \rho\nabla \cdot \mathrm{uu} = -\nabla \mathrm{P} + \rho \mathrm{g} + \mu\nabla^2 \mathrm{u}$$

Where $\nabla \cdot \mathrm{uu}$ is the convection term, use C represent it. $\mu\nabla^2 \mathrm{u}$ is the diffusion term, use D represent it. $\nabla \mathrm{P}$ is the pressure equation, use P represent it. u is velocity, $\mu$ is viscosity, t is time, $\rho$ is density of fluid and g is gravity. In order to present the time discretization, use superscript denote u at different time steps, for example, when t=n u=$u^n$, at time t=n+1 u=$u^{n+1}$, $u^*$ is introduced to denote a temporary value of u between t=n and t=n+1.

After divide the the Navier-Stokes equation by density $\rho$ and move the convection term to the right hand side, the left hand side of Navier-stokes equation transformed into $\frac{\partial \mathrm{u}}{\partial \mathrm{t}}$, it could be rewritten according to the concept of time discretization:

$$\frac{\partial \mathrm{u}}{\partial \mathrm{t}} = \frac{u^{n+1} - u^n}{\Delta t}$$

With the introduce of temporary time $u^*$, the whole Navier-stokes equation can be separated into two terms, which is:

$$\frac{u^* - u^n}{\Delta t} = -C^n + \mathrm{g} + \frac{D^n}{\rho^n}$$

And:

$$\frac{u^{n+1} - u^*}{\Delta t} = -\frac{\nabla \mathrm{P}}{\rho^n}$$

According to the conservation of mass equation for incompressible flow, we have:

$$\nabla \cdot u^{n+1} = 0$$

By taking the divergence of the second part of the separated Navier-stokes equation:

$$\nabla\left(\frac{u^{n+1}-u^{*}}{\Delta t}\right)=\nabla\left(-\frac{\nabla \mathrm{P}}{\rho^{n}}\right)$$

We could conclude that:

$$\frac{\nabla \cdot u^{*}}{\Delta t}=\frac{\nabla^{2} \mathrm{P}}{\rho^{n}}$$

Then we could performance conservation principle to a control volume use FVM, in order to obtain numerical approximation of convection, diffusion and pressure term, we performance volume integral to a control volume. In a two dimensional structured Cartesian coordinate system proposed by Tryggvason in figure 3.2, a control volume with length $\Delta$ x and width $\Delta$ y, the velocity on x direction is u and on y direction is v, the velocity information of u and v storage on the vertical boundary and horizontal boundary of the control volume respectively, the pressure information P storage in the center of the control volume, subscript i and j denote position of u, v and P in the coordinate system.

With above mentioned rules and transformations, the first part of the separated Navier-stokes equation ($\frac{u^{*}-u^{n}}{\Delta t}=-C^{n}+\mathrm{g}+\frac{D^{n}}{\rho^{n}}$), can be rewritten on the following form:

For the x component:

$$\frac{u^{*}_{i+\frac{1}{2},j}-u^{n}_{i+\frac{1}{2},j}}{\Delta t}=-(C_x)^{n}_{i+\frac{1}{2},j}+(g_x)^{n}_{i+\frac{1}{2},j}+\frac{2}{\rho^{n}_{i+1,j}+\rho^{n}_{i,j}}(D_x)^{n}_{i+\frac{1}{2},j}$$

And for the y component:

$$\frac{v^{*}_{i,j+\frac{1}{2}}-v^{n}_{i,j+\frac{1}{2}}}{\Delta t}=-(C_y)^{n}_{i,j+\frac{1}{2}}+(g_y)^{n}_{i,j+\frac{1}{2}}+\frac{2}{\rho^{n}_{i+1,j}+\rho^{n}_{i,j}}(D_y)^{n}_{i,j+\frac{1}{2}}$$

### 3.3.1 Convection term

To performance the spatial discretization, for the convection term, according to Gauss's theory, we can write the volume integral in form of surface integral:

$$C=\frac{1}{V}\int_{V}\nabla \cdot uu\,dV=\frac{1}{V}\oint_{S}u(u\cdot n)\,dS$$

According to above-mentioned coordinate system and theory of FVM, at time t=n, for the x component the convection term can be written as:

$$(C_x)_{i+\frac{1}{2},j}=\frac{(uu)_{i+1,j}-(uu)_{i,j}}{\Delta x}+\frac{(uv)_{i+\frac{1}{2},j+\frac{1}{2}}-(uv)_{i+\frac{1}{2},j-\frac{1}{2}}}{\Delta y}$$

For the y component:

$$(C_y)_{i,j+\frac{1}{2}}=\frac{(vv)_{i,j+1}-(vv)_{i,j}}{\Delta y}+\frac{(uv)_{i+\frac{1}{2},j+\frac{1}{2}}-(uv)_{i-\frac{1}{2},j+\frac{1}{2}}}{\Delta x}$$

### 3.3.2 Diffusion term

Based on same principle, the spatial discretization of diffusion term is:

$$D = \frac{\mu}{\rho}\int_V \nabla^2 u \, dV = \frac{\mu}{V}\oint_S \nabla u \cdot n \, dS$$

For the x component:

$$(D_x)_{\frac{i+1}{2},j} = \mu[\frac{(\frac{\partial u}{\partial x})_{i+1,j} - (\frac{\partial u}{\partial x})_{i,j}}{\Delta x} + \frac{(\frac{\partial u}{\partial y})_{\frac{i+1}{2},\frac{j+1}{2}} - (\frac{\partial u}{\partial y})_{\frac{i+1}{2},\frac{j-1}{2}}}{\Delta y}]$$

For the y component:

$$(D_y)_{i,\frac{j+1}{2}} = \mu[\frac{(\frac{\partial v}{\partial y})_{i,j+1} - (\frac{\partial v}{\partial y})_{i,j}}{\Delta y} + \frac{(\frac{\partial v}{\partial x})_{\frac{i+1}{2},\frac{j+1}{2}} - (\frac{\partial v}{\partial x})_{\frac{i-1}{2},\frac{j+1}{2}}}{\Delta x}]$$

### 3.3.3 Pressure equation

The spatial discretization form of pressure term is:

$$P = \frac{1}{V}\int_V \nabla p \, dV = \frac{1}{V}\oint_S p \cdot n \, dS$$

Based on above mentioned discrete mass conservation equation:

$$\nabla \cdot u^{n+1} = 0$$

The spatial discretization is written on the form:

$$\frac{u^{n+1}_{\frac{i+1}{2},j} - u^{n+1}_{\frac{i-1}{2},j}}{\Delta x} + \frac{v^{n+1}_{i,\frac{j+1}{2}} - v^{n+1}_{i,\frac{j-1}{2}}}{\Delta y} = 0$$

Based on same method, the corrected velocity equation:

$$\frac{u^{n+1} - u^*}{\Delta t} = -\frac{\nabla P}{\rho^n}$$

Can be re-written on the following form:

For the x component:

$$\frac{u^{n+1}_{\frac{i+1}{2},j} - u^*_{\frac{i+1}{2},j}}{\Delta t} = -\frac{2}{\rho^n_{i+1,j} + \rho^n_{i,j}}\frac{P_{i+1,j} - P_{i,j}}{\Delta x}$$

For the y component:

$$\frac{v^{n+1}_{i,\frac{j+1}{2}} - v^*_{i,\frac{j+1}{2}}}{\Delta t} = -\frac{2}{\rho^n_{i,j+1} + \rho^n_{i,j}}\frac{P_{i,j+1} - P_{i,j}}{\Delta y}$$

Substituting the spatial discretization expression of the corrected velocity equation into the discrete mass conservation equation, the pressure equation transformed into:

$$(\frac{P_{i+1,j} - P_{i,j}}{\rho^n_{i+1,j} + \rho^n_{i,j}} - \frac{P_{i,j} - P_{i-1,j}}{\rho^n_{i,j} + \rho^n_{i-1,j}})\frac{1}{\Delta x^2} + (\frac{P_{i,j+1} - P_{i,j}}{\rho^n_{i,j+1} + \rho^n_{i,j}} - \frac{P_{i,j} - P_{i,j-1}}{\rho^n_{i,j} + \rho^n_{i,j-1}})\frac{1}{\Delta y^2} = \frac{1}{2\Delta t}(\frac{u^*_{\frac{i+1}{2},j} - u^*_{\frac{i-1}{2},j}}{\Delta x} + \frac{v^*_{i,\frac{j+1}{2}} - v^*_{i,\frac{j-1}{2}}}{\Delta y})$$

Find solution for the pressure equation is the most difficult part in Direct numerical simulation (DNS) of CFD, advanced pressure solver is introduced in order to achieve reasonable computation. In the following part of this paper, one of the most common algorithm for the pressure term, SIMPLE (Semi-Implicit Method for Pressure Linked Equations) algorithm, will be introduced.

### 3.4 Some important concepts in commercial CFD software

*SIMPLE algorithm*

After discretization, a series of algebraic equations need to be solved simultaneously in every control volumes, SIMPLE (Semi-Implicit Method for Pressure Linked Equations) algorithm is the most popular CFD solution procedure, it developed by Patankar and Spalding (1972) in 1972. For a three dimensional problem, four equations need to be solved, includes Navier-Stokes equation in three directions and one continuity equation. There are four unknown values in the four governing equations: three velocity components in the Navier-Stokes equation at three directions and the pressure. Pressure term is the most time consuming and complex step in CFD solution procedure, because the pressure doesn't have its own explicit equation, special techniques have been devised to extract the pressure term. Currently SIMPLE algorithm is the best known technique for solving the pressure term, in order to implement the SIMPLE algorithm, firstly a guessed pressure field is used to solve the Navier-stokes equations, based on the guessed pressure field, a new velocity can be computed, however, the velocity calculated by the guessed field will not satisfy the continuity equation, so the velocity correction value can be confirmed, based on the velocity correction value, pressure correction also can be determined, the pressure correction then added to the original guessed pressure field, at last, the pressure field updated and remaining unknowns is solved, one iteration is completed. Then in the next iteration above algorithm is repeated.

*Residuals*

Residuals are the differences in the value between two iterations. As we can see from the SIMPLE algorithm, initially, the solution of Navier-stokes equations based on a guessed pressure field, in each steps, the solution of governing equations based on inexact solution from the previous iteration, through repeated iterations, the solution of governing equations refined. Residuals depend from the models and initialization, because residuals related to mathematical convergence, so that during calculating process, residuals should be monitored in order to evaluate the convergence behavior.

*Convergence criteria*

During iterative solution of governing equations, when the residuals decrease to preset level, the solution is regarded as converged, this preset condition for the residuals known as the convergence criteria. The default convergence criteria in Fluent is $10^{-4}$, we use this default value as convergence criteria in this study.

*Under relaxation*

With the governing equations solved iteratively, in each step, the initial value used in current step based on the information from previous iteration, during this process, small difference added to the old values of variable in the previous iteration, generate a new value. When several coupled equations are solved, only a fraction of computed difference is used rather than use the full computed difference, this process is known

as under relaxation, the under relaxation factors decided how much fraction of the computed difference is used, the under relaxation factors varies from 0.1 to 1.0, through adjust under relaxation factors, the convergence behavior of governing equations can be controlled, in general, lower under relaxation factor give stable but slower convergence process.

# Chapter 4 Turbulence models

When the Reynolds number below the critical Reynolds number, flow is smooth, under this condition we name the flow laminar flow. When fluid velocity increase, the Reynolds number will surpass the critical Reynolds number, under this kind of situation, each separated adjacent flow slides will mixing with each other, the main flow properties become chaotic and unsteady, we name this kind of flow turbulent flow.

In reality, most flow is turbulent flow, turbulent model is necessary in fluid dynamics simulation. Currently numerical solution for turbulent flow include: Direct Numerical Simulation (DNS), Reynolds-averaged Navier-Stokes (RANS) and Large Eddy Simulation (LES) (Ferziger and Perić 1996).

## 4.1 Direct numerical simulation (DNS)

DNS solve Navier-stokes equation numerically according to FVM, FEM or FDM, DNS doesn't employ any turbulence models. Because solve equations numerically, the solution of DNS is very accurate, however, it require high computing time, so currently DNS research mainly focus on low Reynolds number flow, in pure mathematic field, DNS can be used to verify turbulence models.

## 4.2 Reynolds-averaged Navier-Stokes (RANS)

In general, the turbulence model can be classified into first order models and second order models, first order models include zero-equation model, one-equation model and two-equation model, second order equation include algebraic stress model and Reynolds stress model. Many turbulence models based on the Boussinesq Hypothesis: turbulence is proportional to the mean rate of deformation, and Reynolds stresses can be linked with the mean rate of deformation. This hypothesis proposed by Boussinesq in 1877 (Schmitt 2007).

For incompressible and Newtonian flow, the continuity equation and Navier-stokes equation can be written as:

$$\frac{\partial u_i}{\partial x_j} = 0$$

$$u_j \frac{\partial u_i}{\partial x_j} = f_i - \frac{1}{\rho}\frac{\partial P}{\partial x_j} + \mu \nabla^2 u_i$$

Where u is velocity, f is body force, P is pressure, i,j denote the x and y direction respectively. Reynolds-averaged methods denote every instantaneous value by two terms, a steady mean value and a time dependent mean value. For example:

$$u_i = \overline{u_i} + u_i'$$

$$P_i = \overline{p_i} + p_i'$$

Substitute above equations into original Navier-Stokes equation and continuity equation, we can derive Navier-Stokes equation and continuity equation under turbulence situation:

$$u_j \frac{\partial u_i}{\partial x_j} = \frac{1}{\rho} \frac{\partial}{\partial x_j} (\sum_{ij} \overline{\rho u_i' u_j'})$$

The Reynold's stress tensor is defined as:

$$\tau_{ij} = -\overline{\rho u_i' u_j'}$$

The Reynold's stress tensor can be denoted in form of:

$$\tau_{ij} = -\overline{\rho u_i' u_j'} = \mu_t [\frac{\partial U_i}{\partial x_j} + \frac{\partial U_j}{\partial x_i}] + \frac{2}{3} \rho k \delta_{ij}$$

Where $k = \frac{1}{2}(\overline{u'^2} + \overline{v'^2} + \overline{w'^2})$, $\delta$ is Kronecker delta, $\mu_t$ is eddy viscosity, it depends on the flow, after transformation, we could turn Reynold's stress tensor problem into how to find the eddy viscosity $\mu_t$. The detailed derivation of RANS is available in papers of Biswas and Wilcox (2002).

### 4.2.1 Zero equation model

The earliest turbulence model is Zero Equation Model or Mixing Length Model, this model use velocity scale and length scale to define the eddy viscosity (Wilcox 1998).

$$\mu_t = \rho l_m^2 [\frac{\partial u_i}{\partial x_j} + \frac{\partial u_j}{\partial x_i}]$$

Where $l_m$ is mixing length, this value need to be determined by experiment. The zero equation model is very simple, for simple flows where the mixing length can be tested by experiments, this model have good performance. But the concept of mixing length doesn't consider diffusion and convection of the turbulence, and the mixing length is difficult to confirm under complex processes. So nowadays this model ignored in commercial CFD software.

### 4.2.2 One equation model (The Spalart-Allmaras)

The one equation model based on zero equation model, the turbulent eddy viscosity is given by:

$$\mu_t = l_m \sqrt{k}$$

The mixing length also determined by experiments. The one equation model is economic and accurate for flow with gentle separation and circulation.

### 4.2.3 Two equations models

The above mentioned eddy-viscosity stress-strain relationship, in addition to equations for turbulent kinetic energy k and dissipation ε, forms the two equation k-ε model. Two equations k-ε models firstly proposed by Jones and Launder (1972) in 1972, it's the most popular turbulence model, in ANSYS-Fluent, there are three types two equations k-ε models, namely standard k-ε model, Re-Normalisation Group (RNG) k-ε model and Realisable k-ε model (Launder and Sharma 1974).

*Standard k-ε model*

The standard k-ε model contain two equations, the turbulence kinetic energy equation k and the dissipation equation $\varepsilon$. In equation for kinetic energy k, we correlate fluctuation terms and the mean flow according to Boussinesq assumption. If we multiplying the k equation by (ε/k) and introducing model constants, then we could derive dissipation equations for ε.

For turbulence kinetic energy k:

$$\frac{\partial(\rho k)}{\partial t} + \frac{\partial(\rho k u_i)}{\partial x_i} = \frac{\partial}{\partial x_j}\left[(\mu + \frac{\mu_t}{\sigma_k})\frac{\partial k}{\partial x_j}\right] + P_k + P_b - \rho\varepsilon - Y_M + S_k$$

For dissipation $\varepsilon$:

$$\frac{\partial(\rho\varepsilon)}{\partial t} + \frac{\partial(\rho\varepsilon u_i)}{\partial x_i} = \frac{\partial}{\partial x_j}\left[(\mu + \frac{\mu_t}{\sigma_\varepsilon})\frac{\partial \varepsilon}{\partial x_j}\right] + C_{1\varepsilon}\frac{\varepsilon}{k}(P_k + C_{3\varepsilon}P_b) - C_{2\varepsilon}\rho\frac{\varepsilon^2}{k} + S_\varepsilon$$

The turbulent viscosity is:

$$\mu_t = C_\mu \rho \frac{k^2}{\varepsilon}$$

Where $P_k$ is production of k:

$$P_k = -\overline{\rho u_i' u_j'}\frac{\partial u_i}{\partial x_j}$$

$P_b$ is effect of buoyancy. $C_{1\varepsilon}$, $C_{2\varepsilon}$ and $C_{3\varepsilon}$ are constants, $\sigma_k$ and $\sigma_\varepsilon$ are prandtl numbers.

Currently, k-ε model is the most widely applied turbulence model, it's easier to

implement in most cases and have good convergence behavior, however, for flow with strong separation, swirling and rotating, the drawbacks of standard k-ε model is apparent. To improve shortcomings of standard k-ε model, modified k-ε model is proposed.

*RNG k-ε model*

RNG k-ε model developed by Yakhot et al (1992) in 1992, Yakhot use Re-Normalisation Group (RNG) methods (a kind of rigorous statistical technique) renormalised the Navier-Stokes equations, derived a turbulence model similar to the standard k-ε model. RNG k-ε model similar to the standard k-ε model, it has an additional term for interaction between turbulence dissipation and mean shear in ε equation. The effect of swirl, Prandtl number and effective viscosity also took into consideration in RNG k-ε model. The RNG k-ε model has better performance for flow with strong swirl and time dependent flow with large scale motions.

The kinetic energy equation of RNG k-ε model is:

$$\frac{\partial(\rho k)}{\partial t} + \frac{\partial(\rho k u_i)}{\partial x_i} = \frac{\partial}{\partial x_j}[(\mu + \frac{\mu_t}{\sigma_k})\frac{\partial k}{\partial x_j}] + P_k - \rho\varepsilon$$

The dissipation equation of RNG k-ε model is:

$$\frac{\partial(\rho\varepsilon)}{\partial t} + \frac{\partial(\rho\varepsilon u_i)}{\partial x_i} = \frac{\partial}{\partial x_j}[(\mu + \frac{\mu_t}{\sigma_\varepsilon})\frac{\partial \varepsilon}{\partial x_j}] + C_{1\varepsilon}\frac{\varepsilon}{k}P_k - C_{2\varepsilon}^{*}\rho\frac{\varepsilon^2}{k}$$

Where $\sigma_k, \sigma_\varepsilon, C_{1\varepsilon}, C_{2\varepsilon}^{*}$ are constants.

*Realisable k-ε model*

Realisable k-ε model have turbulence kinetic energy equation same with the standard k-ε model, it improved the equation for ε, use a variable $C_\mu$ replace the constant, it have better performance for flow with strong separation and recirculation.

In Realisable k-ε model, the turbulence kinetic energy equation is:

$$\frac{\partial(\rho k)}{\partial t} + \frac{\partial(\rho k u_i)}{\partial x_i} = \frac{\partial}{\partial x_j}[(\mu + \frac{\mu_t}{\sigma_k})\frac{\partial k}{\partial x_j}] + P_k + P_b - \rho\varepsilon - Y_M + S_k$$

The dissipation equation is:

$$\frac{\partial(\rho\varepsilon)}{\partial t} + \frac{\partial(\rho\varepsilon u_i)}{\partial x_i} = \frac{\partial}{\partial x_j}[(\mu + \frac{\mu_t}{\sigma_\varepsilon})\frac{\partial\varepsilon}{\partial x_j}]$$
$$+ \rho C_1 S\varepsilon - \rho C_2 \frac{\varepsilon^2}{k + \sqrt{\nu\varepsilon}} + C_{1\varepsilon}\frac{\varepsilon}{k} C_{3\varepsilon} P_b + S_\varepsilon$$

Where $P_k$ is generation of turbulence kinetic energy due to the mean velocity gradients, $P_b$ is the generation of turbulence kinetic energy due to buoyancy and $\mu_t$ is turbulent viscosity. $C_{1\varepsilon}, C_2$, $\sigma_\varepsilon$ and $\sigma_k$ are constant.

*Standard k-ω model*

The standard k-ω model developed by Wilcox et al (1988) in 1988. In k-ω model, ω represent an inverse time scale, it associated with the turbulence. This model consist of a modified turbulent kinetic energy equation, and a transport equation for ω,

In the k-ω model , the Kinematic eddy viscosity calculated as follow:

$$\nu_T = \frac{k}{\omega}$$

Turbulence kinetic energy equation k:

$$\frac{\partial(k)}{\partial t} + U_j \frac{\partial(k)}{\partial x_j} = \tau_{i,j}\frac{\partial U_i}{\partial x_j} - \beta^* k\omega$$
$$+ \frac{\partial}{\partial x_j}[(\nu + \sigma^*\nu_T)\frac{\partial k}{\partial x_j}]$$

Specific dissipation rate equation ω:

$$\frac{\partial(\omega)}{\partial t} + U_j \frac{\partial(\omega)}{\partial x_j} = \alpha\frac{\omega}{k}\tau_{i,j}\frac{\partial U_i}{\partial x_j} - \beta\omega^2$$
$$+ \frac{\partial}{\partial x_j}[(\nu + \sigma\nu_T)\frac{\partial\omega}{\partial x_j}]$$

Where $\beta^*, \alpha, \beta, \sigma^*$ and $\sigma$ are constants.

*Shear Stress Transport (SST) k-ω model*

The Shear Stress Transport (SST) k-ω model developed by Menter et al (1994) in 1994, SST k-ω model is an eddy-viscosity model, it is combination of two different kinds of turbulence models, in region close to the inner boundary layer, it use k-ω model, while outside the boundary layer, it switch to k-ε model.

The SST k-ω model contain following equations.
Kinematic eddy viscosity:

$$\nu_T = \frac{a_1 k}{\max(a_1\omega, SF_2)}$$

Turbulence kinetic energy equation:

$$\frac{\partial(k)}{\partial t} + U_j \frac{\partial(k)}{\partial x_j} = P_k - \beta^* k\omega$$
$$+ \frac{\partial}{\partial x_j}[(\nu + \sigma_k \nu_T)\frac{\partial k}{\partial x_j}]$$

Specific dissipation rate equation:

$$\frac{\partial(\omega)}{\partial t} + U_j \frac{\partial(\omega)}{\partial x_j} = \alpha S^2 - \beta\omega^2$$
$$+ \frac{\partial}{\partial x_j}[(\nu + \sigma_w \nu_T)\frac{\partial \omega}{\partial x_j}] + 2(1 - F_1)\sigma_{\omega^2}\frac{1}{\omega}\frac{\partial k}{\partial x_j}\frac{\partial \omega}{\partial x_j}$$

Where $F_1$ is blending function, $F_2$ is the second blending function, $P_k$ is the production limiter, it is used in the SST model to prevent the build-up of turbulence in stagnation regions, $\beta^*, \sigma_k, \alpha, \beta, \sigma_w$ and $\sigma_{\omega^2}$ are constants.

### 4.2.4 Reynolds stress model (RSM)

Through solving additional transport equations for six independent Reynolds stresses, the RSM close the RANS equations, RSM could predict complex flows accurately, such as swirling flow, strong circulation flow and separation flow.

Expression for the Reynolds stress model is:

$$\frac{DR_{ij}}{Dt} = P_{ij} + D_{ij} + \varepsilon_{ij}$$
$$+ \Pi_{ij} + \Omega_{ij}$$

Where $R_{ij}$ is individual Reynolds stresses, $P_{ij}$ is rate of production, $D_{ij}$ is transport by diffusion, $\varepsilon_{ij}$ is rate of dissipation, $\Pi_{ij}$ is transport due to turbulent pressure-strain interactions and $\Omega_{ij}$ is transport due to rotation. Detailed information about RSM is out the scope of this paper but available in articles of Launder et al (1975).

## 4.3 Large Eddy Simulation (LES)

Large Eddy Simulation (LES) is more accurate but more time consuming than RANS, it can work on large Reynolds numbers and complex flows (You and Moin 2007, Huang and Li 2010). LES based on the theory that large scale eddied are dependent on the geometry, while small scale eddied almost same everywhere in the flow, so that

large scale eddied could solve explicitly and small eddies could calculated implicitly. According to sub-grid scale theory, velocity field could separate into two components, the resolved part and the sub-grid part, which represent large eddies and small eddies respectively. Detailed demonstration of LES is out the scope of this research.

# Chapter 5 Species transport and reaction model

## 5.1 Residence time distribution (RTD)

The Residence Time Distribution (RTD) is one of the most important parameters in reactor design, in the real world, performance of reactors often very different from what we expected, we name these reactors “non-ideal reactor”, the distribution of residence time is a very important method in non-ideal reactor analysis (Fogler 1999). residence time indicates the time spent by fluids in the reactor, RTD usually measured by using tracer test, in order to performance tracer test, certain amount of tracer is injected into inlet of the reactor, concentration of tracer then monitored at the outlet and plot versus time, this kind of drawing namely flow through curve (FTC) or residence time distribution (RTD). The RTD curve can be used to detect potential failures such as dead zone, re-circulation current or bypass. In addition to tracer test, CFD supplies an alternative and simpler method of determining the RTD.

## 5.2 Species transport model

In CFD, RTD can be obtained through two models: the Discrete phase model (DPM) or the species transport model (Bridgeman et al 2009). The DPM performance Lagrangian particle tracking firstly, then analyze discrete phase or discrete particles to get the RTD curve. The DPM require track and analyze large numbers of particles, so it dramatically increase computational time. An alternative of RTD simulation in CFD is treat the tracer as a continuum, by solving the transport equation for the tracer, RTD is obtained:

The transport equation is:

$$\frac{\partial(\rho Y_i)}{\partial t} + \frac{\partial(\rho u_j Y_i)}{\partial x_j} = \frac{\partial}{\partial x_j}[\rho D_i \frac{\partial Y_i}{\partial x_j}] + R_i + S_i$$

Where $Y_i$ is mass fraction of chemical species i, $u_j$ is the velocity, $D_i$ is the diffusion coefficient, $R_i$ is the reaction source term and $S_i$ is other source term. Physical statement of species transport model is: the rate of change and net rate of flow (convection) equal to sum of the rate of change due to diffusion, rate of change due to reaction sources and rate of change due to other sources.


a

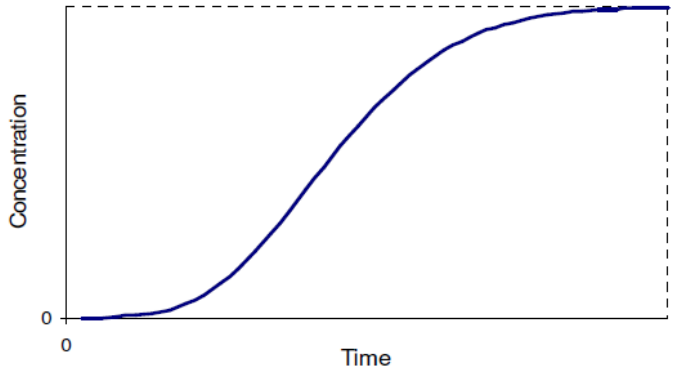


b

**Figure 5.1** Two types of Residence Time Distribution (RTD) curve

There are two major approaches to determine the RTD: pulse approach and step approach, pulse approach start inject tracer into inlet at time t=0, and stop tracer injection after the first time step, in the step approach, the tracer injection species will be maintained over the first time step and subsequent time steps. Figure 5.1 (a) displayed the pulse approach RTD curve, it also called the “E” type RTD curve, Figure 5.1 (b) is the step approach RTD curve or the “F” type RTD curve.

Traditional water process tank design based on assumption of ideal flow pattern, real hydrodynamics characteristics are not take into account, for example, “plug flow” pattern are employed for chlorine contact tank and sedimentation tank design, while “completely mixing” pattern are used for design of chemical or biological reactor with mixing (Stamou 2008). In this study, in addition to determine the RTD curve by CFD approach, the RTD curve analysis will be combined with velocity distribution plot analysis, the combined analysis will give a better understanding about fluid dynamics in the reactors.

# Chapter 6 Multi-phase models

In reality, most of flows are multi-phase flow, multi-phase model is necessary in order to study the multi-phase flow. Currently, multi-phase models available in commercial CFD software can be divided into two major groups: the Lagrangian multi-phase model and the Eulerian multi-phase models. In this chapter, major multi-phase models which employed by current mainstream CFD software and their applications will be introduced.

## 6.1 Lagrangian approach

Lagrangian multi-phase model also name discrete phase model (DPM), it suitable for fluids which contain a continuous phase and a dispersed phase, the primary phase or the continuous phase can be gas or liquid while the secondary phase can be particles, bubbles or liquid drops, the volume fraction of the discrete phase should below 10%. Lagrangian multi-phase model or discrete phase model calculate each particles individually, so Lagrangian multi-phase model require higher computer power and more time consuming.

In DPM, the continuous phase is solved by using transport equations (Buwa et al 2006). The discrete phase is simulated in Lagrangian reference frame, commercial CFD software anticipate the trajectory of discrete particle, as well as heat and mass transfer to or from the discrete phase, by integrating the balance on the particle, particle stream which could stand for the disperse phase is selected and calculated, with a series of conservation, momentum and energy equation are solved, the state of each particle stream can be confirmed.

In Lagrangian reference frame. The force balance on a particle is intergrated, so that behavior of individual particle can be tracked. In a Cartesian coordinate system, equating particle inertia with force acting on this particle, can be written as:

$$\frac{du_p}{dt} = F_D(u - u_p) + \frac{g_x(\rho_p - \rho)}{\rho_p} + F_x$$

Where u is the fluid phase velocity, $u_p$ is the particle velocity, $\rho$ is the fluid density, $\rho_\rho$ is the density of the particle and $F_x$ is an additional acceleration term, $F_D(u - u_p)$ is the drag force per unit particle mass and

$$F_D = \frac{18\mu}{\rho_P d_p^2}\frac{C_D \mathrm{Re}}{24}$$

Where $d_p$ is the diameter, Re is the relative Reynolds number, which is defined as：

$$\mathrm{Re} = \frac{\rho d_p \left| u_p - u \right|}{\mu}$$

After calculate the primary phase and the dispersed phase, two phase coupling can be achieved by calculate interaction terms in the continuous-phase equations. This model applicable when volume fraction of dispersed phase is low (usually require less than 10%), and the discrete phase is injected into primary phase.

To apply DPM in commercial CFD software for steady state problems, the continuous flow phase should be solved firstly, then the discrete phase injector is created, inject the discrete phase into continuous phase and calculate the continuous-discrete phase coupling, so that the particle behavior can be tracked. For transient problems, discrete phase injector should be created before initialize the flow field, particle state and position will update when simulation on going.

Goula et al (2008) studied particle transport for different particle sizes in full-scale sedimentation tanks of potable water treatment with DPM. In his work, the range of the suspended solids was divided into 13 classes based on the experimental data, the simulation firstly solved in absent of particles, after steady state flow field was achieved, several injectors was created, these injectors at same place: the inlet, but with different particle density and particle size, particles released from inlet into sedimentation tank and tracked. Each time particle tracking performance towards one class size, size and density is determined by injectors defined in the previous step, so that the trajectory of particles with different size in steady flow field can be detected.

### 6.2 Eulerian approaches

Eulerian multi-phase model include three major models:

- Volume of Fluid (VOF) Model
- Eulerian Model
- Mixture Model.

Eulerian model is one the most common multi-phase models, compare to Lagrangian approach, Eulerian model require less CPU time in general. Based on interpenetrating continua theory, all phases in the multi-phase flow are governed by the Navier-Stokes equation, co-existed in the same volume, interacted with each other in space and exchange mass, momentum and energy. Physical parameters, such as velocity, energy and volume fraction of each phase are described individually in Eulerian model (ANSYS Inc. 2009).

#### 6.2.1 VOF model

The VOF model is suitable for free surface flow study, this model could model two or more immiscible fluids, the immiscible fluids simulated by solving momentum equations and tracking volume fraction in the whole computational domain. VOF model simulate motion of phases by solve transport equations, and treat interface of

phases via jump boundary condition (Delnoij et al 1998). However, this model can't simulate species mixing and reacting, generally, it mainly applied in gas-liquid two phase simulation, such as the motion of large bubbles in a liquid, dam break, and liquid-gas interface.

According to VOF model theory, besides calculation in each control volume, it regard volume fraction of each phases as a whole, it based on the assumption that all phases couldn't penetrate into each other. All variables field and property field of fluid, is treated by volume averaging method and share between each phases. With one more phases add into model, the volume fraction of the phase in the computational cell for each added phases is included as a variable, so in every control volume, the variables and properties are either purely represented by one of the phases, or represented by a mixture of the phases, depending upon the volume fraction values. If in control volume for fluid q, the volume fraction of the phase is denoted by $\alpha_q$, then we have the following three situations:

$\alpha_q$=0: Volume fraction of the fluid q is 0

$\alpha_q$=1: Volume fraction of the fluid q is 1

$0<\alpha_q<1$: Fluid q mixed with other fluid

Track interface between phases can be validated via get solution of a continuity equation for the volume fraction of the phases, the continuity equation for fluid q can be written as:

$$\frac{\partial \alpha_q}{\partial t} + \vec{v} \cdot \nabla \alpha_q = \frac{S\alpha_q}{\rho q}$$

This volume fraction equation can't give solution for the primary phase, but the primary phase volume fraction can be obtained by following constrain:

$$\sum_{q=1}^{N} \alpha_q = 1$$

In VOF model, a single set of momentum equation is solved and applied over the whole computational zone, the velocity field is same among all the phases, because density ρ and viscosity μ in the momentum equation, the momentum equation decided by volume fraction of all phases.

$$\frac{\partial}{\partial t}(\rho\vec{v}) + \nabla \cdot (\rho\vec{v}\vec{v}) = -\nabla\rho + \nabla \cdot [\mu(\nabla\vec{v} + \nabla\vec{v}^{-T})] + \rho\vec{g} + \vec{F}$$

According to control-volume formulation used by commercial CFD software, convection and diffusion flux through faces of control volume computed in the control volume and balanced with source term, calculation of face flux could enable via the following four schemes:

- Geometric reconstruction scheme
- Donor-acceptor scheme
- Euler explicit scheme

•Implicit scheme

Both Geometric reconstruction scheme and Donor-acceptor scheme performance special treatment to the boundary cell which locate near the interface of two phases. While the Euler explicit scheme and the implicit scheme assume boundary cell filled with one phase or the other. Here Geometric reconstruction scheme and Donor-acceptor scheme will be described.

In geometric reconstruction scheme, when fluid is filled only one phases, the standard interpolation scheme for wall flux calculation is used, geometric reconstruction scheme is used for control volume which near the interface. Geometric reconstruction scheme use piecewise-linear approach treat interface of two phases, within each control volume, interface is transformed into linear sharp boundary with linear slope, wall flux in this control volume then calculated according to the linear sharp interface, it similar to computational method used for unstructured mesh.

Based on volume fraction of each phases, position of linear interface could be confirmed, it relevant to center of each part of the control volume, which filled with one phases in each part. Advection of each phases pass through faces could be calculated according to computed velocity distribution on the interface. Then according to balance of face flux calculated, the volume fraction of each cell could be found.

Similar to geometric reconstruction scheme, standard interpolation scheme is used towards cell filled with one phase, amount of fluid advected through the face is determined on the interface use donor-acceptor scheme. In donor-acceptor scheme, the “donor” donate an amount of fluids in one phase, and the neighboring “acceptor” cell receive same amount of fluids from the “donor”, the direction of the interface then either horizontal or vertical, and used to determine face flux, according to direction of interface and other values such as motion, flux value could obtained by up-winding method, down-winding method or combine two methods together.

Shahrokhi et al (2012) studied the influence of different baffle position on setting effect by using VOF model, in his work, VOF method is used to define suitable boundary condition for free surface, compare to fixed surface flow, VOF have better performance in terms of calculating free surface, VOF method define volume of fluid in each discretized control volume, combine with the Fractional Area/Volume Obstacle Representation (FAVOR), solves unsteady state Navier–Stokes equations. FAVOR method enable using structured mesh, since VOF method ignore motion in the surrounding air, computational time is reduced. In order to verify simulation result, values of dimensionless x and z direction velocity are measured and calibrated with simulation result, although a 2-dimensional model is simulated for simplification purpose and experiments performance in 3-dimensional tank, the simulation result still representative and present good agreement.

### 6.2.2 Eulerian model

When using Eulerian model, the multi-phases can be solid, liquid, gas or any combination, Eulerian model could simulate large numbers of secondary phases, only the computer memory space could limit numbers of the secondary phases. Eulerian model solve momentum and continuity equations for each phase, and single pressure is same in every phases, it have variable interphase drag coefficient functions. However, when using Eulerian model, only k-ε turbulence model is available, particle tracking interaction only happened with the primary phase. Eulerian model use phasic volume fractions describe multiphase flow as an interpenetrating continua, here we use $\alpha_q$ represent it. Volume fraction indicates how much space occupied by each phase, governing equation such as continuity equation and Navier-Stokes equation should satisfied by each individual phase.

Volume fraction $V_q$ defined as:

$$V_q = \int_V \alpha_q dV$$

Sum volume fraction of each phase should equal to 1.

$$\sum_{q=1}^{N} \alpha_q = 1$$

Effective density of phase q is:

$$\hat{\rho}_q = \alpha_q \rho_q$$

Where $\rho_q$ represent density of phase q.
Continuity equation for phase q is:

$$\frac{\partial}{\partial t}(\alpha_q \rho_q) + \nabla \cdot (\alpha_q \rho_q \vec{v}_q) = \sum_{p=1}^{n} \dot{m}_{pq}$$

Where $\vec{v}_q$ is velocity for phase q. $\dot{m}_{pq}$ represent mass transfer between phase q and q. From mass conservation point of view, we could derive following relationship:

$$\dot{m}_{pq} = -\dot{m}_{qp}$$

$$\dot{m}_{pp} = 0$$

Momentum equation for phase q is:

$$\frac{\partial}{\partial t}(\alpha_q \rho_q \vec{v}_q) + \nabla \cdot (\alpha_q \rho_q \vec{v}_q \vec{v}_q) = -\alpha_q \nabla p + \nabla \cdot \bar{\bar{\tau}}_q + \sum_{p=1}^{n} (\vec{R}_{pq} + \dot{m}_{pq} \vec{v}_{pq}) +$$

$$\alpha_q \rho_q (\vec{F}_q + \vec{F}_{lift,q} + \vec{F}_{vm,q})$$

Where $\bar{\bar{\tau}}_q$ is stress-strain tensor for phase q:

$$\overline{\overline{T}}_q = \alpha_q \mu_q (\nabla \vec{v}_q + \nabla \vec{v}_q^T) + \alpha_q (\lambda_q - \frac{2}{3}\mu_q) \nabla \cdot \vec{v}_q \overline{\overline{I}}$$

Where $\mu_q$ is shear viscosity for phase q, $\lambda_q$ is bulk viscosity for phase q, $\vec{F}_q$ external body force, $\vec{F}_{lift,q}$ is lift force, $\vec{F}_{vm,q}$ virtual mass force, $\vec{R}_{pq}$ is interaction force between phases, p is the pressure shared by all phases, $\vec{v}_{pq}$ is interphase velocity.

Mohanarangam and Stephens (2009) modeled behavior of floating and setting phases in a circular sedimentation tank, in this study, Eulerian model is employed as multi-phase model. The multi-phases included in this study were settling phases consist of sand, clay and a floatable phase. Contour plot of turbulent kinetic energy, floating phase and setting phase is presented. Highest turbulent kinetic energy is observed in feedwell region just after of the inlet. For floatable phase study, simulation performance towards two cases: floating particles with diameter 3.0 mm and 1.0 mm respectively, simulation result for volume fraction of floating phase with different diameters is compared, another important parameters, Stokes number which stand for kinetic equilibrium of the particles with the surrounding liquid, also used for evaluate particle behavior, Stokes number defined as ratio of the particle relaxation time to a time characteristic of the fluid motion, because larger particles demonstrate larger slip velocity, it shows tendency that move independently of flow pattern, as well as larger Stokes number. In order to simulate both the floating and settling solids at the same time, this study suggest include diffusion stress term into the momentum equation. Additionally, this research also recommended accurate measurement of the floating phase to increase efficient removal of particles from sedimentation tank overflow.

### 6.2.3 Mixture model

Unlike VOF model, the multi-phases could interpenetrating in Mixture model, Mixture model allow fluids move at different velocity by using slip velocity approach.

Mixture model solve the momentum and continuity equations for the mixture, and the volume fraction equation for the secondary phase. Mixture model performance good for fluids have strong interphase coupling. Under some conditions, such as wide distribution of the particulate phase or interphase reaction is unclear, the Mixture model could replace Eulerian model, although it’s simpler and solve smaller numbers of variables, it still could performance as good as complex multi-phase models such as Eulerian model, in this study, we employ Mixture model as multi-phase model, which is a perfect balance of simulation time and accuracy.

The continuity equation for Mixture model is:

$$\frac{\partial}{\partial T}(\rho_m) + \nabla \cdot (\rho_m \vec{V}_m) = \dot{m}$$

Where $\vec{V}_m$ is mass averaged velocity:

$$\vec{V}_m = \frac{\sum_{k=1}^{n} \alpha_k p_k \vec{V}_k}{\rho_m}$$

$\rho_m$ is density of the mixture:

$$\rho_m = \sum_{k=1}^{n} \alpha_k \rho_k$$

$\alpha_k$ is volume fraction of phase k

$\dot{m}$ is mass transfer due to cavitation or user-definned mass sources

The momentum equation is a sum of individual momentum equations for every phase, the momentum equation is:

$$\frac{\partial}{\partial t}(\rho_m \vec{V}_m) + \nabla \cdot (\rho_m \vec{V}_m \vec{V}_m) = -\nabla p + \nabla[\mu_m(\nabla \vec{V}_m + \nabla \vec{V}_m^T)] +$$

$$\rho_m \vec{g} + \vec{F} + \nabla \cdot (\sum_{k=1}^{n} \alpha_k \rho_k \vec{V}_{dr,k} \vec{V}_{dr,k})$$

Where n is numbers of phases, $\vec{F}$ is body force,

Viscosity of mixture is:

$$\mu_m = \sum_{k=1}^{n} \alpha_k \mu_k$$

$\vec{V}_{dr,k}$ is drift velocity of the secondary phase:

$$\vec{V}_{dr,k} = \vec{V}_k - \vec{V}_m$$

Mixture model allow primary and secondary phase move at different velocity, relationship between the velocity of secondary phase and velocity of primary phase define as relative or slip velocity, which can be written as:

$$\vec{V}_{qp} = \vec{V}_p - \vec{V}_q$$

Relationship between drift velocity and slip velocity is:

$$\vec{V}_{dr,p} = \vec{V}_{qp} - \sum_{k=1}^{n} \frac{\alpha_k \rho_k}{\rho_m} \vec{V}_{qk}$$

A local equilibrium between the phases should be fulfilled over short spatial length scales, so that algebraic relation for the relative velocity can be described, this is basic prerequisite of algebraic slip mixture model. Slip velocity in algebraic slip form is:

$$\vec{V}_{qp} = T_{qp}\vec{a}$$

Where $\vec{a}$ is acceleration of particle in the secondary phase, $T_{qp}$ is particulate relaxation time. According to continuity equation for secondary phase, the volume fraction equation is:

$$\frac{\partial}{\partial t}(\alpha_p \rho_p) \nabla \cdot (\alpha_p \rho_p \vec{v}_m) = -\nabla \cdot (\alpha_p \rho_p \vec{v}_{dr,p})$$

Recent years, Mixture model has appeared in sedimentation tank multi-phase simulation, Tan et al (2009) studied two phases flow in a horizontal sedimentation tank by using Mixture model. The simulation result calibrated with the Froude number theory, numerical result shows that when the Froude number equal to 0.2, there is an interface exist between the two phases, the “density current” phenomena is obvious, while when Froude number surpass 0.7, the two phases mixed with each other. Contour plot of volume fraction of sediments indicates that there are four zones in sedimentation tank from surface to bottom: clean water zone where volume fraction of sediments near zero, flocculation zone where sediments concentration increase dramatically, sedimentation zone with constant concentration of sediments and sludge zone with very high volume fraction of sediments, this “four zone” phenomena also can be found in reality.

Above study based on the assumption that temperature is constant during simulation, however, in really situation, temperature are variable and have influence on the “density current”, temperature difference between incoming fluid and fluid in sedimentation tank, or temperature difference in different seasons also influent the density current. Tan et al (2013) studied effect of different temperature on “density current” by using Mixture model, in his work, multi-phase simulation performance firstly in order to modeling “density current” caused by different density, after stable state achieved, different temperature of the multi-phases is introduced, so that influence of different temperature on existed density current could be studied.

As a relatively simple multi-phase model, there are quite few reports about application of Mixture model in sedimentation tank simulation, based on current available paper, Mixture model is reliable for sedimentation tank design, in this study, Mixture model will be employed as multi-phase model for multi-phase simulation.

# Chapter 7 Single phase and RTD simulation result

Commercial CFD software Fluent is used in this study, in order to study the flow pattern and evaluate the hydraulic performance of the sedimentation tank, single phase simulation and RTD simulation are carried out, the model setup for single phase simulation and RTD simulation described as follows:

- Define a three dimensional, steady state, implicit and pressure-based solver.
- Choose a proper turbulence model. The standard k-ε model is employed for single phase and RTD simulation.
- Enable the "species transport and reaction model".
- Define the fluid properties of sewage material used for the single phase simulation, assume the density of sewage is 1000kg/$m^3$, viscosity is 0,001 kg/m·s.
- Define the fluid properties of tracer material used for the RTD simulation, the tracer have fluid properties same with the sewage material, so that the tracer will not have significant effect on the fluid.
- In the material panel, choose sewage and tracer as mixture species, select volume weighted mixing law for density.
- Define the operating conditions, setup direction and value of gravity.
- Define the boundary conditions: the inlet velocity is 0.5 m/s (define according to the designed detention time 3 hours), volume fraction of tracer at the inlet is 0.
- Define the solution control by choosing the under-relaxation factors and setting discretization schemes.
- In the solution control panel, choose the continuity and momentum equations, disable the tracer species equation.
- Initialize the flow fields.
- Solve the steady state continuity and momentum equations until convergence.

Save the converged solution of steady state continuity and momentum equations, the solution will be used for single phase flow pattern analysis. To performance the residence time distribution simulation and get the "E" type RTD curve, continue above simulation with following setups:

- Enable the transient solver.
- Set volume fraction of tracer at the inlet equal to 1.
- Active the species transport equations, deselect the continuity and momentum equation.
- Define a Surface Monitor, plot area weighted averaged concentration of volume fraction of tracer with flow time at the outlet.
- Iterate one time step.
- Set volume fraction of tracer at the inlet back to 0.
- Solve the species equation under transient solver.

To get the "F" type RTD curve, after defined the Surface Monitor, maintain volume fraction of tracer at the inlet is 1, then solve the transient solution of species equation.

### 7.1 Tracer test

The tracer test was carried out at the Drøbak wastewater treatment plant (WWTP), which is situated about 50 km south of the capital of Norway, Oslo. The WWTP has two rectangular flat-bottom sedimentation tanks with two inlets, three outlet launders in each. The Drøbak WWTP with following geometry parameters: length 32m, width 7m and depth 3.6m. The sedimentation tank is a secondary sedimentation tank, used to settle particles generated by coagulation process.

**Figure 7.1** Sedimentation tank at the Drøbak WWTP, Norway

Tracer test was carried out before CFD simulation, the test use Rhod.B as trace, the tracer was released from the inlet, Rhod.B concentration then monitored at the outlet, recorded and plot versus time. The tracer test last for around 2.5 hours. Following picture is the tracer test result:

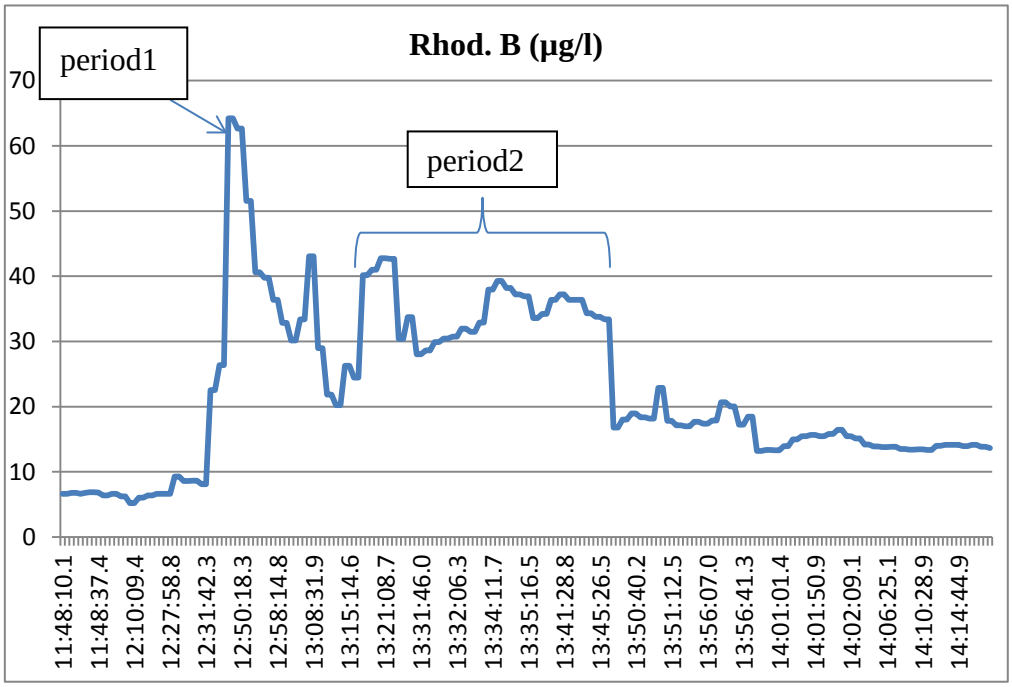


**Figure 7.2** Tracer test result

In Figure 7.2, the x-axis is time, y-axis is concentration of Rhod.B in µg/l, as

indicated from the tracer test result, the whole RTD curve contain two major periods: the first period with a steep peak, and the second period, represented by a longer period with lower tracer concentration. The tracer test indicated following problems in the sedimentation tank:

1) Strong surface current: most tracer arrive the outlet during the first period, with travelling time short than the designed detention time, in an ideal sedimentation tank, entering fluid should stay in the sedimentation tank for the full designed detention time, strong surface current leads to particles or fluids remain in the sedimentation tank shorter than designing detention time, thus reduce effective sedimentation volume and deteriorate sedimentation efficiency. The tracer test result indicates that after released into the sedimentation tank, the tracer bring by strong current on the surface of the sedimentation tank, move to the outlet directly rather than settle to the bottom of the sedimentation tank.
2) Re-circulating current in the sedimentation tank: the second period last for longer time than the first period, it consists of several smaller peaks, it indicates that re-circulating current existed in the sedimentation tank. When tracer arrive the outlet with the surface current, a portion of tracer flow out of the sedimentation tank, form the first peak, while the other portion of tracer move downward, then flow backward towards the inlet direction, thereby form a re-circulating current in the sedimentation tank, with the re-circulating current, tracer move to the surface and finally arrive the outlet of the sedimentation tank again, each time when the re-circulating current arrive the outlet, a portion of tracer flow out of the sedimentation tank, it’s the reason of the several smaller peaks during the second period.

Tracer test is a kind of convenient method to determine flow pattern and potential failures, however, tracer test influenced by a lot of un-controllable factors. For the sedimentation tank tracer test case, the flow rate, the volume fraction of suspended solids, and the wastewater properties are variable during test, these un-controllable factors have influence on tracer behavior, may leads to wrong estimation. To avoid the influence of above mentioned un-controllable factors, an alternative is performance the tracer test in a lab scale pilot plant instead of the full scale sedimentation tank. The pilot plant scaled down according to the geometry of the full scale tank, with more factors under control in lab, the tracer test result of the pilot plant may indicate some problems in the full-scale tank. However, lab scale experiments may expensive and time consuming.

CFD supplied a solution with good balance of accuracy, time and funding. Take advantage of software, geometry of the sedimentation tank, physical properties of the fluid and boundary conditions are all controllable, thereby engineers could modify design with higher flexibility. Additionally, due to all the simulation processed in computer, the amount and cost of experiments also reduced. In the following section, the CFD simulation result for the original sedimentation tank design and several modified designs is displayed.

### 7.2 Single phase simulation result

Due to the fact that in the secondary sedimentation tank, the volume fraction of suspended solids is quite low and in order to performance RTD simulation without the influence of multi-phase flow, single phase simulation firstly ran. Sludge withdrawal is neglected in this study, as it occurs intermittently, and will have a very little influence on the flow patterns.

*The original tank*

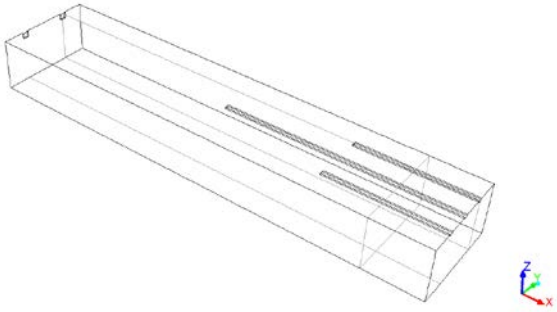

a

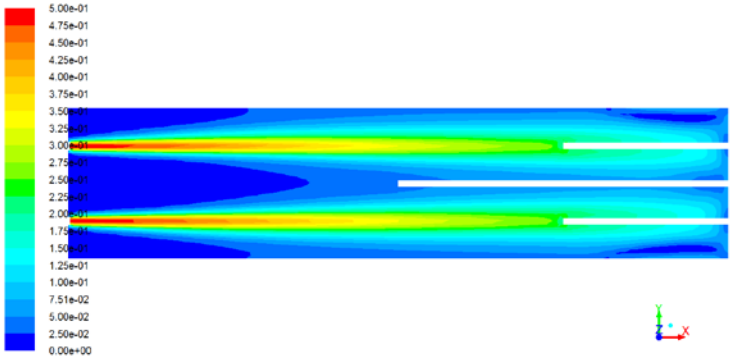


b

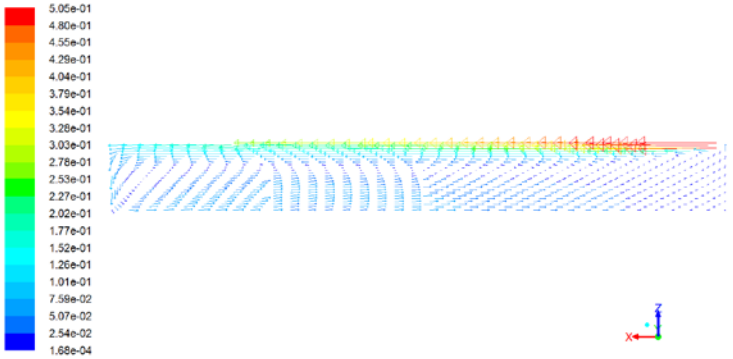


c

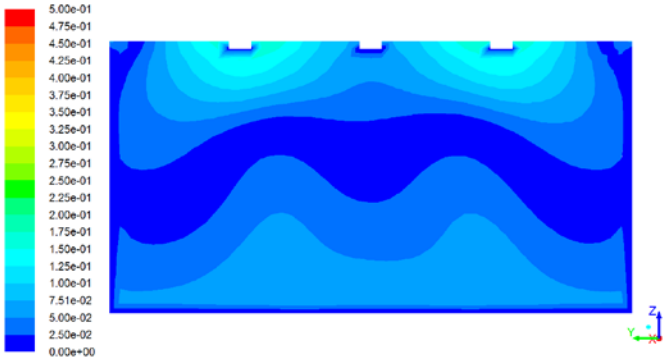


d

**Figure 7.3** Flow pattern of the origin tank

Figure 7.3 (a) is the geometry model for the simulation, it have length, width and depth same with the really wastewater treatment plant, it use three long rectangular represent the outlet launder, all the three trenches have depth 0.1m and width 0.3m, one locate in the middle of the sedimentation tank with length 16m and rest of them locate +1.75 and -1.75m away from the middle trench with length 8m. Use two rectangular represent the inlet, cross section of the inlet is 0.4*0.4 m and penetrate 0.1m along the flow direction. The inlet is defined as velocity inlet, outlet is defined as outflow, baffle and wall define as standard wall and tank surface is defined as free surface.

Figure 7.3 (b) is contour of velocity magnitude of the tank surface, it shows strong surface current, particles bring by the surface current will flow out of the tank directly without enough time for detention, Figure 7.3 (c) is velocity vector on cross-section of x-z plane, the velocity vector indicates besides surface current, there is also strong re-circulating current inside the tank, as we can see from Figure 7.3 (c), the vector direction move downward after reach the outlet side wall, then the downward flow transfer into bottom current with direction opposite to the surface current, thus generate the re-circulating current, the surface current will leads to short detention time, while bottom current will disturb stability of sludge layer at the tank bottom. Figure 7.3 (d) shows contour of velocity magnitude on cross-section of y-z plane, near the tank surface, velocity in range 0.150-0.175 m/s, while at the bottom the velocity in range 0.050-0.075 m/s.

Re-circulating current leads to dead zone in sedimentation tanks, if dead zone occupy volume of the sedimentation tank, effective volume of sedimentation tank will decrease, thus reduce sedimentation volume for suspended solids, on the other hand, re-circulating current cause mixing, strong mixing may bring bottom settled particles back to surface and disturb stability of fluid inside sedimentation tank, so one major goal for sedimentation tank design is reduce the re-circulating current. In sedimentation tank design, baffle often used to reduce re-circulating and re-distribute incoming fluids around inlet hence reduce surface current, Goula et al (2008) research

the influence of baffle on sedimentation tank in potable water treatment by using CFD，a circulation zone exist in the original tank without baffle, after equipped baffle, the circulation zone around inlet in original tank decreased, the baffle enhanced setting of particles. Due to effect of baffle, particles around inlet move downwards and reach the bottom of the tank. In rectangular sedimentation tanks, dissipate energy of incoming fluid is the main task in designing a sedimentation tank. Energy of influent must be dissipating near the inlet zone by changing the position and configuration of inlet or equip baffles around the inlet zone. Based on research of baffle effect, baffle is equipped in two optimized design at +4m and +2m away from the inlet respectively. In following part of this paper, we name these two designs 4m baffle tank and 2m baffle tank respectively.

*4m baffle tank*

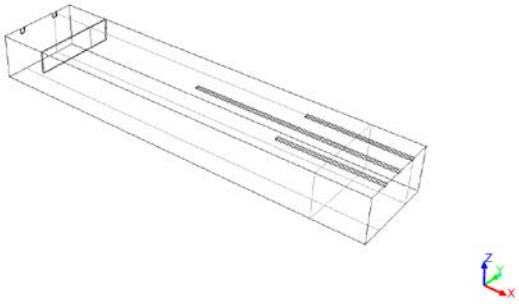

a

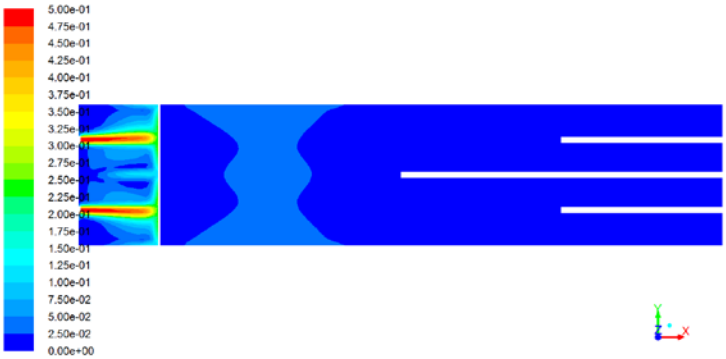


b

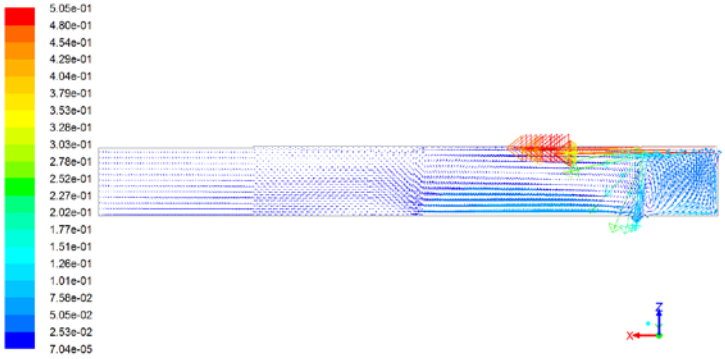


c

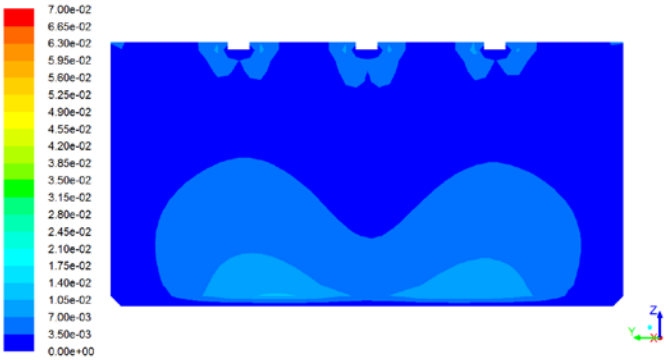


d

**Figure 7.4** Flow pattern of 4m baffle tank

Figure 7.4 (b) displayed the simulation result after installing a baffle with a 4m distance from the inlet. The surface current seems to be improved with the baffle, although a new velocity zone appeared between baffle and outlet, the direct strong surface current still reduced dramatically, from Figure 7.4 (c), we could find the fluid move downward due to effect of baffle, a portion of fluid bypass the baffle and reach surface again, this is the reason for the velocity zone between baffle and outlet depicted in Figure 7.4 (b), but major part of fluid flow at the bottom of tank, near outlet zone, the vector size much more smaller than observed in the original tank Figure 7.3 (c), indicates slower velocity near outlet zone, result from Figure 7.4 (d) shows that bottom current velocity and surface current velocity reduced to around 0.01 m/s and 0.005m/s respectively.

*2m baffle tank*

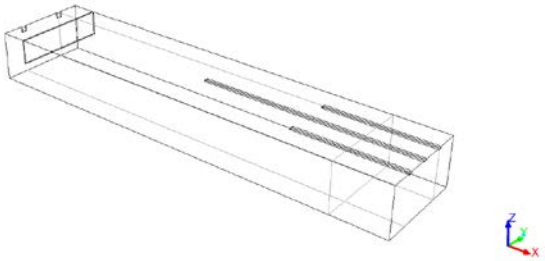

a


5.03e-01
4.78e-01
4.53e-01
4.28e-01
4.03e-01
3.78e-01
3.52e-01
3.27e-01
3.02e-01
2.77e-01
2.52e-01
2.27e-01
2.01e-01
1.76e-01
1.51e-01
1.26e-01
1.01e-01
7.55e-02
5.03e-02
2.52e-02
0.00e+00

b

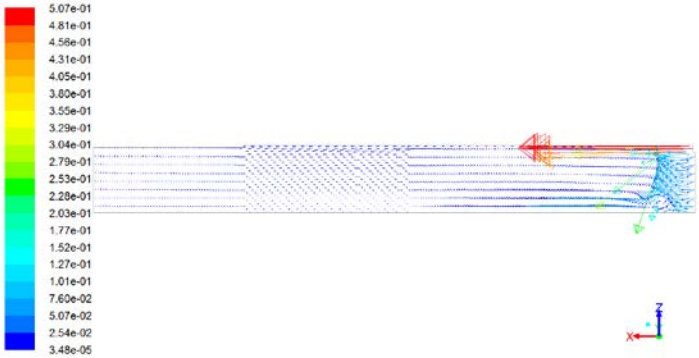
5.07e-01
4.81e-01
4.56e-01
4.31e-01
4.05e-01
3.80e-01
3.55e-01
3.29e-01
3.04e-01
2.79e-01
2.53e-01
2.28e-01
2.03e-01
1.77e-01
1.52e-01
1.27e-01
1.01e-01
7.60e-02
5.07e-02
2.54e-02
3.48e-05

c


1.00e-01
9.50e-02
9.00e-02
8.50e-02
8.00e-02
7.50e-02
7.00e-02
6.50e-02
6.00e-02
5.50e-02
5.00e-02
4.50e-02
4.00e-02
3.50e-02
3.00e-02
2.50e-02
2.00e-02
1.50e-02
1.00e-02
5.00e-03
0.00e+00

d

**Figure 7.5** Flow pattern of 2m baffle tank

To avoid bypass flow around baffle, we ran the simulation with a 2m baffle rather than a 4 m baffle and the results are given in Figure 7.5, the velocity zone and bypass flow that appeared in Figure 7.4 have disappeared, while the velocity vector remains in almost same size and direction after baffle, means the fluid very close to “plug flow” situation, in Figure 7.5 (d), the contour plot almost dark blue (indicates velocity near to zero) while the velocity at the top of tank around 0.005 m/s (light blue zone).

*4m baffle with tilted bottom tank*

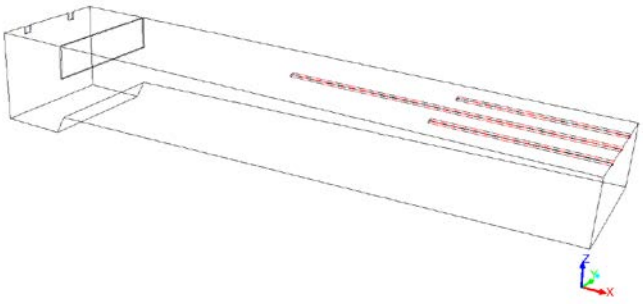

a

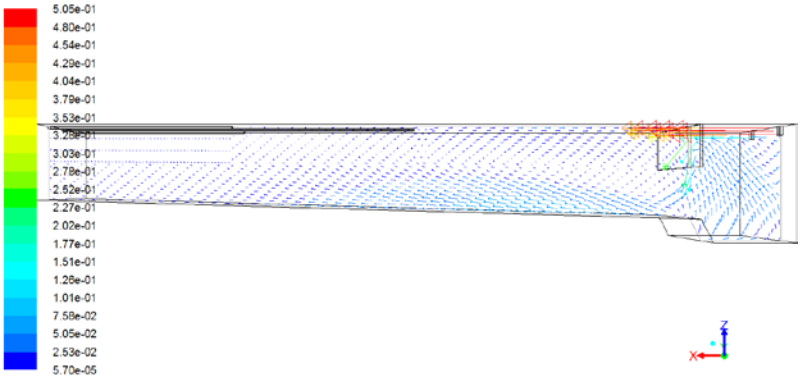


b

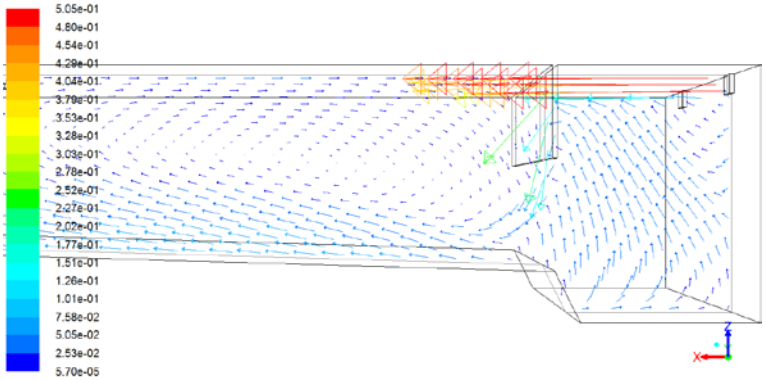


c

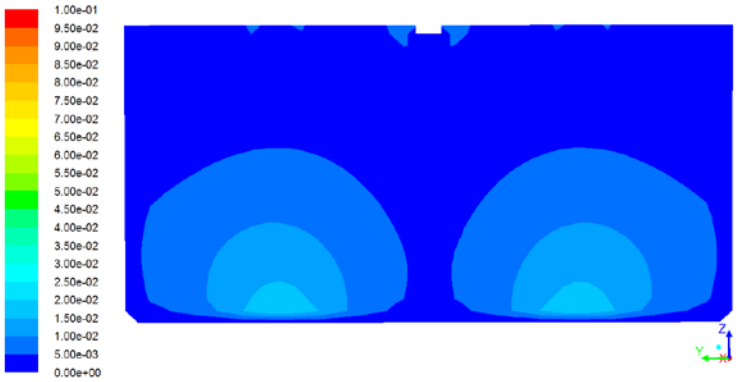


d

**Figure 7.6** Flow pattern of 4m baffle with tilted bottom tank

In this design, in addition to a baffle equipped 4 meters away from the inlet, two more optimization also installed, a sludge hopper with length 3.5m in x direction and depth 5m is added, the bottom of the sedimentation tank is tilted, the slope start from 4m away from the inlet side of the tank, at the inlet side, the depth of the slope is 4m below tank surface, at the outlet side, the depth of the slope is 3.6m below tank surface, so that the slope of tank bottom is 0.0143. These modifications aim at improve sludge removal efficiency.

As displayed in Figure 7.6 (b), after impinging on the baffle, the inflow wastewater is deflected downwards to the bottom of the sedimentation tank. The flow separate just above boundary of the sludge hopper and the tilted bottom, a portion of wastewater bypass the baffle, producing a recirculation eddy in the zone between baffle and outlet, this large recirculation region spanning a large part of the tank. In Figure 7.6 (c), a smaller recirculation region are also found in the sludge hopper zone, after incoming wastewater split around on boundary of sludge hopper and tilted bottom, part of wastewater move backward towards the inlet direction, then move upward again, thereby form a smaller circulation zone in the sludge zone, similar result was also observed by Stamou (1991) and Goula et al (2008). Due to effect of baffle and slope, wastewater current is stronger at the tank bottom than on the tank surface, as displayed in Figure 7.6 (d). Compare to 4m baffle without tilted bottom, in this case the surface current velocity in range 0.005-0.01m/s and bottom current velocity 0.015-0.02 m/s, the surface current velocity is lower than the 4m baffle case, while the bottom current velocity is higher than the 4m baffle design, it means that with the tilted bottom, more incoming wastewater is concentrated to the tank bottom.

*2m baffle with titled bottom tank*

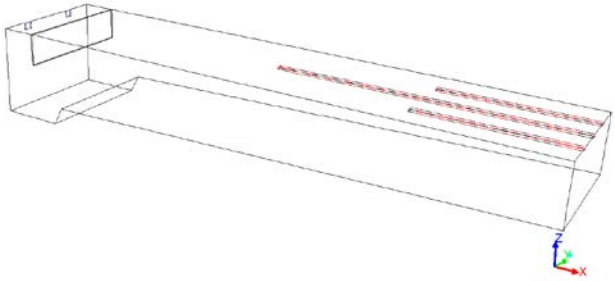

a

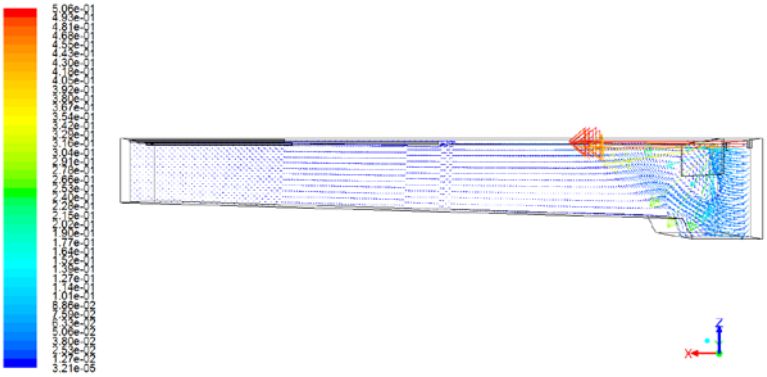

b

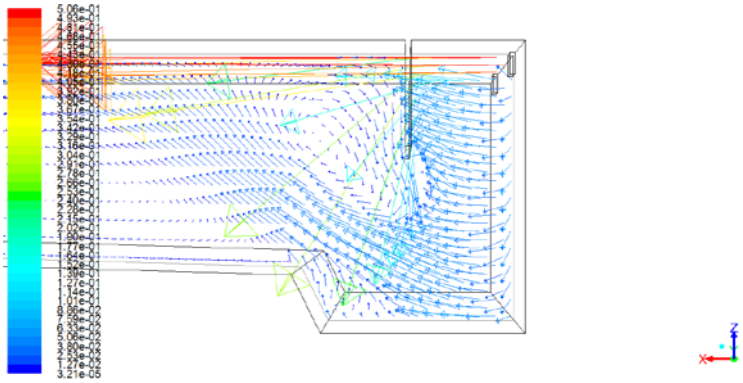

c

d

**Figure 7.7** Flow pattern of 2m baffle with tilted bottom tank

To further study the influence of baffle and tilted bottom on flow pattern, a 2m baffle with titled bottom design is proposed, the sludge hopper and bottom in this case share same geometry parameters as the above mentioned tank.

As displayed in Figure 7.7 (b), compare to the 4m baffle with tilted bottom design, in this case, due to shorter distance between the inlet and the baffle, the downward flow velocity stronger after impinged on the baffle, the deflected wastewater bypass the baffle, produce a recirculation eddy near the baffle zone, the recirculation eddy occupied much smaller volume compare to the 4m baffle with tilted bottom design. As displayed in Figure 7.7 (c), with reduced volume between the inlet and the baffle, the small recirculation region detected in the 4m baffle with tilted bottom design almost disappeared in this case. In Figure 7.7 (d), the surface current velocity in range 0.0067-0.01m/s and bottom current velocity around 0.0033-0.0067m/s, both the surface current and the bottom current slightly higher than 2m baffle without tilted bottom tank, however, the surface current and bottom current velocity still lower than the 4m baffle with tilted bottom tank, 4m baffle tank and the original design, the flow also more evenly distributed compare to these three designs.

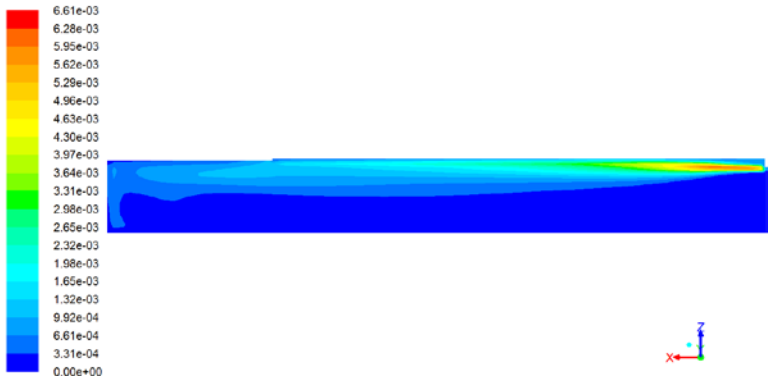


a


b


c


d


e

**Figure 7.8** Contour of kinetic energy for the horizontal tanks

Kinetic energy (unit $m^2/s^2$) is an important parameter for sedimentation tank CFD simulation, strong kinetic energy maybe cause re-suspension of the settled particles, so that one major goal of baffle in sedimentation tanks is reducing the kinetic energy. As displayed in Figure 7.8 (a), in the original tank, kinetic energy spread in the whole tank especially on the tank surface, in order to dissipate kinetic energy of the incoming wastewater, baffle is installed near the inlet, after impact with baffle, the kinetic energy of inflow wastewater is dissipated, Figure 7.8 (b) and Figure 7.8 (c) shows that both 2m baffle and 4m baffle could dissipate the kinetic energy effectively, in the 2m baffle and 4m baffle design, the kinetic energy limited between the baffle

and the inlet, thereby provide a better settle environment in the zone between baffle and outlet. The major drawbacks of flat bottom design is kinetic energy filled in the whole inlet zone, sludge settled in this region may influenced by subsequent wastewater, as displayed in Figure 7.8 (d) and Figure 7.8 (e), with tilted bottom, the kinetic energy reduced in the inlet zone, sludge accumulated in the inlet zone will have less disturbance.

Compare to horizontal flow sedimentation tank, circular sedimentation tank, which has advantages such as smaller volume and higher precipitation efficiency, is employed by more and more wastewater treatment plant recently. To study the performance of circular sedimentation tank, in the following part of this paper, two novel sedimentation tank models is proposed and analyzed by CFD method, the circular sedimentation tank models studied in this paper have radius 8m, depth 3m, the sludge hopper which locate in the center of the sedimentation tank have radius 2m and depth 4m, the reflector have radius 1m and length 1m, the feed tube have radius 0.5m and length 1m. In one circular sedimentation tank, the wastewater in the feed tube move upward, we name it upward flow circular sedimentation tank, in the other circular sedimentation tank, the wastewater move downward in the feed tube, we name it downward flow circular sedimentation tank. The boundary condition is same with the horizontal tank simulation, in the following figures, geometry of tanks, velocity vectors on cross-section of x-z plane, tank surface and on cross-section of x-y plane is displayed in sub-figures a, b, c and d respectively.

*Upward flow circular sedimentation tank*

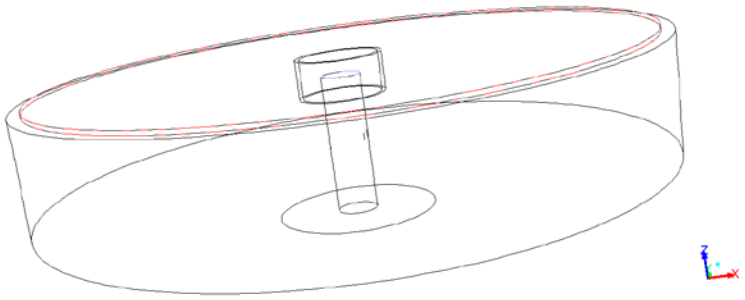

a

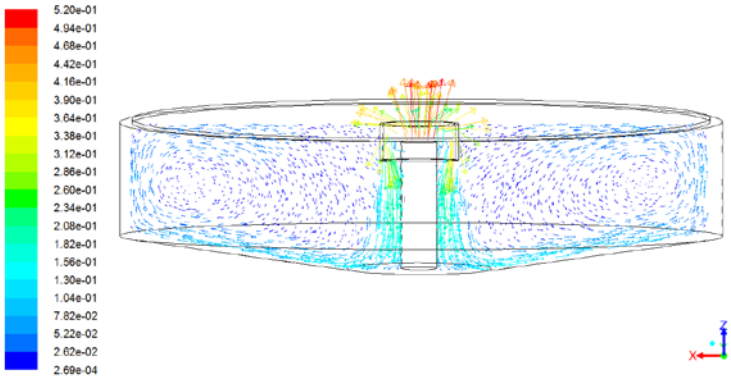


b

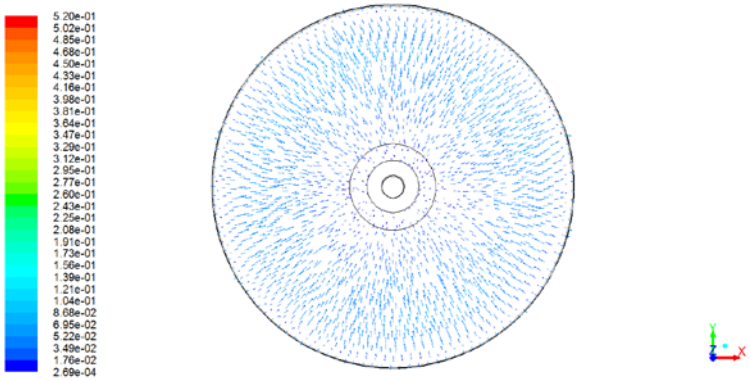


c

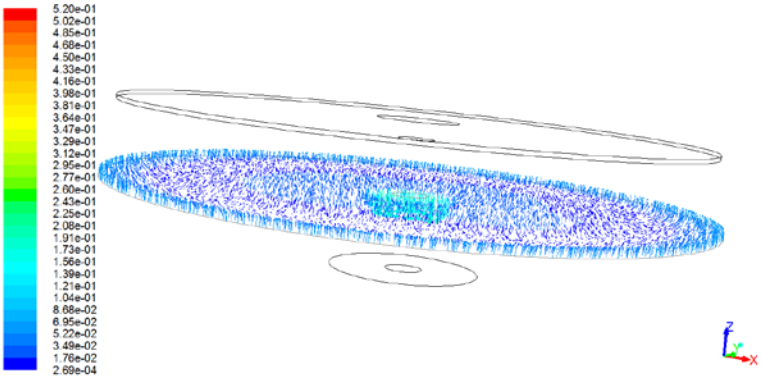


d

**Figure 7.9** Flow pattern of upward flow circular sedimentation tank

Deininger et al (1998) measured flow velocity and solids distribution in a full scale circular secondary sedimentation tank, the measurement result also evaluated by using numerical approach. Circular currents were detected in both numerical simulation result and the full scale measurement, Deininger et al summarized that the circular current contain following properties:

- In the zone near to the tank bottom, flow move forward towards the tank rim.
- In the upper part of the tank where near the tank surface, flow move backward towards the inlet side.
- The forward flow (towards tank rim) is higher in the inlet zone than in the rim zone.

•The backward flow (towards tank inlet) is higher in the inlet zone than in the outlet zone.
•Around the inlet region, backward flow turns into vertical currents towards to the tank bottom. While near to the outlet zone, forward flow move upward to the tank surface.

The above-mentioned circular current characteristics basically in agreement with the simulation result displayed in Figure 7.9, the only difference is higher backward flow velocity is detected in the outlet region rather than in the inlet region, this difference is due to different inlet arrangement, in Deininger's model, the inlet closer to the tank bottom. As displayed in Figure 7.9 (b), after reflected by the baffle, the inflow wastewater deflected downwards and move forward along tank bottom, then move upward after arrive tank rim, a portion of wastewater flow out of the tank, while the other portion of wastewater flow backward to the inlet side, submerged again with the circular current, thereby generate re-circulation current in the whole tank.

*Downward flow circular sedimentation tank*

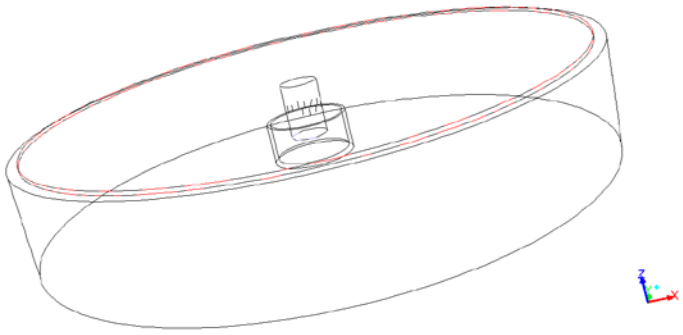

a

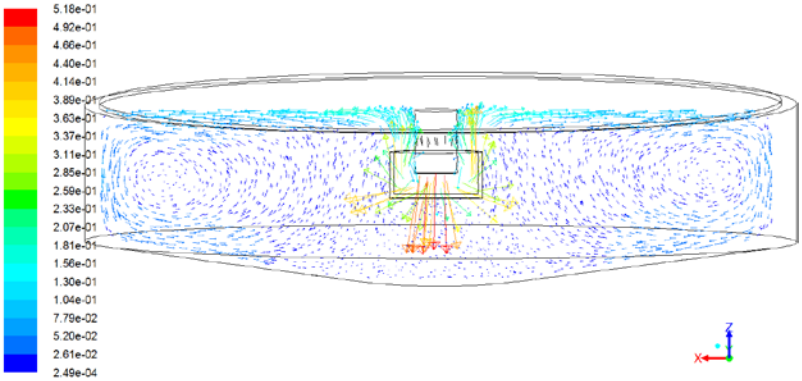


b

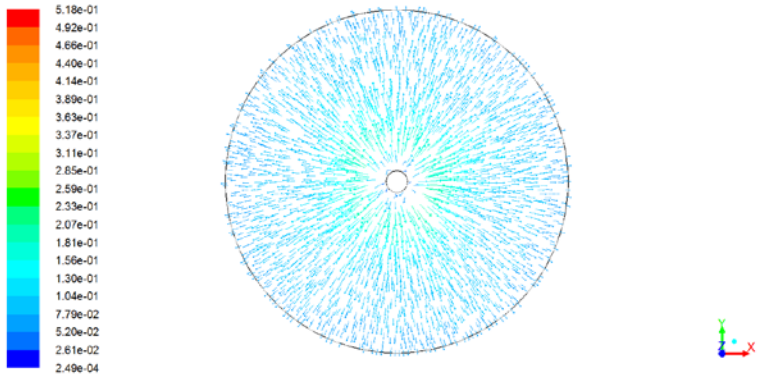


c

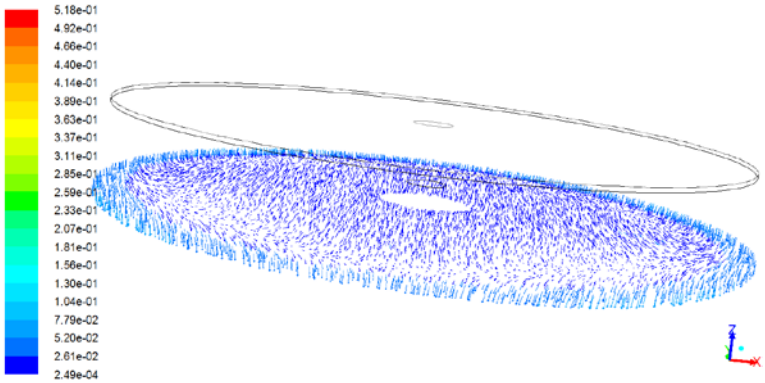


d

**Figure 7.10** Flow pattern of downward flow circular sedimentation tank

Zhu et al (2012) studied a vertical flow sedimentation tank using CFD method, the sedimentation tank studied by Zhu have structure similar to the upward flow circular sedimentation tank. Zhu reported that in a vertical flow sedimentation tank, the reflector at the end of central pipe could change the direction of incoming wastewater, the reflector also spread the incoming wastewater, make the flow distributed uniformly in the whole sedimentation tank, Zhu concluded that the reflector could improve tank performance and efficiency. Similar simulation result also presented in Figure 7.10, as displayed in Figure 7.10 (b), after reflected by reflector, the incoming wastewater move upward and spread to the whole range of radial tank, the reflected wastewater then flow toward the outlet, generate re-circulating current with direction opposite to the upward flow circular tank.

The re-circulating current detected in both upward flow circular sedimentation tank and downward flow circular sedimentation tank, the circulation region decrease effective tank volume and reduce the tank performance, the re-circulating current also result in short circuiting and strong mixing.

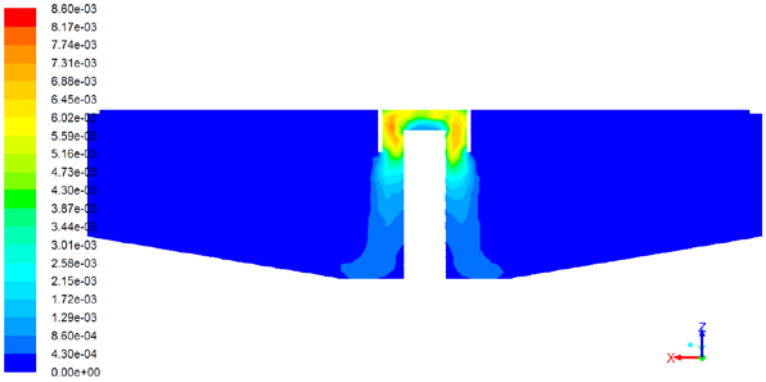


a

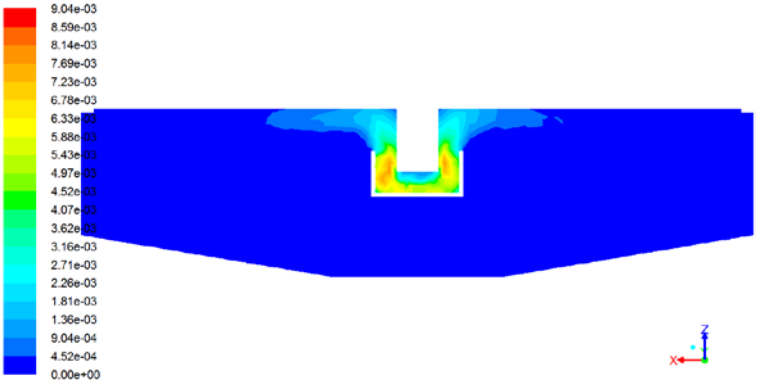


b

**Figure 7.11** Contour of kinetic energy for circular tanks

Figure 7.11 shows the kinetic energy of the upward flow circular sedimentation tank and the downward flow circular sedimentation tank. Figure 7.11 (a) displayed that in the upward flow circular sedimentation tank, maximum kinetic energy appears in the inlet region. After the incoming wastewater reflected by baffle, the magnitude of kinetic energy reduced, the wastewater move downward towards the tank bottom, falls on the sludge hopper. Usually sludge accumulated in the sludge hopper, form a sludge layer, the kinetic energy above the sludge layer indicates that wastewater reflected by the baffle may disturb stability of the sludge layer. As shown in Figure 7.11 (b), in the downward flow circular sedimentation tank, the reflector prevent incoming wastewater splash on the sludge hopper which locate at the tank bottom directly, thus reduce the disturbance of reflected wastewater on the sludge layer.

### 7.3 RTD simulation result

In order to determine the RTD by CFD approach, a converged solution for flow field should be calculated with steady state solver before solve the species equation, however, in reality, the wastewater inlet velocity is always variable, a User Defined Function (UDF, in the form of external C programming file) as displayed in Figure 7.12 which describe the variable inlet velocity should be coupled with commercial CFD software in order to define the variable inlet velocity, thereby the flow field with variable inlet velocity should be solved with transient solver. Now a dilemma

appeared in front of CFD analyst: the steady state solver is required to obtain the RTD, while simulation of variable inlet velocity need to use the transient solver. In this study, due to the tracer test performance in full scale sedimentation tank with variable inlet velocity, while all the CFD simulation assume that the inlet velocity is constant, so that only general trend of experimental tracer test result and CFD simulation result will be analyzed and compared.

```
#include "udf.h"
DEFINE_PROFILE(velocity_magnitude, t, i)
{
real velocity;
real the_current_time;
face_t f;
the_current_time = CURRENT_TIME;
if ((the_current_time>=0) && (the_current_time<5))
{
velocity=-2.8;
}
if ((the_current_time>=5) && (the_current_time<10))
{
velocity=-1.48;
if ((the_current_time>=10))
{
velocity=-2.01;
}
begin_f_loop(f,t)
{
F_PROFILE(f,t,i) = velocity;
}
end_f_loop(f,t)
}
```

**Figure 7.12** Example of User Defined Function for variable velocity

Ahrokhi et al (2012) investigated the influence of different numbers of baffles on sedimentation tank by using CFD, in addition to evaluated by flow pattern parameters, the effect of different arrangements of baffles on hydraulic behavior of sedimentation tank also studied by using the FTC method. The whole study conducted under laboratory condition, a rectangular primary sedimentation tank model is used for experimental measurement, wastewater injected by a pump with constant velocity, so that the measured tracer test result could calibrate with CFD simulation. Ahrokhi suggested use following RTD parameters study the performance of sedimentation tank:

•Dead zone or short circuiting problems in the sedimentation tank could be detected

by $t_{10}$, it indicates how fast tracer arrive the outlet. With higher values $t_{10}$, comes less possibility of dead zone.

•Other parameters, such as $t_{75}–t_{25}$, $t_{90}–t_{10}$, and $t_{90}/t_{10}$, is used to investigate the degree of mixing in the sedimentation tank, higher values of these parameters indicates stronger mixing in the sedimentation tank.

•Parameter $t_{50}$ is employed for evaluating the performance of the tank. Higher $t_{50}$ value means better sedimentation efficiency.

The residence time parameters is firstly non-dimensioned by theoretical detention time, after the non-dimension performance, the ratio of tracer concentration at the outlet $C_{out}$ and mean tracer concentration $C_O$, $C_{out}/ C_O$, marked as subscript to indicate the outlet tracer concentration after certain time, for example, $t_{10}$ means 10 percent of tracer has passed through the outlet. With flow rate 0.08$m^3$/s, The volume of original tank, 4m baffle tank and 2 baffle tank is around 806.4 $m^3$, so that the theoretical detention time for these three tanks is 10080s, the volume of 4m baffle with tilted bottom tank and 2m baffle with tilted bottom tank is around 883.05 $m^3$, so that the theoretical detention time for these two tanks is 11038s. With flow rate 0.4 m/s, the volume of two circular sedimentation tanks is around 686 $m^3$, so that the theoretical detention time for circular tanks is 1715s.

**Table 7.1** Residence Time Distribution parameters

| | Original tank | 2m baffle tank | 4m baffle tank | 2m baffle + tilted bottom | 4m baffle + tilted bottom | Upward circular tank | Downward circular tank |
|---|---|---|---|---|---|---|---|
| $t_{10}$ | 0.016 | 0.2 | 0.16 | 0.22 | 0.18 | 0.11 | 0.05 |
| $t_{25}$ | 0.10 | 0.28 | 0.26 | 0.30 | 0.27 | 0.27 | 0.07 |
| $t_{50}$ | 0.33 | 0.44 | 0.42 | 0.42 | 0.41 | 0.70 | 0.63 |
| $t_{75}$ | 0.72 | 0.66 | 0.65 | 0.59 | 0.61 | 1.50 | 1.54 |

| | | | | | | | |
|---|---|---|---|---|---|---|---|
| $t_{90}$ | 1.24 | 0.90 | 0.94 | 0.80 | 0.87 | 2.56 | 2.74 |
| $t_{75}$-$t_{25}$ | 0.65 | 0.38 | 0.39 | 0.29 | 0.35 | 1.23 | 1.47 |
| $t_{90}$-$t_{10}$ | 1.22 | 0.71 | 0.78 | 0.58 | 0.70 | 2.45 | 2.68 |
| $t_{90}/t_{10}$ | 78.16 | 4.65 | 5.84 | 3.62 | 2.12 | 24.22 | 53.92 |

To investigate the effect of baffle and tilted bottom on hydraulic behavior of sedimentation tank, the RTD curve and parameters for the original rank, the 2m baffle tank and 2m baffle with tilted bottom tank is displayed and studied.

*Original tank*

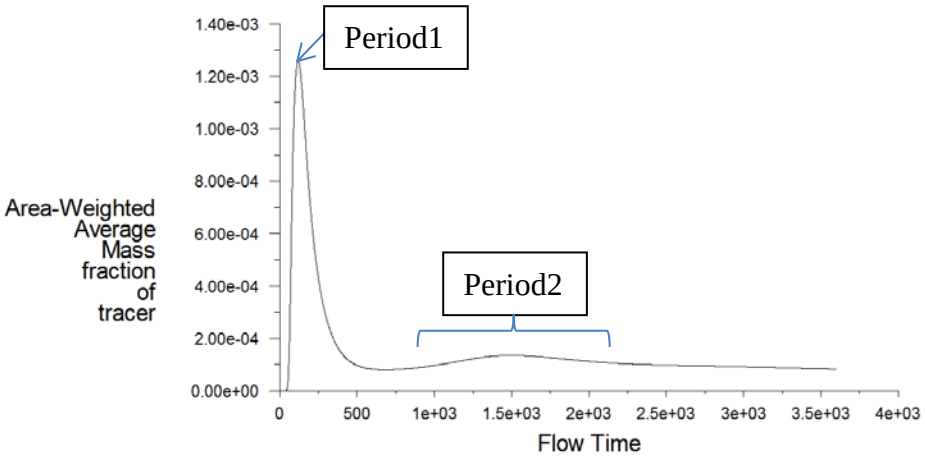


a

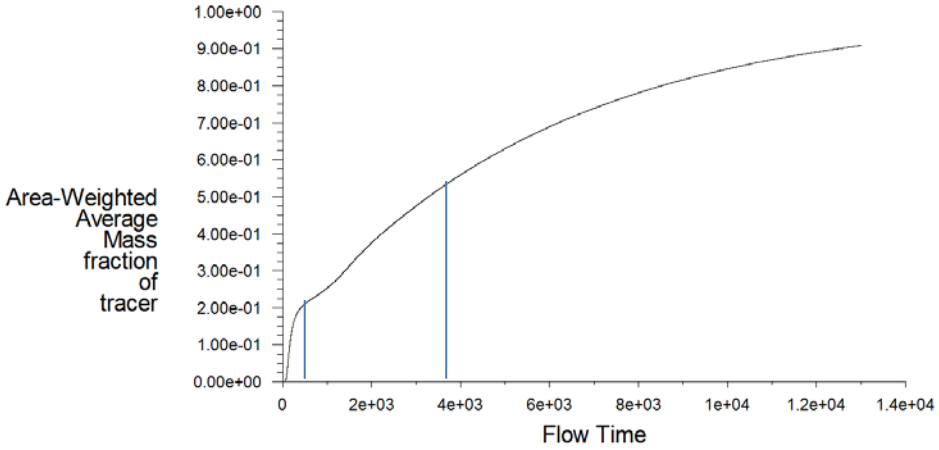


b

**Figure 7.13** RTD curve of the original tank

The RTD simulation curve for the original tank design in agreement with both the tracer test result and the CFD simulation result, as described in previous section, the tracer test result consists of two periods: the first period with a steep peak, and the second period with several smaller peaks. The RTD curve obtained by CFD simulation also following similar trend of experimental data, a two period phenomena also detected by the RTD simulation, the first period corresponds to the strong surface current detected in the single phase simulation, as described by the Figure 7.13 (a), the first period range from time 0 to around 500s after tracer released, the second period begin at around 1000s, last for around 1000s. According to the Figure 7.13 (b), over 20 percent of total tracer pass through the outlet during the first period, indicates too short detention time. The second period is the result of the re-circulating current. Through analyze The RTD parameters, the original tank have the lowest $t_{10}$ and $t_{50}$ value and highest $t_{75}–t_{25}$, $t_{90}–t_{10}$, and $t_{90}/t_{10}$ values among horizontal sedimentation tanks, indicates dead zone and strong degree of mixing in the original sedimentation tank, the parameters also indicates the existence of re-circulating current. Both RTD simulation and the single phase simulation result confirm the assumed potential failures through analyze the experimental tracer test result. The correspondence among experimental data, single phase simulation result and RTD curve verify that the CFD simulation is reliable.

*2m baffle tank*

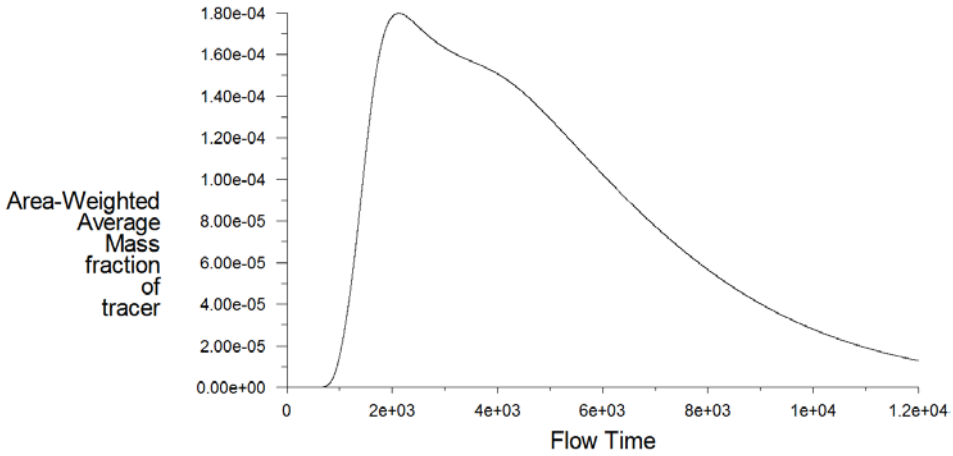


a

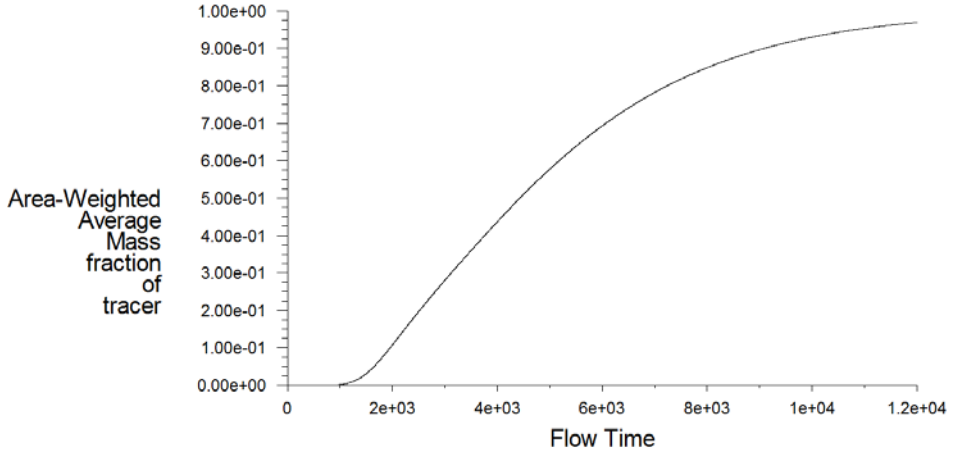


b

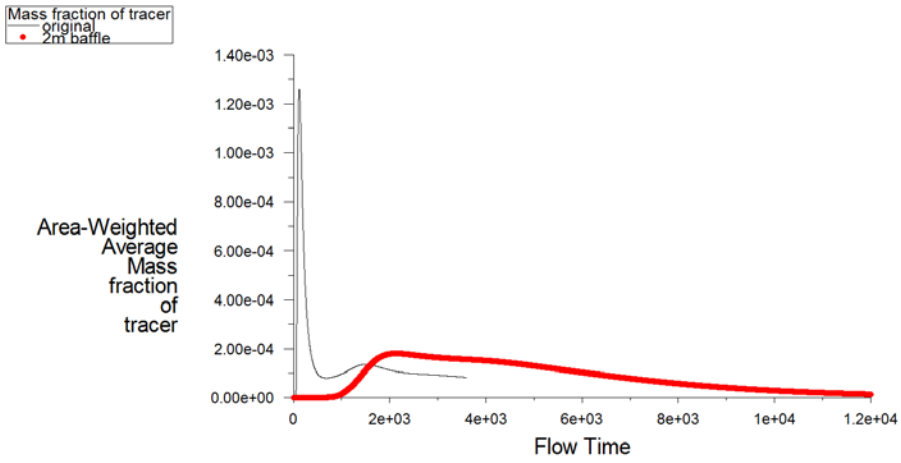


c

**Figure 7.14** RTD curve of the 2m baffle tank

In Figure 7.14 (c), the red curve is RTD curve of the 2m baffle tank, the black curve is RTD curve of the original tank. As displayed in Figure 7.14, with installation of baffle, the first peak caused by strong surface current is removed. According to RTD simulation result, the $t_{10}$ value of original sedimentation tank is 0.016, after equipped with baffle, this value increase to 0.2, it means dead zone reduced in the baffle assisted sedimentation tank, parameters used to evaluate the degree of mixing, such as

$t_{75}$–$t_{25}$, $t_{90}$–$t_{10}$, and $t_{90}/t_{10}$, all decreased dramatically, the $t_{75}$–$t_{25}$ value decreased from 0.65 to 0.38, the $t_{90}$–$t_{10}$ value decreased from 1.22 to 0.71, the $t_{90}/t_{10}$ value decreased from 78.16 to 4.65. Baffle remove the strong surface current, thereby stop the re-circulating current caused by the strong surface current, after re-distributed by the baffle, the incoming wastewater spread on the whole cross section of the sedimentation tank.

*2m baffle with tilted bottom tank*

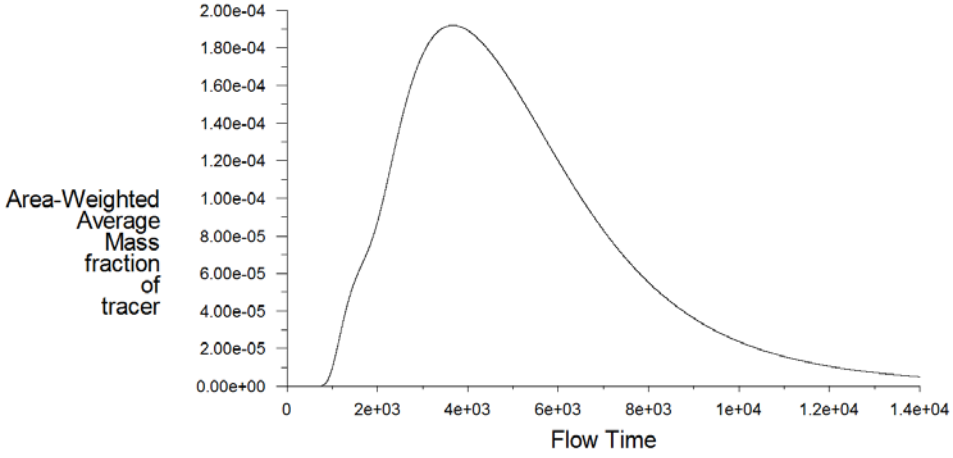


a

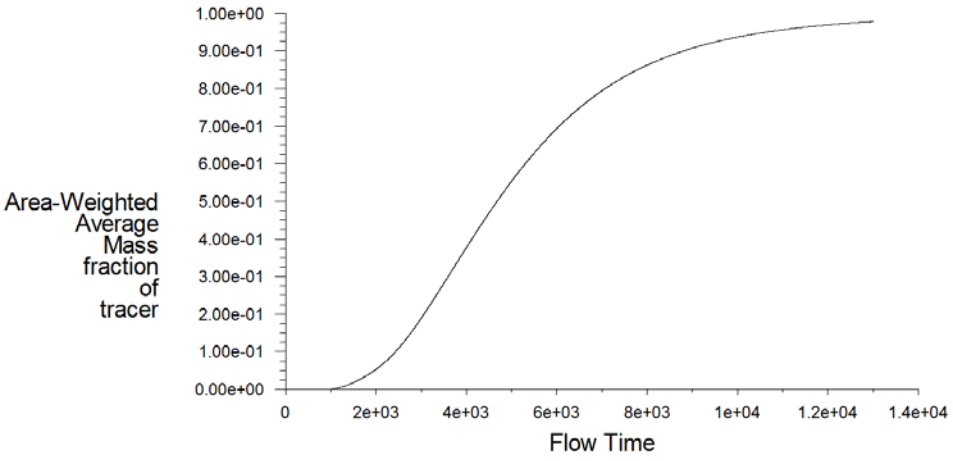


b

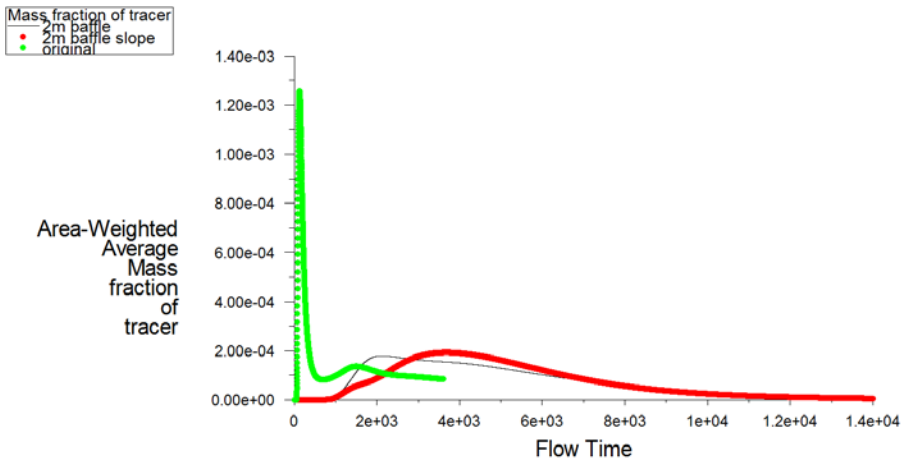


c

**Figure 7.15** RTD curve of the 2m baffle with tilted bottom tank

In Figure 7.15 (c), the green curve is RTD curve of the original tank, the black curve is RTD curve of the 2m baffle tank and the red curve is RTD curve of the 2m baffle with tilted bottom tank. As displayed in Figure 7.15, with a tilted bottom, the hydraulic efficiency of baffle equipped sedimentation tank further improved. RTD simulation result provide some major parameters for hydraulic efficiency evaluation, the $t_{10}$ value for the original tank, 2m baffle tank and 2m baffle with tilted bottom tank is 0.160, 0.2 and 0.22 respectively, these values indicates dead zone in the 2m baffle tank reduced a lot compare to the original tank, while the tilted bottom further reduce the volume of the dead zone, in terms of parameters used to investigate the degree of mixing, all the values of 2m baffle with tilted bottom tank decreased compare to 2m baffle design, the $t_{75}–t_{25}$ value decreased from 0.38 to 0.29, the $t_{90}–t_{10}$ value decreased from 0.71 to 0.58s, the $t_{90}/t_{10}$ value decreased from 4.65 to 3.62, the simulation parameters corresponding to the single phase simulation result, in the 2m baffle with tilted bottom design, the circulation in the zone between the baffle and outlet, as well as the circulation in the sludge zone improved.

*Upward flow circular sedimentation tank*

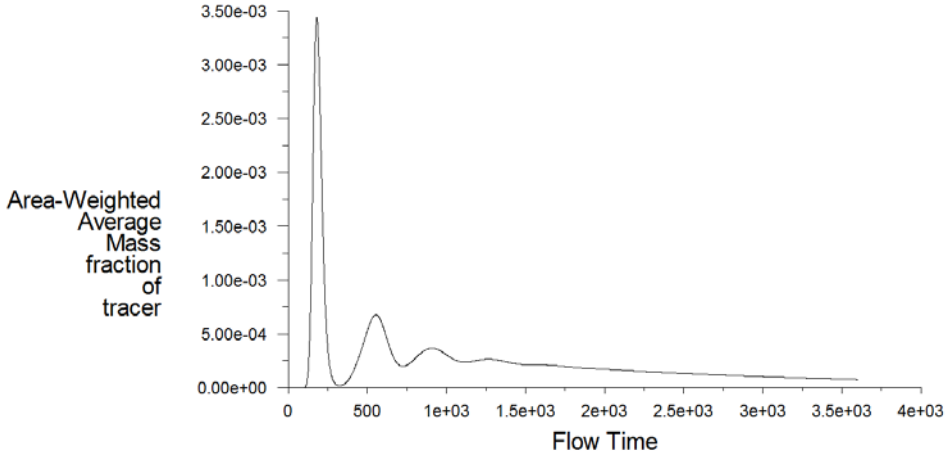


a

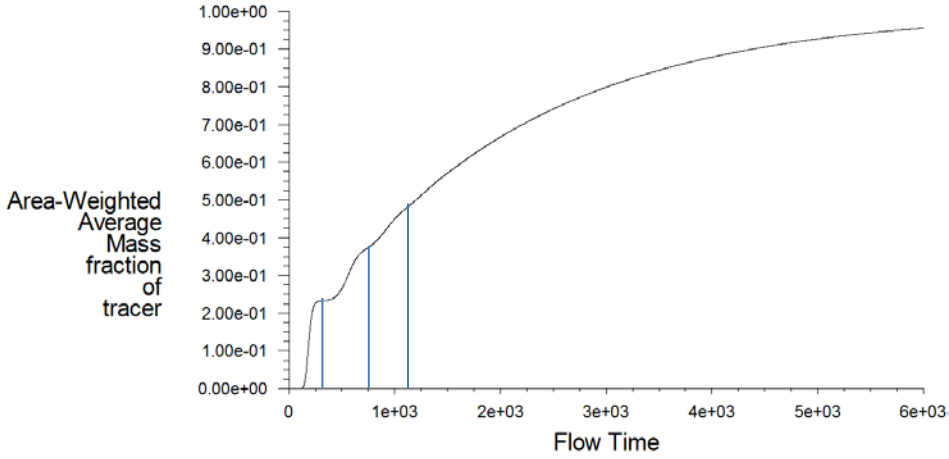


b

*Downward flow circular sedimentation tank*

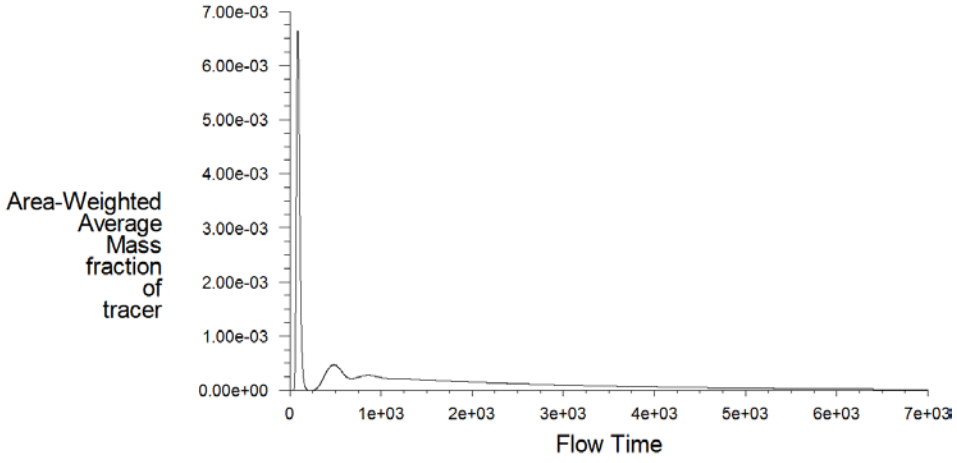


c

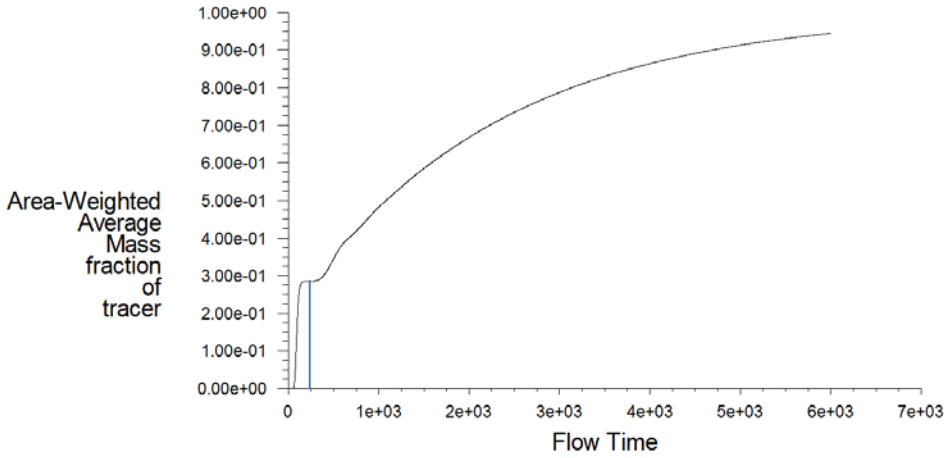


d

**Figure 7.16** RTD curve of the circular tanks

As displayed in Figure 7.16 (a) and Figure 7.16 (c), the "E" type RTD curve for both upward flow and downward flow circular sedimentation tank consists of several peaks and a long tail, which indicates strong recirculating current inside the sedimentation tank. As RTD curve of upward flow circular sedimentation tank displayed in Figure 7.16 (a), the first peak range from around 100s to around 300s after tracer released, in Figure 7.16 (b), it is detected that more than 20 percent tracer pass through the outlet during the first peak, the second peak last from around 300s to around 750s after tracer released, near 40 percent tracer flow out of the sedimentation tank during this period, after the third peak which range from 750s to 1000s, around 50% tracer pass through the sedimentation tank. In the downward flow circular sedimentation tank, around 30 percent tracer flow out of the sedimentation tank during the first peak. According to RTD simulation result, the $t_{75}$–$t_{25}$ value for the upward flow circular sedimentation tank and downward flow circular sedimentation tank is 1.23 and 1.47 respectively, the $t_{90}$–$t_{10}$ value for both tanks is 2.45 and 2.68 respectively, while the $t_{90}/t_{10}$ value for the two circular tanks is 24.22 and 53.92, these value used to evaluate the degree of mixing, from above mentioned values, we can concluded that strong re-circulating current and strong degree of mixing detected in both tanks.

# Chapter 8 Multi-phase simulation result

The model setup procedure for multi-phase simulation described as follows:

- Define a three dimensional, transient, implicit and pressure-based solver.
- Choose proper turbulence model from the viscous model panel. The standard k-ε model is employed in this study.
- Choose proper multi-phase model from the multi-phase model panel. The Mixture model is employed in this study.
- Define two materials: sewage and sediments. The density of sewage is 1000kg/$m^3$, viscosity is 0,001kg/m·s, the sediments with density 1200kg/$m^3$, viscosity is 0,01 kg/m·s and particle diameter 0.1mm.
- Define sewage as the primary phase and sediments as the secondary phase.
- Define the operating conditions, set up direction and value of gravity.
- Define the boundary conditions: set inlet, outlet and wall. The inlet velocity is 0.5m/s, volume fraction of sediments at the inlet is 0.05.
- Define the solution control, modify the under-relaxation factors and choose discretization schemes.
- Initialize the flow fields.
- From the transient solver panel, set the time step size, number of time steps, and maximum iterations per time step.
- Solve the flow fields, record simulation result.

In reality, “density current” could enhance sedimentation process in some case, due to effect of “density current”, fluid move along bottom of sedimentation tank, thereby a relatively steady clean fluid layer appear on the top of layer upon density current, this “relatively clean” layer could constrain upward movement of sediment particle in bottom density current. Nevertheless, “density current” also bring problems for sedimentation tanks, circular flow caused by density current may deteriorate sedimentation of particles and sedimentation effect, due to incoming fluid couldn’t distributed evenly at inlet of sedimentation tank, so under high inlet velocity condition, incoming fluid will disturb stability of sludge layer at the bottom of sedimentation tank, bring settled particles back into density current and reduce efficiency of sedimentation tank, circular flow formed by density current will bring sludge out of sedimentation tank.

Efficient sludge accumulation and removal also very critical to performance of sedimentation tanks, apparently, mechanical sludge removal require electricity, in an area where the electricity is insufficient or energy consumption is a limiting factor for wastewater treatment plant, gravitational sludge removal thereby become the most preferable alternative solution. To remove sludge by gravity, sludge hoppers are installed close to the inlet side of the sedimentation tank, the bottom of the sedimentation tank should be tilted, so that sludge at the bottom of the sedimentation tank could move towards the inlet side, finally accumulated in sludge hopper, after certain interval, the sludge hoppers should be cleaned. Inlets should be designed to

dissipate energy of influent wastewater and distribute the incoming flow in order to establish the expected “plug flow” pattern in the tank. Because sludge collector usually equipped immediately beneath the inlet, if turbulence appeared in the inlet zone, stability of settled sludge in sludge collector may disturbed and hence influence performance of the tank, to stabilize incoming wastewater, baffle always equipped around inlet, in sedimentation tank without mechanically sludge scraper, the floor should be tilted sufficiently for gravitational self-sludge removal. Although the principle is simple, sludge hoppers are difficult to operate, sludge may stay on the slope or accumulated in corners. Incoming wastewater can be drawn downward, pass through the sludge hoppers or even bypass accumulated sludge, result to “rat hole” phenomena (Metcalf 2002).

To study the influence of density current and sludge accumulation in sedimentation tank, we have considered two phases simulation. Figure 8.1 presents the simulation results for volume fractions of sediments after 100s, 200s, 300s, 400s, 500s, 1000s, 2000s on cross-section of x-z plane, volume fraction of sediments at the tank bottom and plot of sediments along bottom of tank from inlet (position -16m) to outlet (position +16m) at time=2000s respectively.

## 8.1 Original sedimentation tank

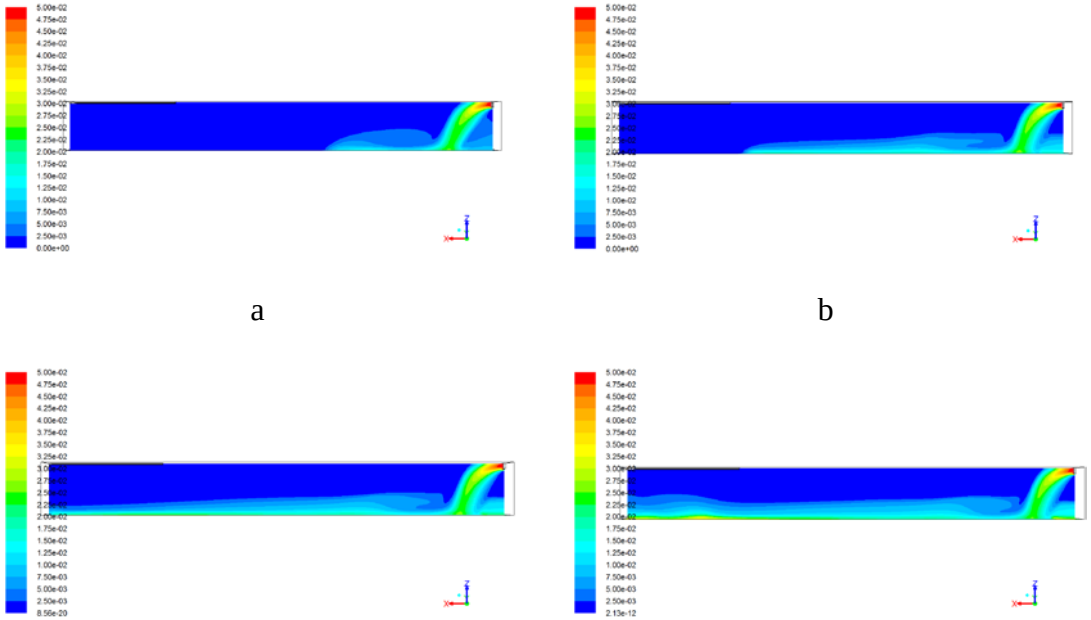

a b

c d

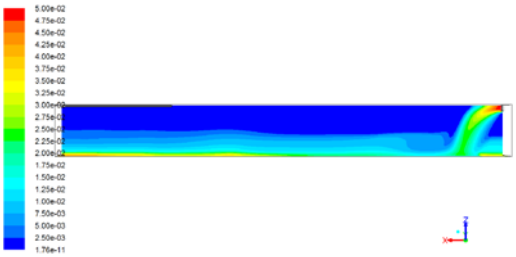

e

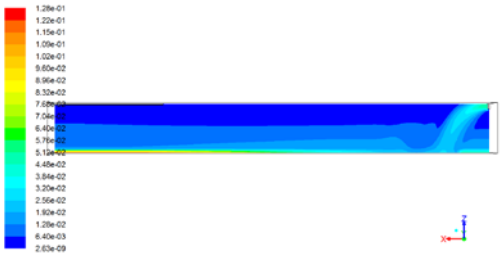

f

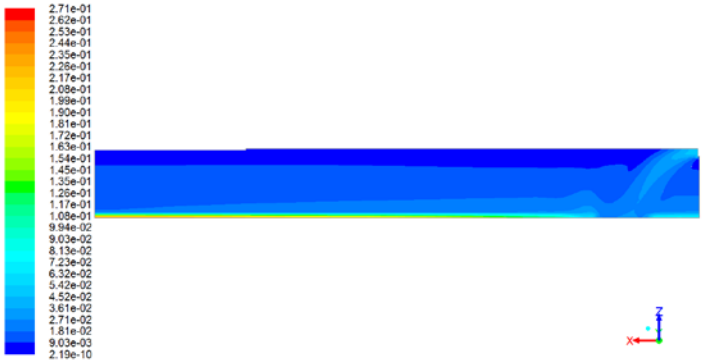

g

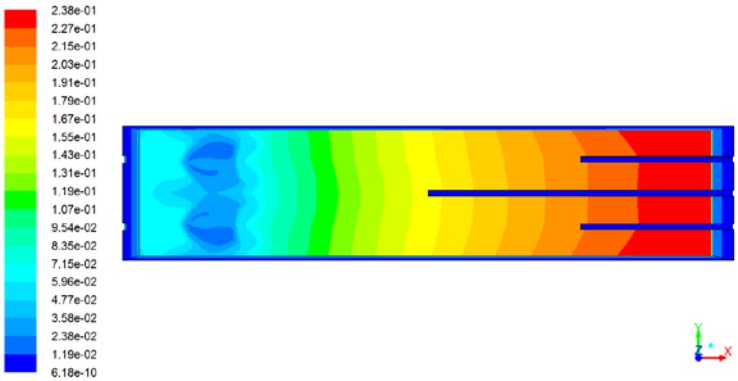

h

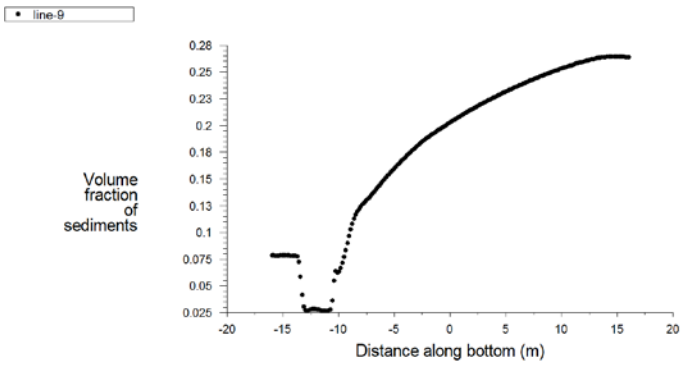
line-9
Volume fraction of sediments
0.26
0.25
0.23
0.2
0.18
0.15
0.13
0.1
0.075
0.05
0.025
-20
-15
-10
-5
0
5
10
15
20
Distance along bottom (m)

i

**Figure 8.1** Multiphase simulation of original tank

Figure 8.1 (a)-Figure 8.1 (g) show the evolution of density current in the original tank, the two phases fluid enter into inlet, due to the sediments phase have higher density, it sink to bottom of the tank and flow along the bottom, thus generate density current in sedimentation tank. Figure 8.1 (i) is plot of volume fraction of sediments along the bottom of tank from inlet to the outlet after 2000s simulation, at position -16 — -13 m, volume fraction around 0.075, from position -13m to -10 m, volume fraction of sediments decrease to 0.025, it mainly caused by splash effect of the density current, at position from -10m to +16m, volume fraction of sediments increase along bottom of tank, the highest value around 0.27.

## 8.2 Sedimentation tank with 4m baffle

a

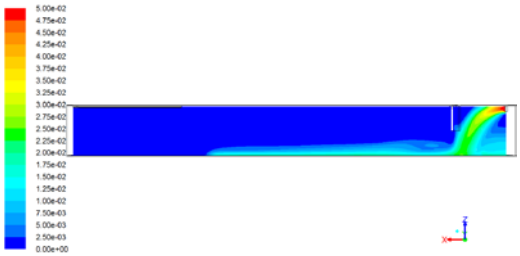

b

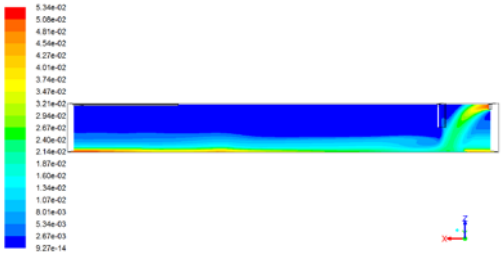

c

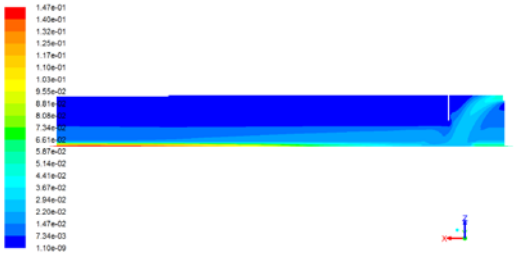

d

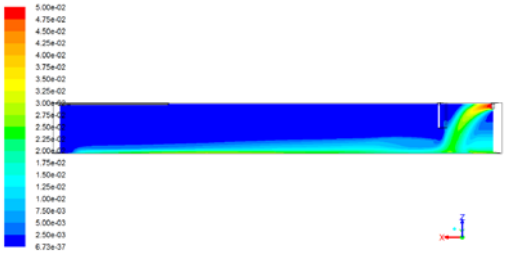

e

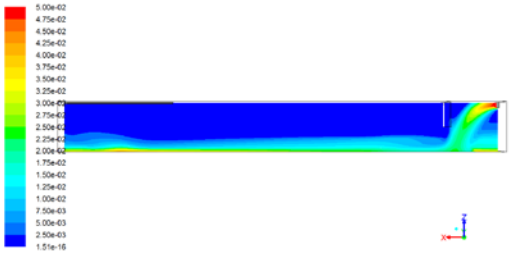

f

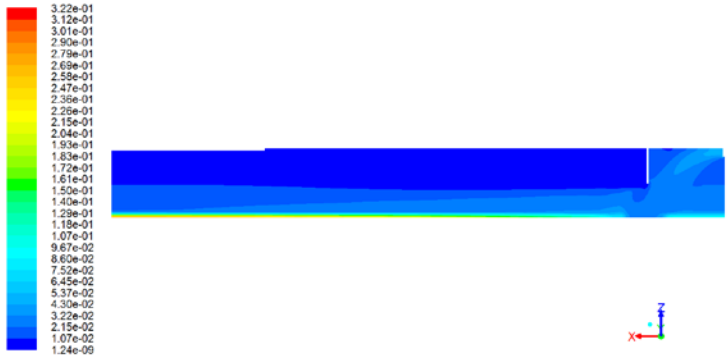


g

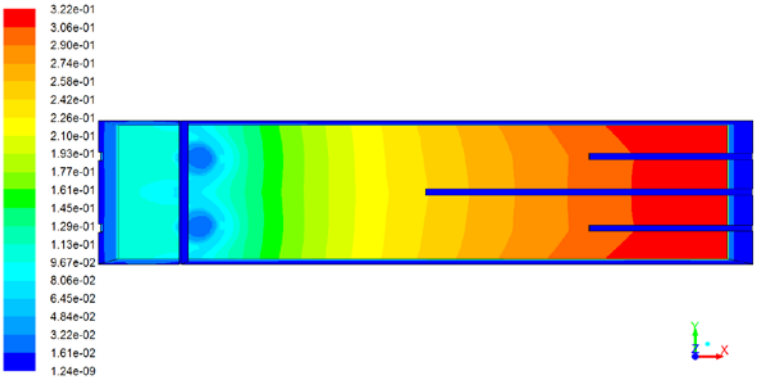


h

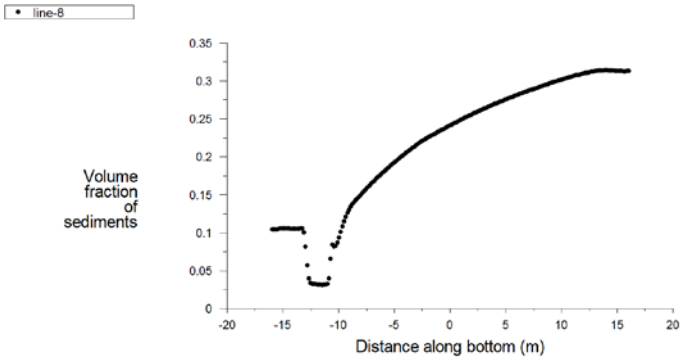


i

**Figure 8.2** Multiphase simulation of 4m baffle tank

Figure 8.2 (a)-Figure 8.2 (g) show the evolution of density current in the 4m baffle tank, the baffle direct fluid move downward and enhanced sedimentation effect. Figure 8.2 (i) is plot of volume fraction of sediments along the bottom of tank after 2000s simulation, at position -16 — -13 m, volume fraction around 0.1, from position -13m to -10 m, volume fraction of sediments decrease to 0.025 because of splash effect, at position from -10m to +16m, volume fraction of sediments increase along bottom of tank, highest value around 0.30. Compare to original tank, volume fraction of sediments in 4m baffle tank higher than original tank along the bottom of tank, which indicates the sedimentation effect in 4m baffle tank higher than original tank.

## 8.3 Sedimentation tank with 2m baffle

a

b

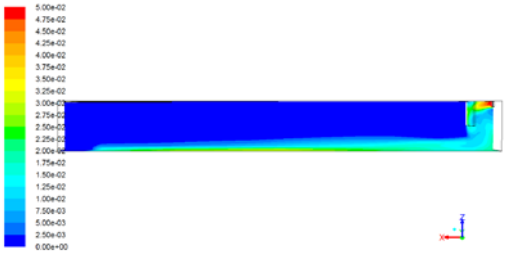

c

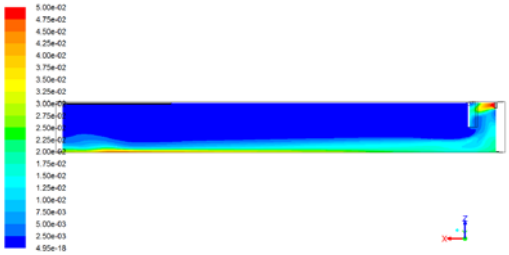

d

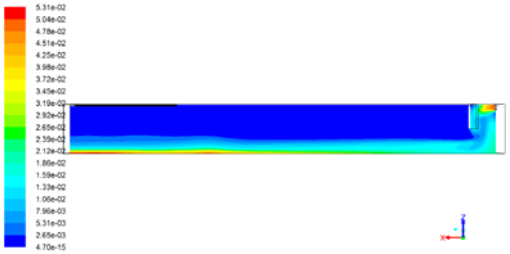

e

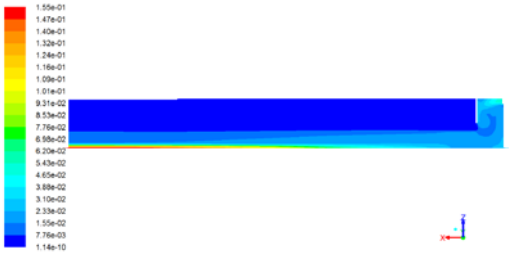

f

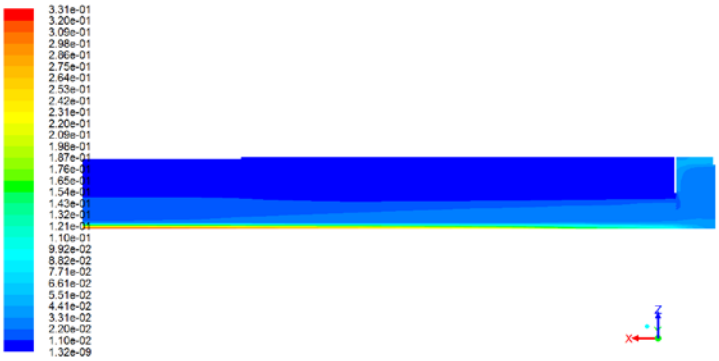

g

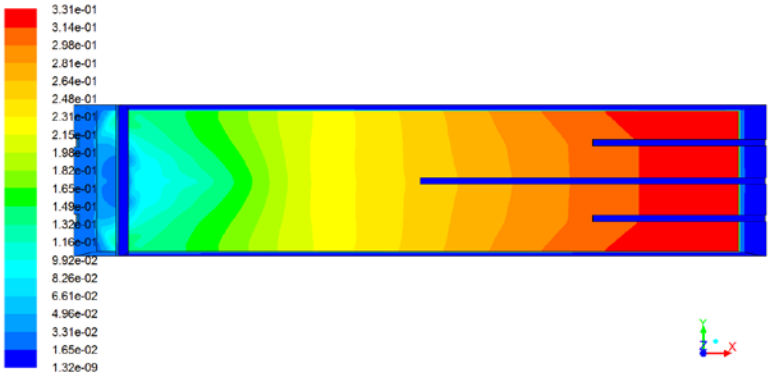


h

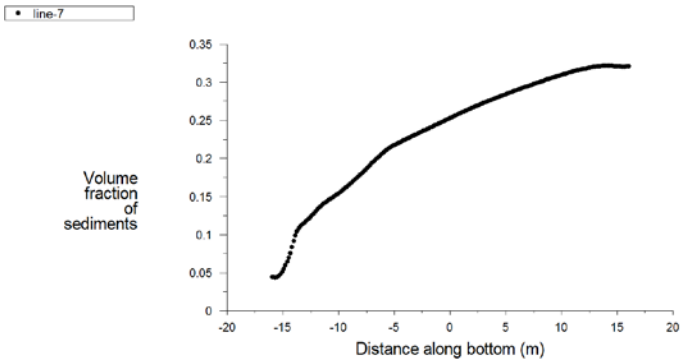


i

**Figure 8.3** Multiphase simulation of 2m baffle tank

Figure 8.3 (a)-Figure 8.3 (g) show the evolution of density current in the 2m baffle tank, the 2m baffle further enhanced sedimentation effect compare to the 4m baffle. Figure 8.3 (i) is plot of volume fraction of sediments along the bottom of tank after 2000s simulation, volume fraction of sediments increase along bottom of tank, the highest value around 0.33. Compare to original tank and 4m baffle tank, volume fraction of sediments in 2m baffle tank is the highest. Besides, splash effect due to density current almost removed.

### 8.4 4m baffle with titled bottom tank

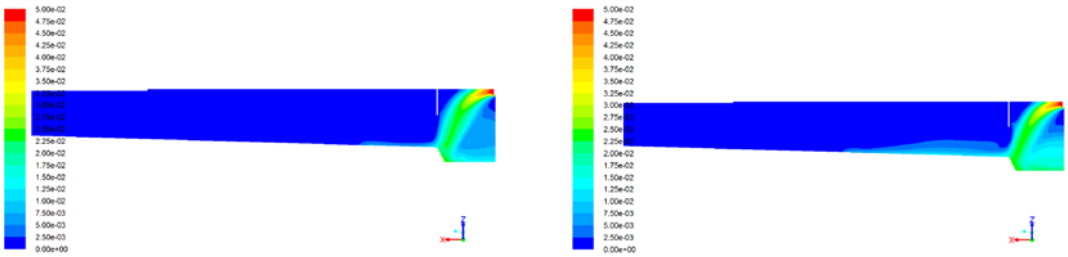

a b

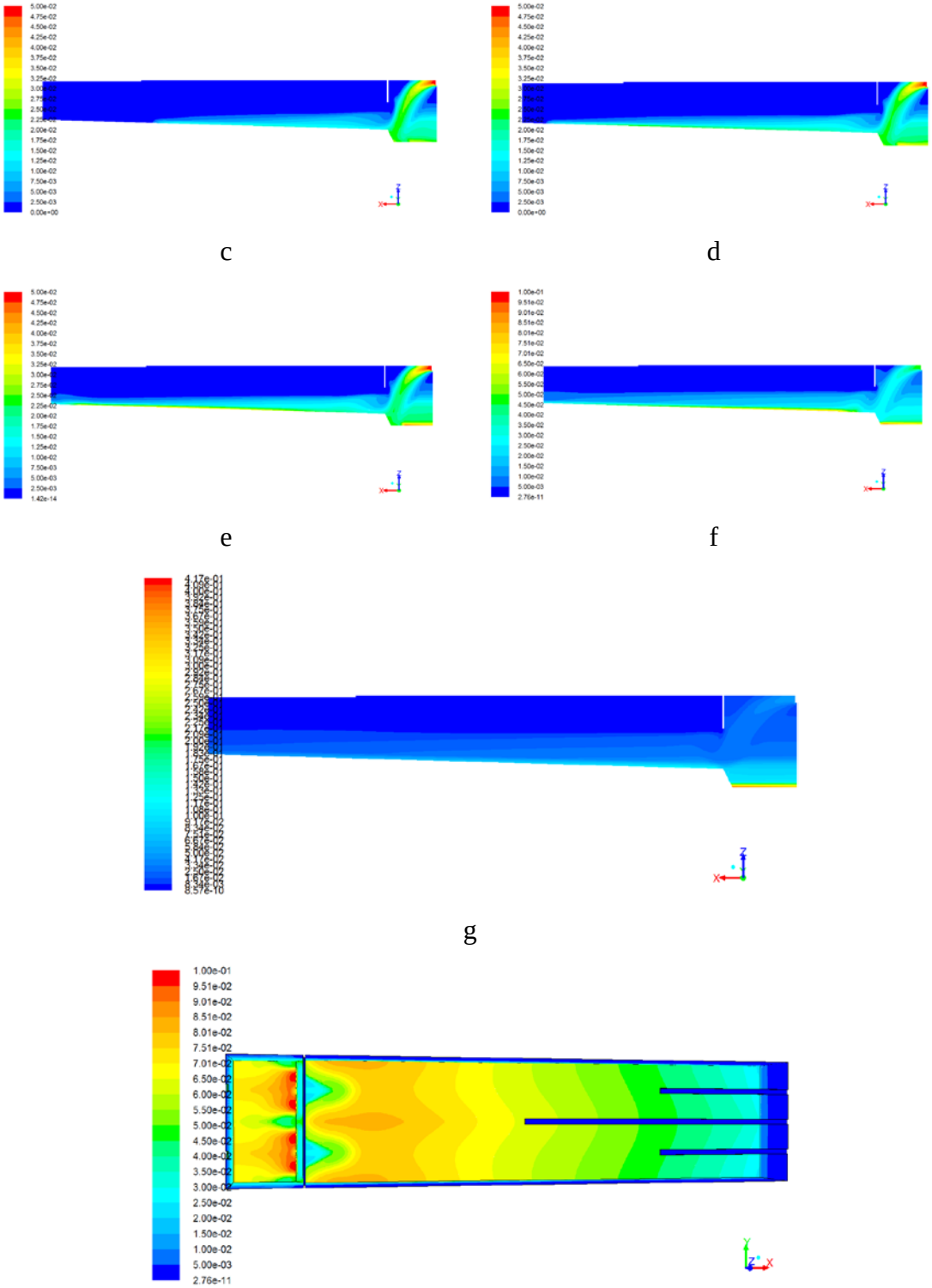

c d e f g h

**Figure 8.4** Multiphase simulation of 4m baffle with tilted bottom tank

As displayed in Figure 8.4 (h), with tilted bottom and sludge hopper, the highest sludge concentration appears near the inlet zone. Previous simulation results show that baffle, no matter 2 meters or 4 meters away from the inlet, could effectively forces the particles to move towards the bottom of the tank, the baffle also decreases

the recirculation zone occupied in the whole tank, thereby significantly improve performance of the sedimentation tank. Although the effect of baffle is significantly, one major problem still existed in the 2m baffle design and the 4m baffle design, which is distribution of sludge at the tank bottom, the highest sludge concentration detected near the outlet zone, volume fraction of sediments increase along tank bottom from the inlet to the outlet, with efficient sludge removal, this problem is neglectable, however, solids may accumulated near the outlet side with inappropriate sludge removal.

The above mentioned problem can be solved by install sludge hopper and tilt the tank bottom. As displayed in Figure.8.4 (a)-Figure.8.4 (g), the inflow wastewater move downward due to effect of baffle and gravity, unlike in the flat bottom tank, a portion of solids trapped in the sludge hopper rather than move towards the outlet side, the other portion of solids still could move alone tank bottom, however, because of the tank bottom is tilted, these solids will move back to the inlet side due to gravity.

The advantage of tilted bottom and sludge hopper is apparent, with effect of gravity, sludge hopper could trap incoming solids, tilted bottom could concentrate sludge in the sludge hopper, thereby the sedimentation tank can be cleaned without mechanical sludge removal, thus reduce overall energy consumption and financial investment.

### 8.5 2m baffle with titled bottom tank

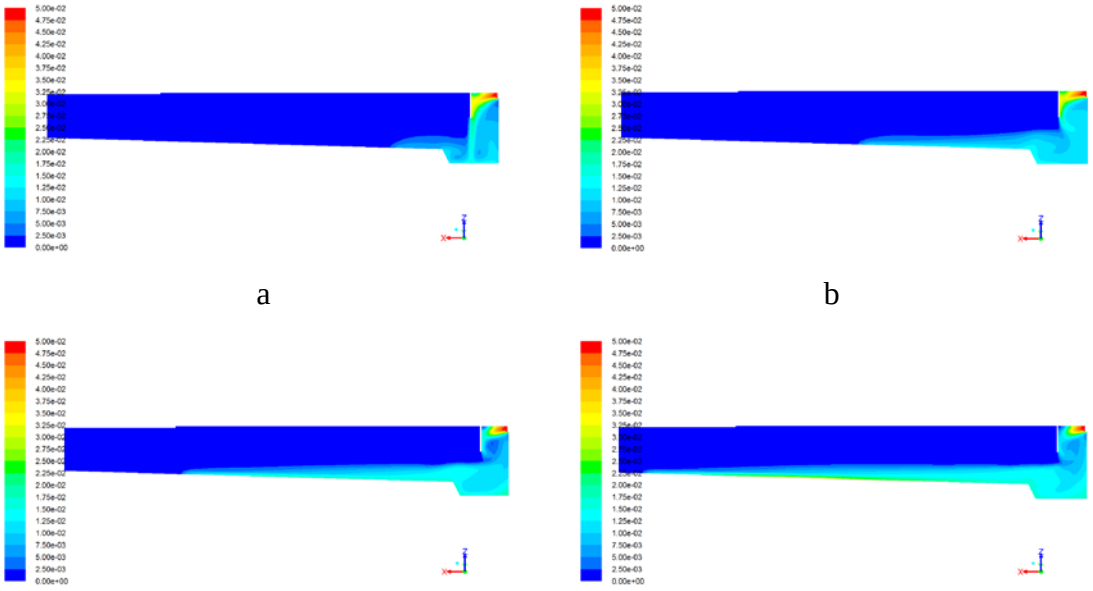

a b

c d

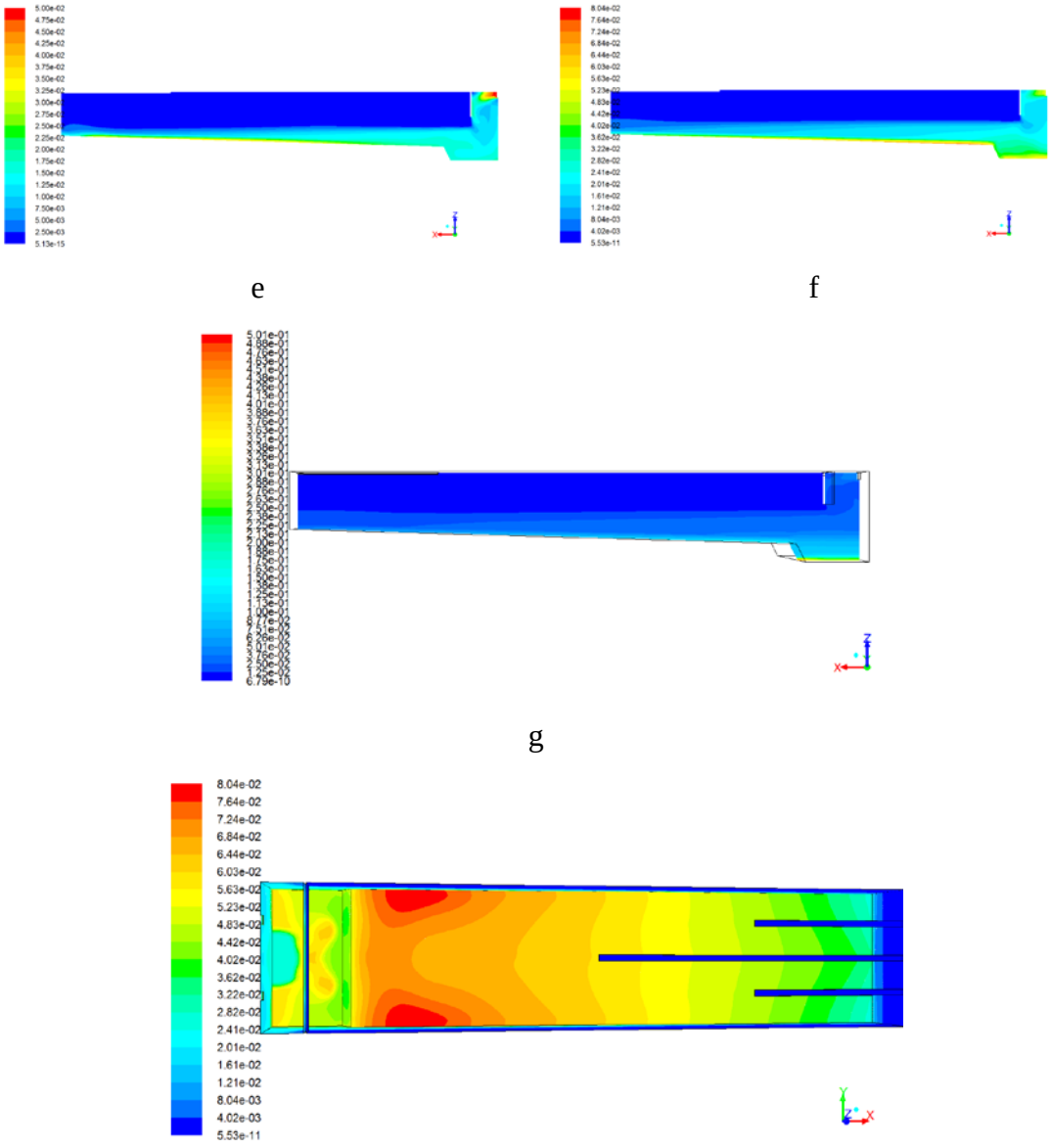

e f g h

**Figure 8.5** Multiphase simulation of 2m baffle with tilted bottom tank

Figure 8.5 is simulation result for the 2m baffle with tilted bottom design, with shorter distance between the inlet and baffle, the effect of baffle is more apparent. Incoming wastewater impact on the 2m baffle with higher velocity, thus the incoming wastewater also move downward with higher velocity, the incoming wastewater splash on the bottom of sludge hopper, solids influenced by the incoming wastewater, move towards the outlet along tank bottom, however, due to the tank bottom is tilted, the solids on the tank bottom also drag by the gravity force, thus move towards the inlet side. The splash force of incoming wastewater and gravity force finally balanced at the boundary of sludge hopper and slope, where is the highest solids concentration detected in Figure 8.5 (h).

## 8.6 Upward flow circular sedimentation tank

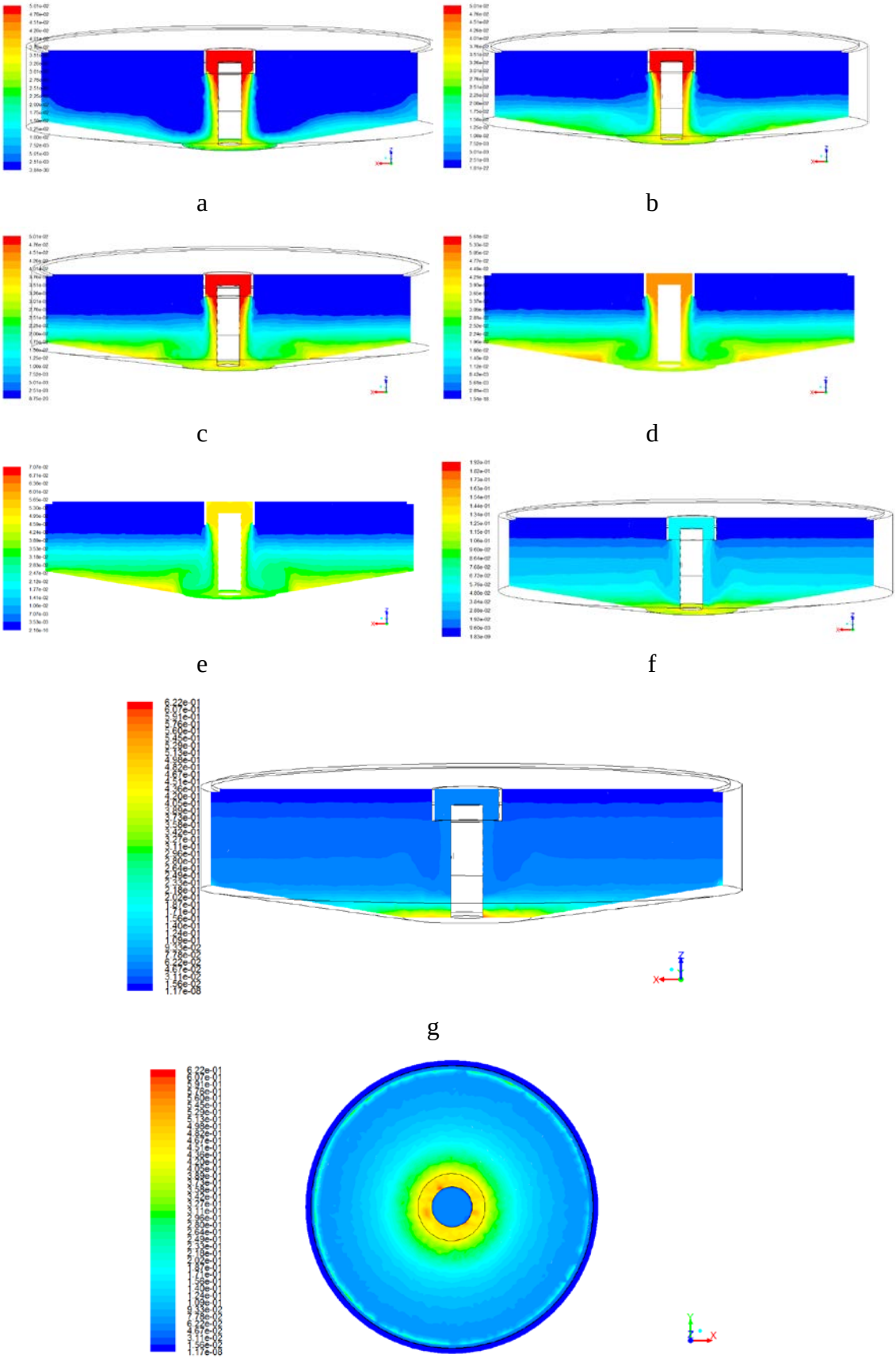

**Figure 8.6** Multiphase simulation of upward flow circular tank

As presented in Figure 8.6, a density current is detected, the density current due to higher density of the incoming solids. After reflected by the baffle around the inlet, this density current sinks toward the sludge blanket at the tank bottom, then flows towards the tank rim along tank bottom. With simulation time increase, solids accumulated in the sedimentation tank. In reality, the solids are discharged from the sludge discharger at the tank bottom, but this process is ignored in this study. It is obviously that the volume fraction of sludge is larger at the bottom and smaller at the top, larger at the tank center and smaller at the tank rim.

As illustrated in Figure 8.5 (h), near the center of the tank, there is a zone just below the baffle have smaller volume fraction of sediments, the solids concentration lower because of disturbance of fallen down wastewater, due to the sludge collector also locate in the center of the sedimentation tank, the disturbance of reflected wastewater may influence the removal efficiency of sedimentation tank.

### 8.7 Downward flow circular sedimentation tank

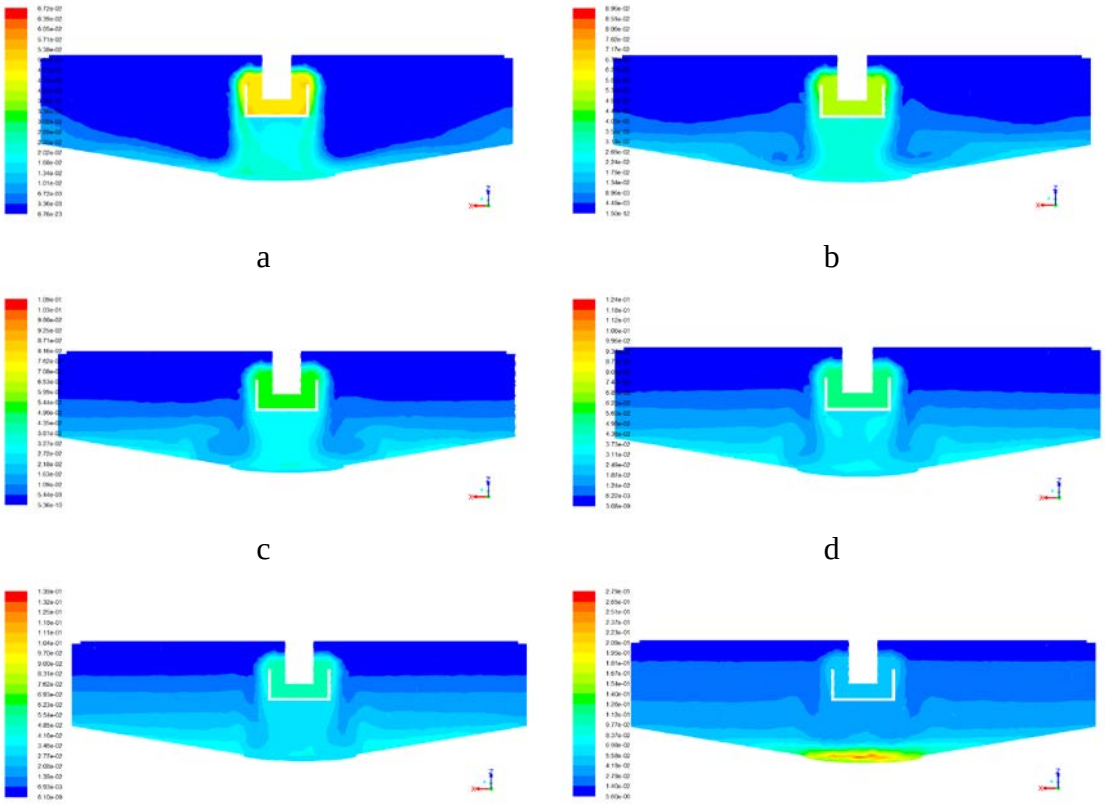

a b c d e f

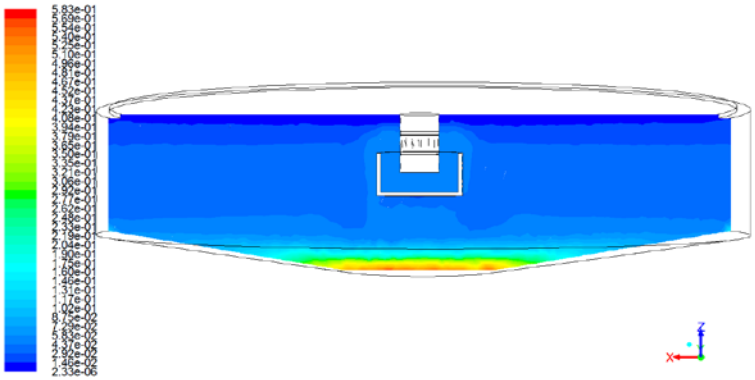

g

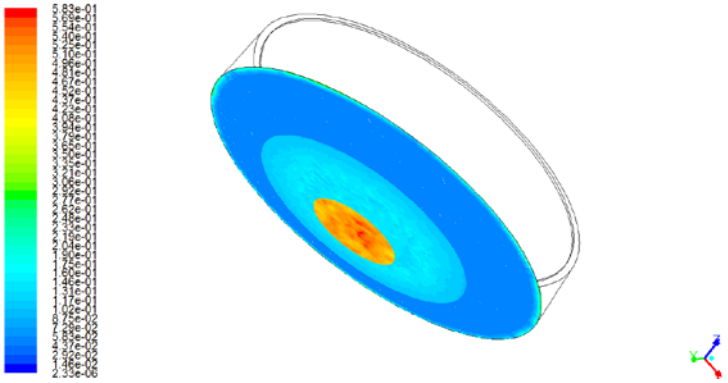

h

**Figure 8.7** Multiphase simulation of downward flow circular tank

As presented in Figures 8.7, unlike the upward flow circular sedimentation tank in which the incoming wastewater splash on the sludge layer directly, in the downward flow circular sedimentation tank, the incoming wastewater firstly reflected by the baffle at the end of the central pipe, after reflected by baffle, the incoming wastewater move upward towards tank rim, in this design, the sludge zone in the center of the tank protected by the baffle above it, so that the accumulated sludge will not disturbed by fallen down wastewater.

# Chapter 9 Lab flocculation unit simulation result

The model setup procedure for implementation of Multi-reference frame (MRF) and mixing simulation procedure described as follows:

•Define a three dimensional, steady state, implicit and pressure-based solver.

•Choose proper turbulence model from the viscous model panel. The standard k-ε model is employed in this study.

•Define material, the material used in this study is water.

•Define the operating conditions, set up direction and value of gravity.

•Define the boundary conditions: the whole computational zone is divided into moving zone and static zone in order to implement MRF, in the moving zone, the rotational speed is 150rpm. Define the impeller blades inside the moving zone as moving wall with rotate speed relative to the adjacent cell zone.

•Define the solution control, modify the under-relaxation factors and choose discretization schemes.

•Initialize the flow fields.

•Solve the flow fields until convergence.

Under laboratory condition, flocculation process optimization often achieved through jar test, the jar test procedure start with a glass vessel with agitator mixing the content, coagulants add into vessel and mixed for a short period of high speed rotating, this period represent the coagulation process, after this high speed mixing period, rotating speed of agitator slow down, this gentle mixing period represent flocculation, after mixing finished, flocs are settled and analyzed for flocculation effect and particle size distribution, jar test result can be used for flocculation procedure optimization.

In this part, hydraulic behavior of one flat blade turbine (FBT) and two pitched blade turbines (PBT) with different inclined angles used for jar test unit mixing are investigated by using CFD, the FBT is a jar test unit produced by Kemira. It had paddle with length 56 mm, width 2 mm and height 30 mm, which was located 45mm above bottom of beaker and the shaft had a diameter 4 mm and length 165mm. The beakers were 175mm tall and diameter 90 mm. The two PBTs have inclined angle 45° and 60° respectively. In further discussions, we name PBT with inclined angle 45°as PBT45 and PBT with inclined angle 60°as PBT60.

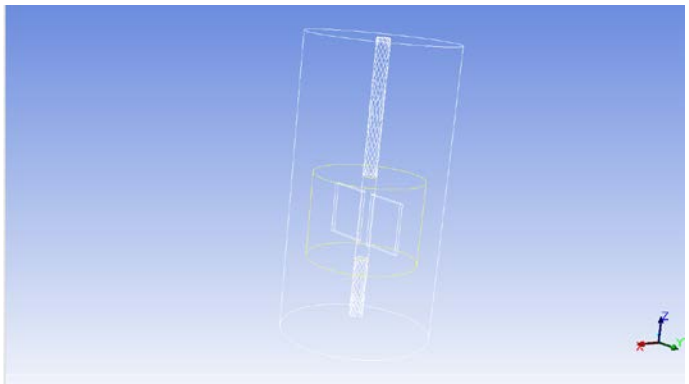

**Figure 9.1** The multi reference frame (MRF)

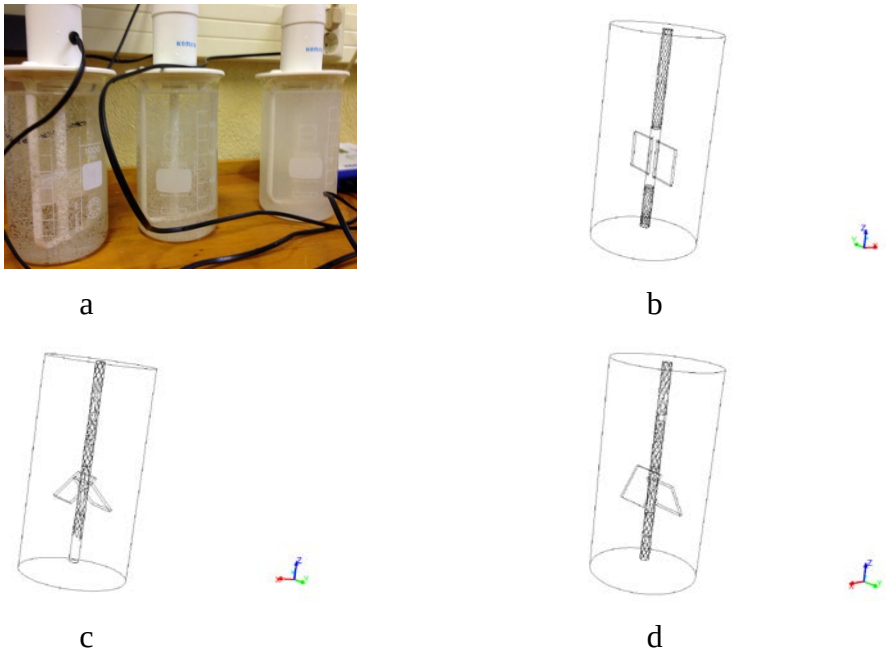

a b c d

**Figure 9.2** (a) the Kemira jar test unit and geometry models of: (b) FBT, (c) PBT 45 and (d) PBT 60

In order to implement MRF, the whole computational zone should be divided into several sub-zones. The Multi Reference Frame (MRF) is a modification of rotating frame model, in rotating frame model, momentum equation is solved for the whole computational domain, in MRF, several rotating frame is implemented and used in the simulation, so that complex reactor configuration, such as baffles, internal walls and heat exchangers can be simulated. The momentum equation inside rotating frame are solved in the frame of impeller, and outside rotating frame, equations are solved in static frame, at the interface between rotating frame and stationary frame, steady transfer should be achieved in order to exchange calculation result between two frames (Luo et al 1994). Figure 9.1 displayed the Multi-reference frame (MRF).

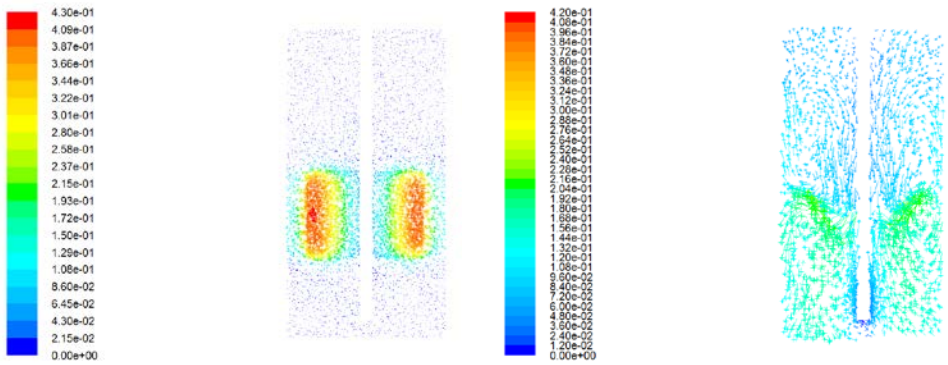


a b

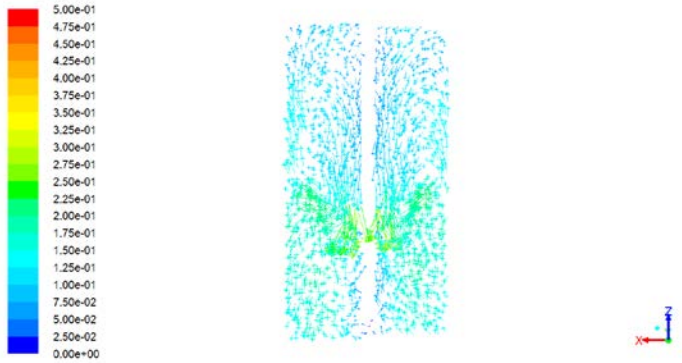


c

**Figure 9.3** Velocity vectors with different paddles and angles: (a) FBT, (b) PBT 45 and (c) PBT 60

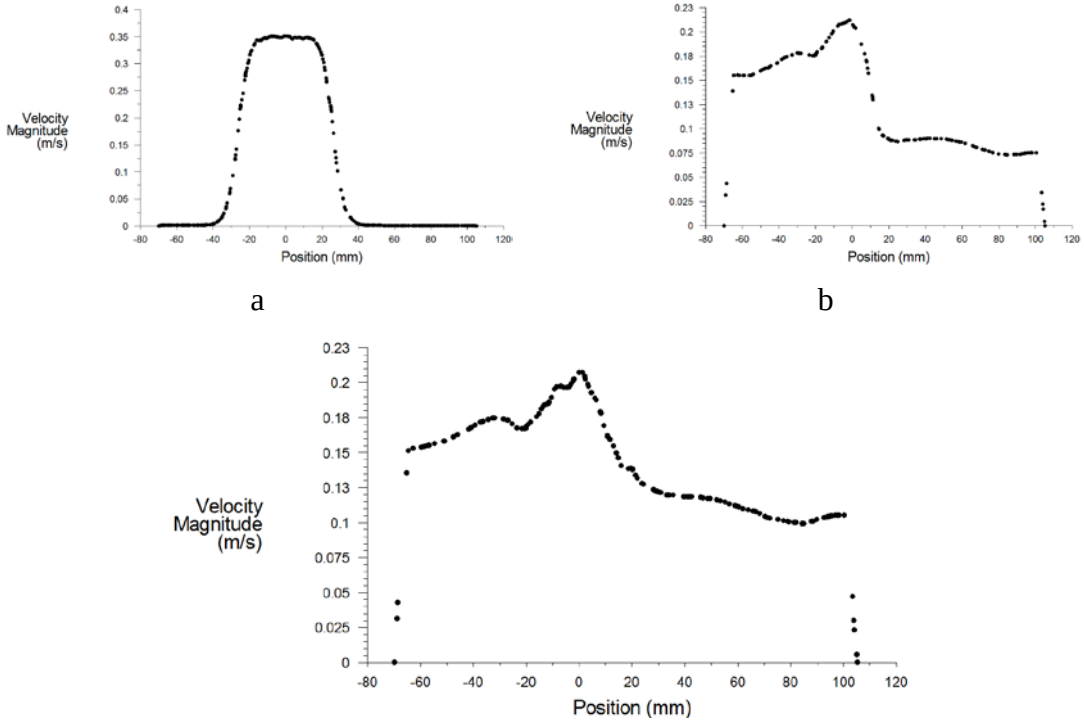


a b

c

**Figure 9.4** Plot of velocity gradient with different paddles and angles: (a) FBT, (b) PBT 45, (c) PBT 60

Figure 9.3 shows the velocity vectors of different paddles. In Figure 9.4, position refers to the point where the velocity gradient information was collected, which were located midway of shaft and beaker wall, along longitudinal direction of the beaker.

According to Figure 9.3 (a), in FBT the highest velocities are limited in the paddle zone. Figure 9.4 (a) shows that velocity is around 0.35m/s within the paddle zone,

while it decrease to near zero in other zones, indicating a poor mixing. Figure 9.4 (b) shows an enhancement in mixing by PBT45, where larger vectors indicating higher velocities also outside paddle zone. The direction of velocity vector indicates an increase movement of liquid. Figure 9.4 (b) shows improved velocity distribution compared with FBT, where the velocities vary 0.15-0.2 m/s from the bottom of beaker to paddle zone, while 0.075m/s above paddle zone. Figure 9.3 (c) and Figure 9.4 (c) follow tendency similar to PBT45, but superior performance.

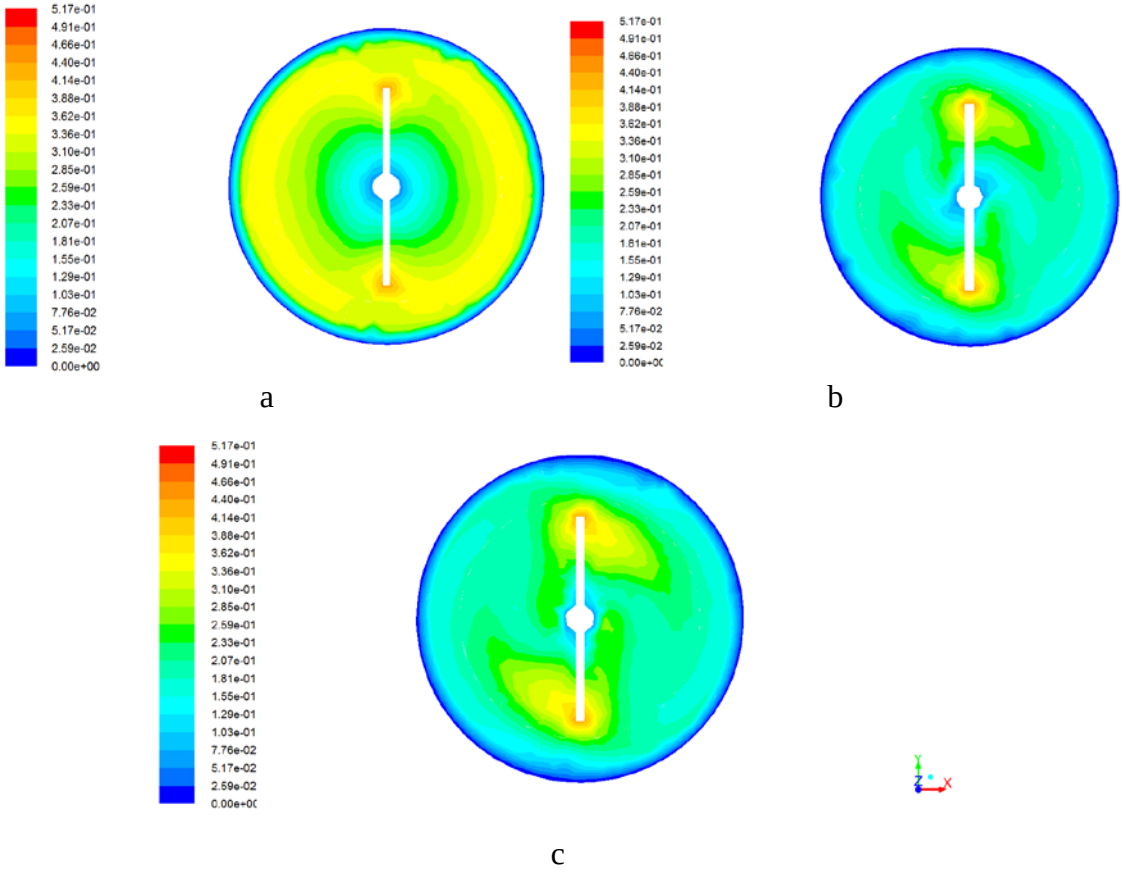


**Figure 9.5** Contours of velocity magnitude with different paddles and angles: (a) FBT, (b) PBT 45, (c) PBT 60

Contours of velocity magnitude for the FBT, PBT45 and PBT60 are displayed in Figure 9.5, the cross-section used for velocity magnitude display taken through the horizontal plane corresponding to the centreline of the FBT and PBTs. As displayed in Figure 9.5 (a), the mixing velocity of FBT is stronger compare to PBTs, in Figure 9.5 (b) and Figure 9.5 (c), the highest velocities are limited to the paddle tip zone. There is good distribution of velocities in both the PBT45 vessel and PBT60 vessel, for the FBT, it is apparent that the velocity in the center of vessel is lower, the uneven velocity distribution indicates poor mixing.

# Chapter 10 Conclusions and perspectives

In order to achieve objectives mentioned above, relevant literature which about sedimentation tank, jar test and CFD firstly studied, the major problems in current sedimentation tank and jar test unit, mathematical background of CFD, available models which describe turbulence flow and multi-phase flow, as well as mesh generation strategy then summarized. Based on background knowledge, single phase simulation and RTD simulation firstly performance towards the Drøbak WWTP, combine with tracer test result, several modified designs are proposed. The modified designs also studied and evaluated by using single phase simulation and RTD simulation. In addition, multi-phase simulation performance for all sedimentation tank designs. At last, the jar test unit also studied by using CFD and Multi-reference frame (MRF).

This study mainly focus on numerical study, it has demonstrated that CFD can be applied successfully to sedimentation tank and lab flocculation unit optimization. As mentioned above, the tracer test conducted in a full scale sedimentation tank with variable inlet velocity and wastewater properties, while in order to simplify the simulation due to limited computer power we assumed the inlet velocity and wastewater properties are constant, so that it's difficult to fully calibrate simulation result with the tracer test, however, even with so much assumptions and simplifications, the simulation result still follow trend similar to the tracer test result and supplied answers for problems detected in the original design, it means although there are a lot of simplifications in the simulation, CFD still could supply some references for engineers, it's an useful, economic alternative design tools. Commercial CFD software could provide reasonable simulation result and can be employed as a powerful tool in optimizing sedimentation tank and lab flocculation unit. CFD may serve as a useful instrument to estimate the different effects of design and performance of sedimentation tank and lab flocculation unit. However, it should be realized that all the simulations in this study were based on a series of simplification and assumption, Van der Walt (1998) pointed out, although there is a lot of simplification and approximation in numerical simulation process, numerical method still could improve our understanding about reality. For engineers, CFD is a reliable powerful tool rather than mathematical toy (Van der Walt and Haarhoff 2000), CFD can be applied in almost every process to optimize design and process operation, with the assistance of CFD, potential failures and optimization of water and wastewater treatment devices such as sedimentation tank and jar test unit can be detected and tested.

In this research, in addition to tracer test, single phase simulation and RTD simulation firstly performance by using CFD towards the Drøbak WWTP, from the tracer test and RTD simulation, a "two periods" phenomena is detected, the first period characterized by a steep peak and the second period represented by several smaller peak but last for longer time, from the single phase simulation, potential failures such

as strong surface current and internal circulation is detected, the single phase simulation result illustrated the reason of the “two periods” phenomena which detected from both the tracer test result and the RTD simulation result, the first steep peak caused by the strong surface current and the second period correspond to the re-circulating current. In general, re-circulating current is always existed in sedimentation tanks, circulation zones also known as dead zones, dead zones occupy the effective sedimentation volume, so that the sedimentation tank will have less volume for settling, thereby the existence of re-circulating current or circulation zones will reduce tank efficiency.

The original design was characterized by strong surface current and large re-circulation zones. In order to solve problems caused by the strong surface current and re-circulating current, four optimized design with baffle at different positions and tilted bottom thus proposed and tested by using CFD approach, baffle can be installed easily and economically without significant influence on the operation. Single phase CFD simulation result shows that baffle re-distribute incoming wastewater on the whole cross-section, reduced surface current and re-circulation regions. By displaying contour of velocity magnitude, contour of kinetic energy and velocity vectors, we found baffle in suitable location and tilted bottom reduces the circulation zone and kinetic energy, create uniform velocity vector inside the sedimentation tank. Therefore, the baffle and tilted bottom improved the hydraulic efficiency of the original sedimentation tank. Moreover, for comparison of the effect of different sedimentation tank designs, the RTD simulation was ran, some key RTD parameters, such as $t_{10}$, $t_{75}$–$t_{25}$, $t_{90}$–$t_{10}$, and $t_{90}/t_{10}$ value, is used to compare efficiency of different designs.

To study the application of CFD in different tank sharps, two novel circular sedimentation tank designs are proposed and simulated, re-circulating current in radial direction is detected in both upward flow and downward flow circular sedimentation tank, the re-circulating current characterized by forward current towards tank rim in the lower tank region and backward current towards tank inlet in the zone close to tank surface, in the downward flow circular sedimentation tank design, simulation result shows that the reflector under the center tube could distribute the inflow wastewater, help the wastewater distributed evenly throughout the radial range of sedimentation tanks, thus improve the hydraulic efficiency. However, problems such as strong re-circulating and strong degree of mixing are detected through check the RTD parameters.

Two-phase simulation also performance with purpose of density current and sludge accumulation study, in terms of the flat bottom tanks simulation, it shown that 4m baffle and 2m baffle designs could enhance sedimentation effect, plot of volume fraction of sediments along bottom of tank testify the volume fraction of sediments in baffle equipped tank higher than original tank, which means more sediments stay inside the tank rather than escape from outlet, 2m baffle tank even remove splash effect caused by density current, give bottom sludge more stable condition.

In flat bottom tanks, volume fraction of sediments increase along the tank bottom from the inlet side to the outlet side, in baffle equipped tanks with tilted bottom, an apparent improvement is the highest volume fraction of sediments appear near the inlet side rather than the outlet side, this improvement is important for sedimentation tank without mechanical cleaning, a tilted bottom could accumulate sludge in the sludge hopper which locate just beneath the inlet, help the sedimentation tank achieve self-gravitational cleaning.

In circular sedimentation tank, two-phase simulation also performance, for the upward flow circular sedimentation tank case, it is detected that the incoming sediment sinks to the sludge blanket which locate in the center of the circular tank, then flows towards the tank rim. One major problem for the upward flow circular sedimentation tank is incoming wastewater splash on the sludge layer directly, which may disturb the stability of settled sludge, so that the downward flow circular sediment tank is proposed, with reversed feed tube and reflector, the sludge layer is protected by above reflector, thus the sludge layer will have less disturbance.

In addition to sedimentation tank, CFD simulation also performance towards mixing unit used in jar test, the mixing efficiency of one FBT and two PBTs are studied through display contour of velocity magnitude and velocity vectors. For the jar test unit simulation, our conclusion is that CFD gives a unique insight to the hydraulics in jar tests as well as suggestions for improvements, which should be considered in construction of mixing units, since it is necessary to secure even and immediate mixing of the coagulants with the whole water mass to optimally utilize the hydrolysis spices produces within fractions of seconds in coagulation processes.

In general, CFD provides new insight into the sedimentation tank and lab flocculation unit design, CFD supply useful information for further research and design. CFD can model internal changes (e.g. baffles, hopper shape and mixer) as well as external changes (inlet velocity, volume fraction and hydraulic load). So that CFD is a powerful tool that can optimize both the operation and geometry of water and wastewater treatment devices. The application of CFD is significant cost savings, because the effects of different geometry models and operation conditions were examined in computer, without implementation of any modification in the real world. The application of CFD can be employed as the first step in the process of optimizing wastewater treatment reactors.

This work has demonstrated clearly the benefits can be gained from CFD. As mentioned above, CFD can be applied in the design of almost every processes of water and wastewater treatment, in the future, with increasing computer power and simplified software, the application of CFD will spread from academic environment to industries. In physical treatment processes, in order to find potential failures such as dead zone, short circuiting and eddy, CFD can be used to detect hydraulic

performance of treatment unit. Besides, multi-phase simulation is suggested for further evaluation of physical treatment unit, for example, liquid-liquid or liquid-solid simulation, represent wastewater with different density and wastewater with particles, is recommended in sedimentation tank research, air-water or air-water-solid simulation is more suitable for DAF research, porous media model is perfect for filtration or membrane devices research.

In chemical treatment processes, CFD research currently mainly focus on coagulation or flocculation simulation, besides study mixing effect of different mixing equipment and configuration or flocculation tank, more and more research begin to coupling chemical reaction model with CFD, the most advanced model is population balance model (PBM), this model could describe particle-particle interaction, such as breakage, aggregation and nucleation, make it perfectly suitable for flocculation simulation, so that in flocculation and coagulation field, the CFD-PBM model will play an important role in the foreseeable future. For other complex chemical treatment processes, chemical reaction can be studied use species transport and reaction model, this model simulate chemical reaction through define volume fraction of different elements and Stoichiometric coefficient.

Biological treatment also can be optimized by CFD, besides hydro-dynamics simulation and multi-phase model mentioned above, biological kinetics could couple with CFD via User Define Function (UDF), UDF in CFD means coupling commercial CFD software with an extra C programming file, commercial CFD software users could programing according to their individual requirement, UDF supply a flexible method for CFD software users and extend application area of CFD.

All in all, no matter in physical, chemical and biological treatment processes, as well as other components in wastewater treatment, such as disinfection, sludge treatment, odour control, pumping station or even sewer line optimization, CFD can be used in all of these processes. CFD will bring new concepts and ideas for water and wastewater industries, change the traditional design methodology of water and wastewater devices, in the foreseeable future, we will see more and more applications of CFD in water and wastewater treatment field.

# References:


Anderson, J. D. (1995). Computational fluid dynamics (Vol. 206). New York: McGraw-Hill.

ANSYS Inc. (2009). ANSYS Fluent 14.0 Theory Guide. *Fluent documentation*.

Ahrokhi, M., Rostami, F., Md Said, M. A., & Sabbagh Yazdi, S. R. (2012). The effect of number of baffles on the improvement efficiency of primary sedimentation tanks. *Applied Mathematical Modelling*, *36*(8), 3725-3735.

Biswas, G., & Eswaran, V. (Eds.). (2002). *Turbulent flows: fundamentals, experiments and modeling*. CRC Press

Buwa, V. V., Deo, D. S., & Ranade, V. V. (2006). Eulerian–Lagrangian simulations of unsteady gas–liquid flows in bubble columns. *International Journal of Multiphase Flow*, *32*(7), 864-885.

Bridgeman, J., Jefferson, B., & Parsons, S. A. (2009). Computational fluid dynamics modelling of flocculation in water treatment: a Review.

Bridgeman, J., Jefferson, B., & Parsons, S. A. (2010). The development and application of CFD models for water treatment flocculators. *Advances in Engineering Software*, *41*(1), 99-109.

Camp T. R. and Stein P. C. (1943) Velocity gradients and internal work in fluid motion. *J. Boston Soc. Civ. Eng.* 30, 219±237.

Chambers, B. (1993). Batch operated activated sludge plant for production of high effluent quality at small works. *Water Science & Technology*, *28*(10), 251-258.

Calhoun, D. A., Helzel, C., & LeVeque, R. J. (2008). Logically rectangular grids and finite volume methods for PDEs in circular and spherical domains.*SIAM review*, 723-752.

Crittenden, J. C., Trussell, R. R., Hand, D. W., Howe, K. J., & Tchobanoglous, G. (2012). *MWH's Water Treatment: Principles and Design*. Wiley.

Delnoij, E., Kuipers, J. A. M., & Swaaij, V. W. (1998). Numerical simulation of bubble coalescence using a Volume of Fluid (VOF) model.

Deininger, A., Holthausen, E., & Wilderer, P. A. (1998). Velocity and solids distribution in circular secondary clarifiers: full scale measurements and numerical modelling. *Water Research*, *32*(10), 2951-2958.

Ding, A., Hounslow, M. J., & Biggs, C. A. (2006). Population balance modelling of activated sludge flocculation: Investigating the size dependence of aggregation, breakage and collision efficiency. *Chemical engineering science*, *61*(1), 63-74.

Edzwald, J. K. (2010). Dissolved air flotation and me. *Water research*, *44*(7), 2077-2106.

Fromm, J. E., & Harlow, F. H. (1963). Numerical solution of the problem of vortex street development. *Physics of Fluids*, *6*, 975.

Ferziger, J. H., & Perić, M. (1996). *Computational methods for fluid dynamics* (Vol. 3). Berlin: Springer.

Fogler, H. S. (1999). Elements of chemical reaction engineering.

Fluent, I. N. C. (2006). FLUENT 6.3 user's guide. *Fluent documentation*.

Fayolle, Y., Cockx, A., Gillot, S., Roustan, M., & Héduit, A. (2007). Oxygen transfer prediction in aeration tanks using CFD. *Chemical Engineering Science*, *62*(24), 7163-7171.

Gentry, R. A., Martin, R. E., & Daly, B. J. (1966). An Eulerian differencing method for unsteady compressible flow problems. *Journal of Computational Physics*, 1(1), 87-118.

Gavrilescu, M., & Macoveanu, M. (1999). Process engineering in biological aerobic waste‐water treatment. *Acta biotechnologica*, *19*(2), 111-145.

Gubelt, G., Lumpe, C., Verstraeten, E., & Joore, L. (2000). Towards zero liquid effluent at Niederauer Mühle: the validation of two novel separation technologies. *Paper technology*, *41*(8), 41-48.

Goula, A. M., Kostoglou, M., Karapantsios, T. D., & Zouboulis, A. I. (2008). The effect of influent temperature variations in a sedimentation tank for potable water treatment—A computational fluid dynamics study. *Water research*, 42(13), 3405-3414.

Goula, A. M., Kostoglou, M., Karapantsios, T. D., & Zouboulis, A. I. (2008). A CFD methodology for the design of sedimentation tanks in potable water treatment: Case study: The influence of a feed flow control baffle. *Chemical Engineering Journal*, *140*(1), 110-121.

Hazen, A. (1904). On sedimentation. *Transactions of the American Society of Civil Engineers*, *53*(2), 45-71.

Harlow, F. H., & Welch, J. E. (1965). Numerical Calculation of Time‐Dependent Viscous Incompressible Flow of Fluid with Free Surface. *Physics of fluids*, *8*, 2182.

Hess, J.L.; A.M.O. Smith (1967).Calculation of Potential Flow About Arbitrary Bodies. *Progress in Aerospace Sciences* **8**: 1–138.

Harleman, D. R. F., & Murcott, S. (1999). The role of physical-chemical wastewater treatment in the mega-cities of the developing world. *Water Science and Technology*, *40*(4), 75-80.

Huang, S., & Li, Q. S. (2010). A new dynamic one‐equation subgrid‐scale model for large eddy simulations. *International Journal for Numerical Methods in Engineering*, *81*(7), 835-865.

Jones, W. P., & Launder, B. (1972). The prediction of laminarization with a two-equation model of turbulence. *International journal of heat and mass transfer*, *15*(2), 301-314.

Kynch, G. J. (1952). A theory of sedimentation. *Transactions of the Faraday society*, *48*, 166-176.

Katz, V. J. (1979). The history of Stokes' theorem. *Mathematics Magazine*, 146-156.

Kim, T., Kato, S., & Murakami, S. (2001). Indoor cooling/heating load analysis based on coupled simulation of convection, radiation and HVAC control. *Building and Environment*, *36*(7), 901-908.

Kim, J. K., Oh, B. R., Chun, Y. N., & Kim, S. W. (2006). Effects of temperature and hydraulic retention time on anaerobic digestion of food waste. *Journal of Bioscience and Bioengineering*, *102*(4), 328-332.

Khalil, E. (2012). CFD History and Applications. CFD Letters, 4(2), 43-46.

Launder, B. E., & Sharma, B. I. (1974). Application of the energy-dissipation model of turbulence to the calculation of flow near a spinning disc. *Letters in heat and mass transfer*, *1*(2), 131-137.

Launder, B. E., Reece, G. J., & Rodi, W. (1975). Progress in the development of a Reynolds-stress

turbulence closure. *Journal of fluid mechanics*, *68*(03), 537-566.

Larsen, P. (1977). *On the hydraulics of rectangular settling basins: experimental and theoretical studies*. Department of Water Resources Engineering, Lund Institute of Technology, University of Lund.

Luo, J. Y., Issa, R. I., & Gosman, A. D. (1994). Prediction of impeller induced flows in mixing vessels using multiple frames of reference. In *Institution of Chemical Engineers Symposium Series* (Vol. 136, pp. 549-549). HEMSPHERE PUBLISHING CORPORATION.

Laari, D. S. A. (2010). *CFD Simulation of Two-phase and Three-phase Flows in Internal-loop Airlift Reactors* (Doctoral dissertation, LAPPEENRANTA UNIVERSITY OF TECHNOLOGY).

Menter, F. R. (1994). Two-equation eddy-viscosity turbulence models for engineering applications. *AIAA journal*, *32*(8), 1598-1605.

Metcalf, E. (2002). Wastewater engineering: treatment and reuse. *McGraw-Hill, New York*.

Meroney, R. N., & Colorado, P. E. (2009). CFD simulation of mechanical draft tube mixing in anaerobic digester tanks. *water research*, *43*(4), 1040-1050.

Mohanarangam, K., & Stephens, D. W. (2009, December). CFD Modeling of floating and settling phases in settling tanks. In *Seventh International Conference on CFD in the Minerals and Process Industries* (pp. 9-11). CSIRO.

Norcross, K. L. (1992). Sequencing batch reactors-an overview. *Water Science & Technology*, *26*(9-11), 2523-2526.

Patankar, S. V., & Spalding, D. B. (1972). A calculation procedure for heat, mass and momentum transfer in three-dimensional parabolic flows. International Journal of Heat and Mass Transfer, 15(10), 1787-1806.

Peyret, R. (Ed.). (1996). *Handbook of computational fluid mechanics*. Academic Press.

Paul, E. L., Atiemo-Obeng, V., & Kresta, S. M. (Eds.). (2004). *Handbook of industrial mixing: science and practice*. Wiley. com.

Prosperetti, A., & Tryggvason, G. (Eds.). (2007). *Computational methods for multiphase flow*. Cambridge University Press.

Richardson, L. F. (1910). On the approximate arithmetical solution by finite differences of physical problems involving differential equations, with an application to the stresses in a masonry dam. Proceedings of the Royal Society of London. Series A, 83(563), 335-336.

Ravina, L., & Moramarco, N. (1993). Everything you want to know about Coagulation & Flocculation. *Zeta-Meter, Inc*.

Rajvaidya, N., & Markandey, D. K. (1998). *Advances in Environmental Science and Technology. Vol 7: Treatment of Pulp-and Paper Industrial Effluent*. New Delhi: A P H Pub. Corp.

Rauen, W. B., Angeloudis, A., & Falconer, R. A. (2012). Appraisal of chlorine contact tank modelling practices. *water research*.

Stamou, A. I. (1991). On the prediction of flow and mixing in settling tanks using a curvature-modified k-ϵ model. *Applied mathematical modelling*, *15*(7), 351-358.

Schlichting, H., & Gersten, K. (2000). *Boundary-layer theory*. Springer.

Schmitt, F. G. (2007). About Boussinesq's turbulent viscosity hypothesis: historical remarks and a direct evaluation of its validity. *Comptes Rendus Mécanique*, *335*(9), 617-627.

Stamou, A. I. (2008). Improving the hydraulic efficiency of water process tanks using CFD models. *Chemical Engineering and Processing: Process Intensification*, *47*(8), 1179-1189.

Shahrokhi, M., Rostami, F., Md Said, M. A., & Sabbagh Yazdi, S. R. (2012). The effect of number of baffles on the improvement efficiency of primary sedimentation tanks. *Applied Mathematical Modelling*, *36*(8), 3725-3735.

Shahrokhi, M., Rostami, F., & Said, M. A. M. (2012). Numerical modeling of baffle location effects on the flow pattern of primary sedimentation tanks. *Applied Mathematical Modelling*.

Thomas, D. N., Judd, S. J., & Fawcett, N. (1999). Flocculation modelling: a review. *Water Research*, *33*(7), 1579-1592.

Thompson, G., Swain, J., Kay, M., & Forster, C. F. (2001). The treatment of pulp and paper mill effluent: a review. *Bioresource Technology*, *77* (3), 275-286.

Tryggvason, G., Bunner, B., Esmaeeli, A., Juric, D., Al-Rawahi, N., Tauber, W., ... & Jan, Y. J. (2001). A front-tracking method for the computations of multiphase flow. *Journal of Computational Physics*, *169*(2), 708-759.

Terashima, M., Goel, R., Komatsu, K., Yasui, H., Takahashi, H., Li, Y. Y., & Noike, T. (2009). CFD simulation of mixing in anaerobic digesters.*Bioresource technology*, *100*(7), 2228-2233.

Tan Lixin, Li Kaizhan, & Li Bo. (2009). Two-Dimensional Numerical Simulation of the Two-Phase Flow in Rectanangular Secondary Settling Tanks. *Journal of Xi'an University of Technology 25*(2), 197-201.

Tryggvason, G., & Scardovelli, R. (2011). Direct numerical simulations of gas-liquid multiphase flows. Cambridge University Press.

Tan Lixin, Li Bo, & Li Erkang. (2013). Numerical Simulation of the effect of temperature difference on gravity flow in Rectanangular Secondary Settling Tanks. *Journal of Xi'an University of Technology* 29(2), 182-187.

Van der Walt, J. J. (1998). Is a sedimentation tank really that simple. In *Proceedings of the WISA Biennale Conference and Exhibition, Cape Town, South Africa*.

Van der Walt, J. J., & Haarhoff, J. (2000). Is CFD an engineering tool or toy. In *Proceedings of the Sixth Biennial Conference of the Water Institute of Southern Africa, Sun City*.

Versteeg, H. K., & Malalasekera, W. (2007). *An introduction to computational fluid dynamics: the finite volume method*. Pearson Education.

Wilcox, D. C. (1988). Reassessment of the scale-determining equation for advanced turbulence models. *AIAA journal*, *26*(11), 1299-1310.

Wilcox, D. C. (1998). *Turbulence modeling for CFD* (Vol. 2, pp. 103-217). La Canada, CA: DCW industries.

Wilderer, P. A., Irvine, R. L., & Goronszy, M. C. (Eds.). (2001). *Sequencing batch reactor*

*technology* (Vol. 10). IWA publishing.

Wenta B. & Hartmen B. (2002). Dissolved air flotation system improves wastewater treatment at Glatfelter *Pulp Pap*, 76 (3), 43–47.

Wu, B. (2012). Advances in the use of CFD to characterize, design and optimize bioenergy systems. *Computers and Electronics in Agriculture*.

Yakhot, V. S. A. S. T. B. C. G., Orszag, S. A., Thangam, S., Gatski, T. B., & Speziale, C. G. (1992). Development of turbulence models for shear flows by a double expansion technique. *Physics of Fluids A: Fluid Dynamics (1989-1993)*, *4*(7), 1510-1520.

You, D., & Moin, P. (2007). A dynamic global-coefficient subgrid-scale eddy-viscosity model for large-eddy simulation in complex geometries. *Physics of Fluids (1994-present)*, *19*(6), 065110.

Zhu, G., Zhang, Y., Ren, J., Qiu, T., & Wang, T. (2012). Flow Simulation and Analysis in a Vertical-Flow Sedimentation Tank. *Energy Procedia*, *16*, 197-202.

Žarković, D. B., Todorović, Ž. N., & Rajaković, L. V. (2011). Simple and cost-effective measures for the improvement of paper mill effluent treatment–A case study. *Journal of Cleaner Production*, *19*(6), 764-774.